5-21-2020

Investigation of azo-bond cleavage in Methyl Orange and Direct Yellow 12 using soybean peroxidase

Amanpreet Kaur
University of Windsor

Investigation of azo-bond cleavage in Methyl Orange and Direct Yellow 12 using soybean peroxidase

By

Amanpreet Kaur

A Thesis
Submitted to the Faculty of Graduate Studies
through the Department of Civil and Environmental Engineering
in Partial Fulfillment of the Requirements for
the Degree of Master of Applied Science
at the University of Windsor

Windsor, Ontario, Canada

2020

Investigation of azo-bond cleavage in Methyl Orange and Direct Yellow 12 using soybean peroxidase

by

Amanpreet Kaur

APPROVED BY:

_____

T. Bolisetti
Department of Civil and Environmental Engineering

_____

R. Seth
Department of Civil and Environmental Engineering

_____

N. Biswas, Co-Advisor
Department of Civil and Environmental Engineering

_____

K. E. Taylor, Co-Advisor
Department of Chemistry and Biochemistry

April 06, 2020

DECLARATION OF ORIGINALITY

I hereby certify that I am the sole author of this thesis and that no part of this thesis has been published or submitted for publication.

I certify that, to the best of my knowledge, my thesis does not infringe upon anyone's copyright nor violate any proprietary rights and that any ideas, techniques, quotations, or any other material from the work of other people included in my thesis, published or otherwise, are fully acknowledged in accordance with the standard referencing practices. Furthermore, to the extent that I have included copyrighted material that surpasses the bounds of fair dealing within the meaning of the Canada Copyright Act, I certify that I have obtained a written permission from the copyright owner(s) to include such material(s) in my thesis and have included copies of such copyright clearances to my appendix.

I declare that this is a true copy of my thesis, including any final revisions, as approved by my thesis committee and the Graduate Studies office, and that this thesis has not been submitted for a higher degree to any other University or Institution.

ABSTRACT

Removal of dyes released in water by textile industries presents a major challenge for the researchers. Soybean peroxidase (SBP) has been widely explored for removal of a variety of toxic aromatics consisting of phenolic or anilino functional groups. Also, it has been known to possess the ability of azo-bond cleavage. This thesis was aimed to investigate azo-bond cleavage by SBP in the presence of hydrogen peroxide, if possible, in the absence of these functional groups. Direct Yellow 12 and azobenzene were chosen as a model compounds for this study. Experiments were conducted at a range of pHs, SBP and hydrogen peroxide to investigate the hypothesis. Enzymatic removal of *p*-anisidine and Methyl Orange (MO) and azo-bond cleavage of MO were also studied. Optimization of pH, hydrogen peroxide-to-substrate ratio and SBP activity were performed to achieve ≥95% removal of these substrates in 3 hours, analyzed using high-performance liquid chromatography. A time course study was conducted to calculate pseudo-first-order rate constants and half-lives for degradation of these compounds. Mass spectrometry analysis showed oligomerization of *p*-anisidine and for MO, evidence of azo-bond cleavage was obtained after the enzymatic treatment.

DEDICATION

“ਕਬੀਰ ਮੇਰਾ ਮੁਝ ਮਹਿ ਕਿਛੁ ਨਹੀ ਜੋ ਕਿਛੁ ਹੈ ਸੋ ਤੇਰਾ”

(Kabeer, nothing is mine within myself. Whatever there is, is Yours, O Lord.)

To my late father, Kamaljit Singh for showering his blessings from heaven and teaching me the true essence of life.

ACKNOWLEDGEMENTS

I owe my deepest gratitude to my supervisors, Dr. Nihar Biswas and Dr. Keith E. Taylor, for their patience, motivation, encouragement and guidance throughout my thesis. I have been extremely fortunate to have got an opportunity to be their student and gain a small chunk of the astute knowledge that they have. My sincere thanks to my committee members, Dr. Tirupati Bolisetti and Dr. Rajesh Seth, for their valuable suggestions and comments that helped me in my thesis.

I would like to thank Mr. Bill Middleton and Mr. Joe Lichaa, for their guidance and technical support with all the instrumentation and troubleshooting in lab. My profound gratitude to Dr. Janeen Auld, for mass spectrometry analysis, sharing her knowledge and answering all my queries patiently.

My sincere thanks to Dr. Debjani Mukherjee, for constantly supporting me during my thesis and to all my lab colleagues, Xiaoyang Zhang, Negin Ziayee Bideh, Baturh Yarkwan and Dr. Neda Mashhadi, for their valuable suggestions at all times. Thanks to all the volunteer students, Lily Xu, Victoria Funmilayo, Zeina Sibaei, Kiana Mokrian and Rose Simard, for their help with my lab work. Special thanks to Anju Tiwari, for her help with my experimental work.

Thanks to the Natural Sciences and Engineering Research Council of Canada (NSERC) and University of Windsor for financial support.

My profound gratitude to Dr. M.K. Jha, for his support and motivation to work towards the accomplishment of this goal.

My deepest thanks to my father, Kamaljit Singh, for his hard work, love and sacrifice. His lessons of honesty, perseverance and belief in the Almighty, helped me to fulfill his dreams. My profound indebtedness to my mother, Harpreet Kaur, for her continuous love, motivation and belief in me. Her inspiration and unconditional support at all times helped me to finish this journey.

Finally, my sincere thanks to my friends, Kulvir Singh, Arshi Mehta and Arshdeep Singh, who have always supported me as a family during my toughest times. This journey would have been impossible without their unconditional support.

TABLE OF CONTENTS

LIST OF FIGURES

LIST OF TABLES

LIST OF ABBREVIATIONS/SYMBOLS

4-AAP	4-aminoantipyrine
ARP	*Arthromyces ramosus* peroxidase
ASAP	Atmospheric solid analysis probe
BOD	Biological oxygen demand
CIP	*Coprinus cinereus* peroxidase
COD	Chemical oxygen demand
CPO	Chloroperoxidase
DAD	Diode array detector
DMPD	N,N-Dimethyl-*p*-phenylenediamine
DY12	Direct Yellow 12
ESI	Electrospray ionization
HOBT	Hydroxybenzotriazole
HPLC	High-performance liquid chromatography
HRP	Horseradish peroxidase
MO	Methyl Orange
MS	Mass spectrometry
RZ	*Reinheitzahl* number (purity number)
SA	Sulfanilic acid
SBP	Soybean peroxidase
TDS	Total dissolved solids
TRI	Toxics Release Inventory
UV-VIS	Ultraviolet-Visible

Symbols used

H_2O_2	Hydrogen peroxide
K_m	Michaelis constant
kDa	kilo-Dalton
m/z	mass-to-charge ratio
mDa	milli-Dalton
pK_a	$-\log_{10}(K_a)$, K_a = Acid dissociation constant
ppm	parts per million
V_{max}	maximum velocity

CHAPTER 1: INTRODUCTION

1.1 Dyes

Dyes are important in industries such as textile, paper, food, pharmaceutical, plastic, tannery and electroplating. The annual consumption of dyes is estimated to be around one million tons (Ali *et al*. 2013). In Canada, the textile industry is located primarily in the provinces of Quebec and Ontario. Around 653 establishments, manufacturing textile products and clothing, were operational in Canada in 2016, generating revenue of $1.8 billion (Statistics Canada 2018). The total value of textile exports from Canada to U.S. in 2018, was 1.1 billion CAD (Statistics Canada 2019). Discharge of coloured effluents in the wastewater by textile industries is one of the most difficult problems faced by the environmentalists. Inefficiencies in industrial processes and effluent treatment techniques result in release of large quantities of synthetic dyes into the water bodies. Around 15% of synthetic organic dyes are released into the environment after their usage (Naghizade Asl *et al*. 2016). The textile industry is the highest consumer of water and the most significant contributor to water pollution amongst all industries. This water is high in biological oxygen demand (BOD), chemical oxygen demand (COD) and total dissolved solids (TDS). Dyeing and rinsing steps generate the largest coloured fraction in effluent water and they are characterized by sudden variations in parameters such as pH, COD, BOD, temperature and salinity (Carmen and Daniela 2012).

Several problems arise with coloured water. It not only inhibits photosynthesis but also interferes with the habitats of several aquatic species. Dyes are xenobiotic and have complex, chemically stable structures that resist degradation. Most of the dyes are toxic, carcinogenic and non-biodegradable. They can accumulate in the aquatic species which are

ultimately consumed by humans and can lead to severe interference in the functioning of reproductive, digestive and nervous systems and even lead to kidney and liver damage (Husain 2010).

1.2 Classification of dyes

Dyes can be classified into several categories based on their structure, applications and colour. Based on chemical structure, they are classified as azo-dyes, indigoid dyes, anthraquinone dyes, triarylmethane dyes, nitro dyes and nitroso dyes (Yagub *et al*. 2014). The structures are shown in Figure 1.1.

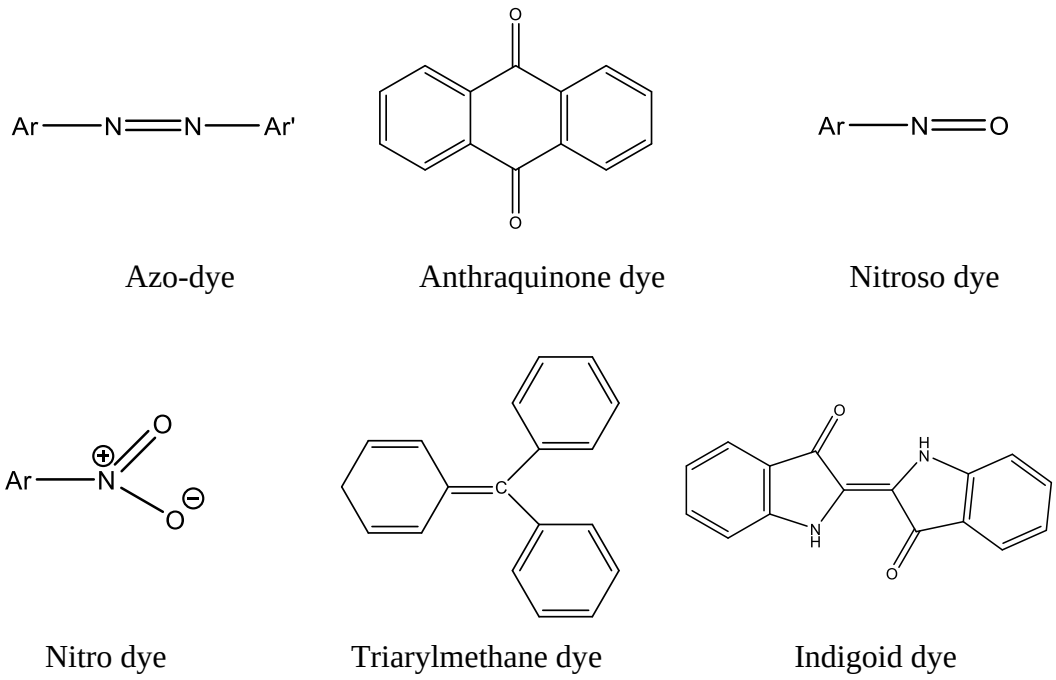

Figure 1.1. Classification of dyes (Ar and Ar' denote aryl groups).

Based on the applications of dyes, they are classified as acidic, basic, sulfur, vat, disperse, direct, azoic and reactive dyes. Based on colour, the categorization of dyes is quite complex owing to the complexities of colour. Hence, classification based on structure and applications is preferred. Amongst the dyes being used in the textile industry, azo-dyes

contribute to two-thirds of it. These are used for imparting red, yellow and orange colours. Azo-dyes are highly toxic and carcinogenic due to the breakdown of azo-dyes into amines (Freeman and Mock 2007). Azo-bond cleavage is the first step in the degradation of azo-dyes (Seshadri *et al*. 1994) Some azo-dyes release benzidine and other anilines that can be carcinogenic and mutagenic. Hence, a study of degradation products of dyes is important (Rauf and Ashraf 2012).

1.3 Treatment processes for dyes

The need for removal of dyes from wastewater can be inferred from the fact that even the presence of minor amounts of dyes, as low as <1 ppm, can be easily observed and is unacceptable (El Nemr *et al*. 2018). Treatment methods are generally classified as physical, chemical and biological. Physical methods consist of coagulation-flocculation, adsorption and filtration techniques. Chemical methods comprise ion-pair extraction, advanced oxidation and other chemical oxidations. Biological methods consist of treatment using enzymes and micro-organisms (Holkar *et al*. 2016).

Biological methods represent the most effective treatment method since these are eco-friendly, economical and do not have substantial sludge disposal issues. Biological methods include treatment using enzymes and micro-organisms such as algae, bacteria and fungi aerobically or anaerobically or even a combination of aerobic and anaerobic processes. Some microbial industrial processes are activated sludge process, trickling filters, aerobic and anaerobic digestion and rotary biological contractors (Carmen and Daniela 2012). Long acclimation time and inhibition of microorganisms prior to enzyme production present major drawbacks for practical use in water treatment. The capital cost for selected enzymatic treatment is 5-8 times less than the conventional treatment methods

(Mukherjee *et al.* 2020). Isolated enzymes such as tyrosinases, laccases and peroxidases have been explored for removal of dyes and various phenolic and anilino compounds from wastewater (Ćirić-Marjanović *et al.* 2017). Many peroxidases have been investigated for removal of toxic substances from wastewater. Soybean peroxidase (SBP) has been known to be effective for dye decolourization (Cordova Villegas 2017).

1.4 Structures of the dyes and related compounds of interest in this thesis

These are shown in Figure 1.2.

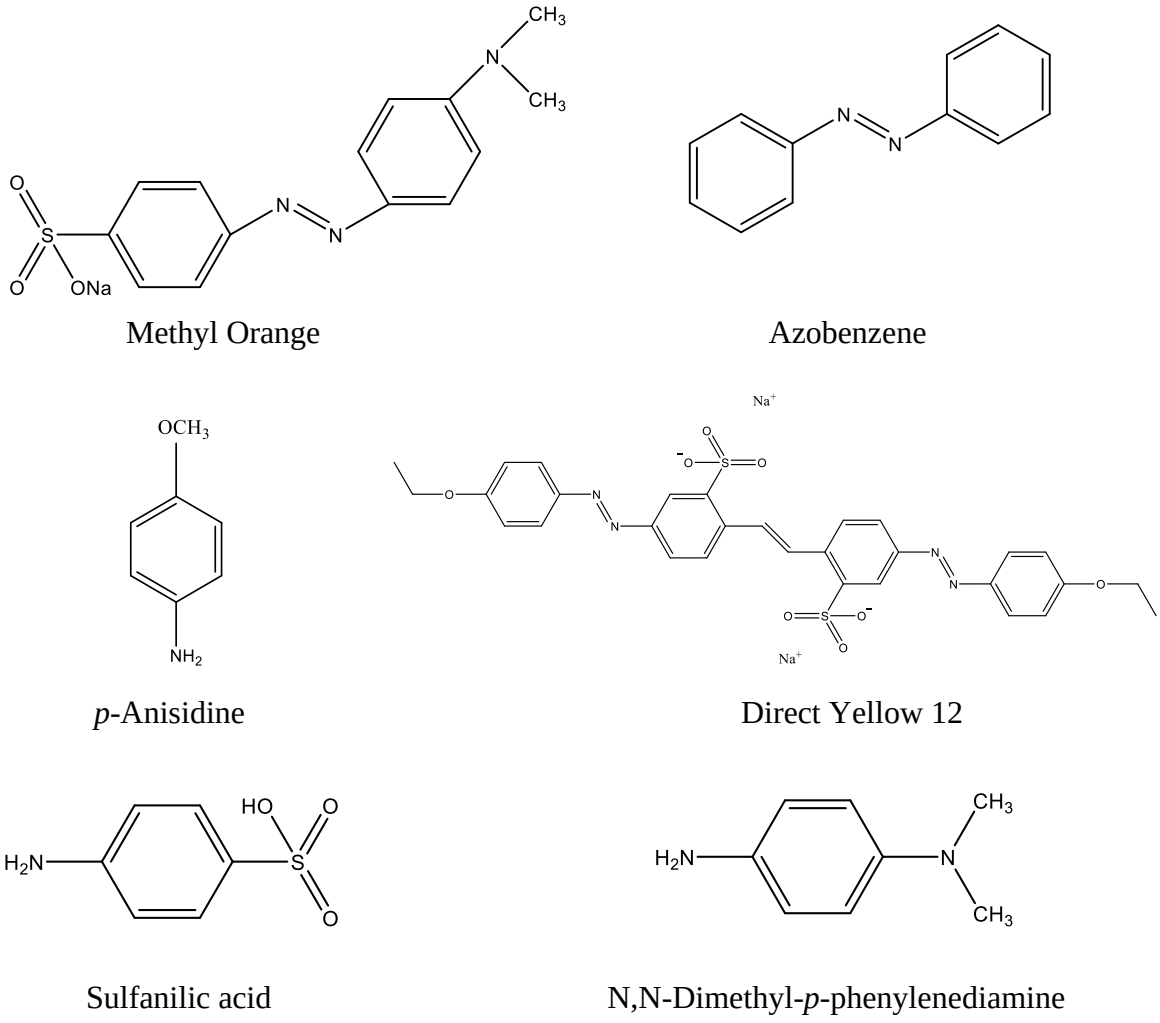

Figure 1.2. Compounds studied in this thesis.

Although real wastewater is not part of the scope of this thesis, it is always a general long-term objective of enzymatic treatment.

1.5 Research objectives

The major objectives of the research are to:

1. Seek evidence of SBP reactivity with azo-dyes that have no other enzyme-active phenolic or anilino functional groups; optimize any reactivity
2. Characterize azo-cleavage reaction products by their SBP reactivity and structurally

1.6 Scope of research

Part I: Optimization of reaction conditions

1. Determine feasibility of SBP for removal of DY12, a bis-azo dye, and MO, a mono-azo dye
2. Optimization of parameters (pH, SBP activity and H_2O_2 concentration) for ≥95% removal of the dyes and some of the putative azo-cleavage products
3. Establish initial first-order rate constants and half-lives for enzymatic conversion of the compounds

Part II: Product identification

1. Investigate the formation of dimers and higher oligomers of *p*-anisidine using mass spectrometry
2. Conduct HPLC analysis of dye reaction products, if any, and standards of possible azo-cleavage products of dye to confirm their presence
3. Conduct MS analysis of dye reaction products, if any, to characterize possible products formed as a result of azo-bond splitting and/or radical polymerization

CHAPTER 2: LITERATURE REVIEW

2.1 Wastewater treatment methods

Wastewater treatment methods can include physical, chemical and biological methods, as reviewed by Holkar *et al*. (2016). A brief description of these methods is provided in this section. Coagulation-flocculation, filtration and adsorption comprise the most widely used physical methods. Szygula *et al*. (2008) used coagulation-flocculation for the removal of sulphonated azo-dyes with chitosan, an aminopolysaccharide. However, the coagulation-flocculation technique has a major drawback of having low efficiency and generation of a significant amount of sludge requiring facilities for appropriate treatment and disposal. Adsorption techniques using activated carbon and other low-cost adsorbents such as polymeric resins also generate large quantities of sludge and are not suitable for higher pollutant concentrations (Mugdha and Usha 2012). Filtration methods such as reverse osmosis, nanofiltration and ultrafiltration have disadvantages of high membrane cost and membrane fouling, rendering the process infeasible for large-scale treatment (Koyuncu and Güney 2013, Liang *et al*. 2014).

Several chemical methods have been proposed for degradation of dyes such as use of Fenton's reagent (Fe^{2+}/H_2O_2) for degradation of MO, *p*-Methyl Red and azobenzene (Guivarch *et al*. 2003), ozonation for removal of MO (Chen 2000), electrocoagulation for removal of Acid Red 14 (Aleboyeh *et al*. 2008) and combination of electrochemical and ion-exchange for decolourization of textile wastewater (Raghu and Ahmed Basha 2007). These processes present major drawbacks of large amount of sludge generation, high energy costs, short half-life and/or generation of environmentally hazardous by-products

(Chuah *et al*. 2005). According to Husain (2010), industrial applications of the physical and chemical treatment methods proposed for wastewater treatment are very limited.

As discussed in Section 1.3, enzymatic treatment presents one of the most efficient and cost-effective technique for removal of a wide variety of wastewater pollutants (Bilal *et al*. 2018).

2.2 Enzymatic treatment

Enzymes are biocatalysts that catalyze reactions, specifically under mild conditions. The ability of oxidoreductase enzymes to polymerize arylamines using H_2O_2 or O_2 as oxidants has led to extensive research in this field in the last few decades. The first enzymatic treatment of substituted anilines was reported in 1925 for oxidative dimerization of *o*-phenylenediamine by peroxidase/H_2O_2, as reviewed by Ćirić-Marjanović *et al*. 2017. Use of peroxidases for oligomerization and polymerization of arylamines has been a major interest since then for researchers.

Bollag and his co-workers in 1979 were the pioneers to use an enzyme (a laccase) extracted from *Rhizoctonia praticola* fungus for polymerization of 2,6-dimethoxyphenol (Bollag *et al*. 1979). During the same period, Klibanov and his group used horseradish peroxidase (HRP) for removal of more than 30 phenols and aromatic amines from wastewater and achieved removal efficiencies of more than 99% for some of these compounds (Klibanov *et al*. 1980). Since then, there has been comprehensive research on treatment of a wide range of phenols and anilines that have been listed as hazardous pollutants by various regulatory agencies or can potentially become pollutants in the future (emerging contaminants/micropollutants), using peroxidases (Morsi *et al.* 2020). Extensive research has also been devoted to understand the kinetics/mechanism of enzymatic treatment of

arylamines, phenols and azo-dyes (Ali *et al*. 2013, Arregui *et al*. 2019, Mukherjee *et al*. 2019).

Enzymatic treatment is becoming one of the most explored alternatives owing to its effectiveness in acting over a wide range of pH and temperature, ease of control, simple operation, higher reaction rates, ability to treat a wide range of concentrations, less sludge generation and ease of handling and storage (Bodalo *et al*. 2006, Morsi *et al*. 2020). With advancements in engineering and new methods, the major barriers in the applicability of enzyme at large scale, cost and availability, are being overcome. Enzymes can also be used to generate value-added products from waste by transformation or render a compound suitable for its treatment by decomposition of its chemical structure (O'Neill *et al*. 1999, Fernandes *et al*. 2020).

Oxidoreductases, including laccases and peroxidases, have proven to be ideal for industrial wastewater treatment since they have the ability to oxidize phenols and anilines to free radicals which couple to form dimers, which can further undergo enzymatic cycles to be converted to higher oligomers until they precipitate out of the solution and can be removed through sedimentation or filtration (Ali *et al*. 2013, Steevensz *et al.* 2014). Laccases are enzymes that can remove many phenolic and anilino contaminants in the presence of oxygen. However, a major drawback of using laccase is the cost of white-rot fungi, from which it is produced, susceptibility to inactivation due to changes in conformation and modification of amino groups and slow activity of the enzyme. Also, it requires oxygen as a co-substrate, which poses a problem of low oxygen solubility in water (Ba *et al*. 2013).

2.3 Peroxidases

Peroxidases come to be the most preferred alternative for biodegradation of environmentally harmful synthetic dyes. A major advantage of peroxidases is their non-specific nature i.e., the ability to degrade a wide range of pollutants including herbicides, phenols, anilines, polycyclic aromatic hydrocarbons, polychlorinated biphenyls among others (Bilal *et al*. 2018).

Peroxidases can broadly be classified into two major classes: heme peroxidases, with iron (III) in a prosthetic heme group, and non-heme peroxidases. Another classification of peroxidases is based on the origin of these peroxidases as plant peroxidase superfamily, animal peroxidase superfamily and catalase superfamily (Dunford 1999). Plant peroxidases are further sub-classified into three classes based on amino acid sequence analogies. These include class I peroxidases of prokaryotic origin such as chloroplast and yeast cytochrome peroxidases, class II fungal peroxidases such as lignin and manganese peroxidases and class III plant peroxidases such as SBP, HRP, peanut peroxidase and barley peroxidase.

Amongst all the peroxidases, HRP is one of the most explored peroxidases (Mukherjee 2019). A major issue with using heme-dependent peroxidases is the oxidative degeneration of the heme group contributing to their low operational stability. However, SBP has been known to have better operational stability compared to HRP (Ryan *et al*. 2006). Some other advantages of SBP in contrast to HRP include: (1) ability to treat a wide variety of substrates owing to more exposure of its catalytically active delta heme site, (2) more economical, (3) can function over wide pH range of 2-10 compared to 4-8 for HRP, since HRP loses heme at lower pH values while SBP does not, (4) lower susceptibility to irreversible inactivation by hydrogen peroxide, (5) higher inactivation temperature of

90.5ºC compared to 81.5ºC for HRP, (6) existence as a single isozyme compared to other peroxidases such as HRP that occur as multiple isozymes, which makes it more substrate specific (McEldoon *et al*. 1995, McEldoon and Dordick 1996, Ryan *et al*. 2006, Steevensz *et al.* 2014).

2.4 Soybean peroxidase

SBP belongs to the class III secretory plant peroxidase family with a molecular weight of 37 kDa (Henriksen *et al*. 2001). It is an oxidoreductase enzyme that can be used to remove organic pollutants (consisting of various amines and phenolic compounds) released from industries through oxidation/polymerization. SBP exhibits an extensively anionic heterogeneous glycoprotein covalent structure with 306 residues; pyrrolidine carboxylic acid residue occupying the first position and serine residue at the last (Welinder and Larsen 2004). All peroxidases have ferriprotoporphyrin (IX), known as heme, at the active site with Fe (III) complex occupying the center position and methine-bridges joining the four pyrrole rings which complex Fe (III) (Figure 2.1) (Welinder and Larsen 2004, Al-Ansari *et al*. 2011). Enzymatic activity of soybeans can be found in the seed hulls, leaves and roots of soybean plant. However, seed hulls that comprise 4-8% of total mass of the seed, contain the maximum amount of activity (Geng *et al*. 2001, Al-Ansari *et al*. 2011).

SBP has been proposed to be the preferred enzyme in comparison to other peroxidases for wastewater treatment according to McEldoon and Dordick (1996). SBP possesses unusual thermal stability at temperatures as high as 90ºC at pH 5.0, compared to HRP and *Coprinus cinereus* peroxidase (CIP) that have a melting temperature of 81.5 and 65ºC, respectively. This is because SBP can tightly bind the heme group to its structure. At temperatures above 90ºC, the heme is lost, leading to formation of inactive apo-SBP.

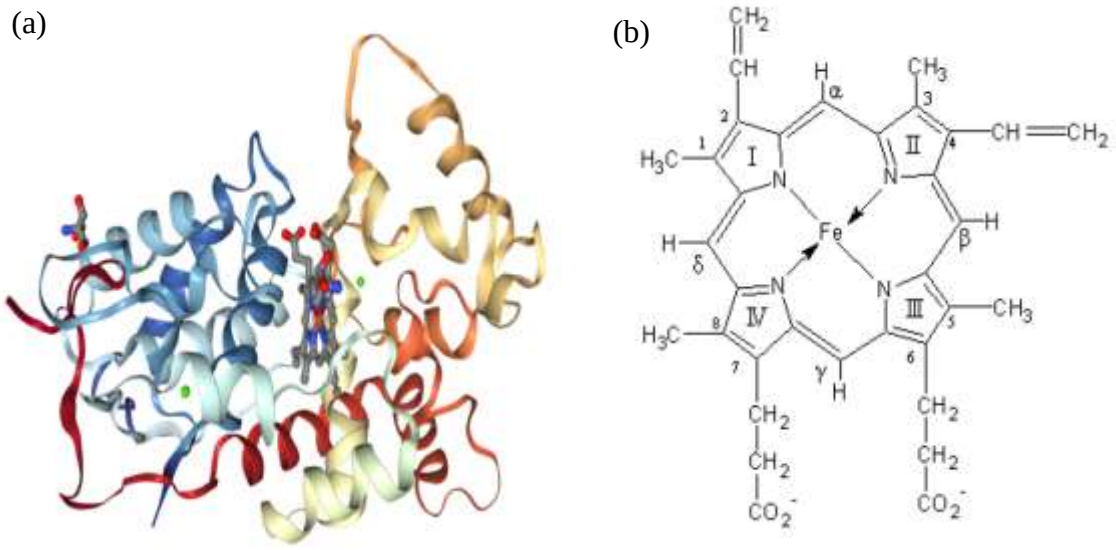

Figure 2.1. (a) 3-D structure of SBP (generated from RCSB-Protein Data Base, category no. 1FHF, 2020) and **(b)** ferriprotoporphyrin IX (heme) prosthetic group (adopted from Al-Ansari *et al*. 2011).

The catalytic efficiency (k_{cat}/K_M) of SBP has been reported as 7.1±0.1 μMs^{-1} at pH 6.8 using ABTS [2,2'-azino-bis-(3-ethylbenzthiazoline-6-sulphonate)] as a substrate (Kamal and Behere 2003). This value is 1.7 times higher than that observed for HRP. SBP is relatively more resistant to inactivation in the presence of high concentrations of H_2O_2 compared to lignin peroxidase and HRP (McEldoon *et al*. 1995). A study conducted on the degradation of Sulforhodamine B dye using SBP and chloroperoxidase (CPO) has proven SBP to be more efficient in the elimination of toxicity of the dye than the other peroxidase (Alneyadi *et al*. 2017).

Another advantage of SBP is that the enzyme does not need any purification since the crude enzyme can perform better than the purified enzyme. Flock *et al*. (1996) compared raw and purified soybean for the treatment of phenol and 2-chlorophenol and observed that in comparison to 10% removal of phenol observed by purified enzyme, raw seed hulls

exhibited removal of 96.4 %. This could be, in part, due to the absorption of polymeric products by seed hulls as well as to the slow rate of leaching of enzymes from the seed hulls, thus providing protection to the enzymes from free radicals.

Purity of SBP is denoted by the *Reinheitzahl* (RZ) number, also known as the purity number. It is measured as the ratio of absorbance at 403 nm to absorbance at 280 nm. A higher RZ value shows the purity of the preparation of the enzyme (reaching a maximum in the range 3.0 – 3.3). However, this does not denote higher activity necessarily (Dunford 1999). Nicell and Wright (1999) observed RZ value of 0.49±0.6 for crude SBP. Similar value of ~0.5 was reported by Kamal and Behere (2003). Al-Ansari *et al*. (2010) observed a value of 0.75±0.10 for crude SBP.

2.4.1 SBP production in Canada

Soybean production is the fifth largest amongst the principal field crops in Canada (USDA 2020). The area harvested for soybean production in the world in 2019 was 122 million hectares (HA). Brazil is expected to be the leading producer of soybean with a production of 123 million metric tons (36.4% of the world) surpassing United States for the year 2019-2020. North America contributes 25.8% of world soybean production. United States ranks second in the worldwide production of soybeans with a contribution of 24.7% in the world and 92.5% in North America. The total area harvested in Canada for 2019 was 2.3 million HA in comparison to 1.5 million HA in 2010 as depicted in Figure 2.2 (Statistics Canada 2020), with the production rising from 4 million metric tons in 2009 to 6 million metric tons in 2019. There has been an increase of 36% in production of soybeans during the last decade in Canada (USDA 2020).

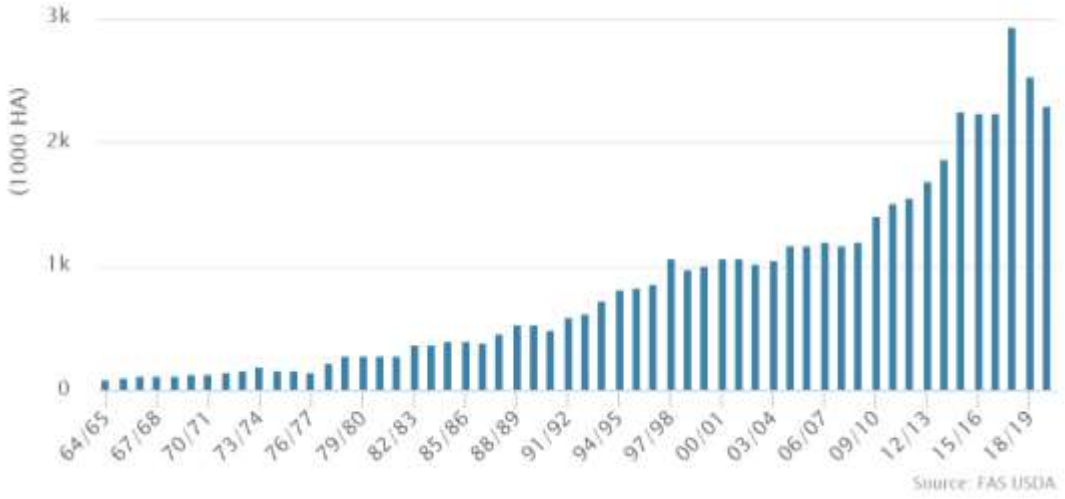

Figure 2.2. Area harvested for soybeans in Canada. Data reported on 01/2020. USDA, 2020.

2.4.2 SBP reaction mechanism

The reaction mechanism for the SBP catalytic reaction, Figure 2.3, is a modified bi-bi ping pong mechanism (Mousa 2008). The enzyme in its resting state (E_N) consists of Fe (III) protoporphyrin at the active site. It reacts with H_2O_2 by a two-electron oxidation step leading to the formation of compound I with Fe (IV) oxo-ferryl at the active center (Equation 1) (Steevensz *et al*. 2014). Compound I oxidizes the aromatic substrate (AH) and forms a free radical (A·) through a one-electron oxidation step, and SBP compound II is formed as an intermediate (Equation 2). Compound II again reacts with the reducing substrate to generate another free radical (A·) and the enzyme reverts to its native form (Equation 3) (Nicell *et al*. 1992, Krainer and Glieder 2015, Ćirić-Marjanović *et al*. 2017).

$$\text{Native peroxidase} + H_2O_2 \longrightarrow \text{Compound I} + H_2O \quad (1)$$

$$\text{Compound I} + \text{AH (Reducing substrate)} \longrightarrow \text{Compound II} + \text{A}\cdot \quad (2)$$

$$\text{Compound II} + \text{AH} \longrightarrow \text{Native peroxidase} + \text{A}\cdot + H_2O \quad (3)$$

The mechanism of enzymatic reaction of SBP is illustrated in Figure 2.3.

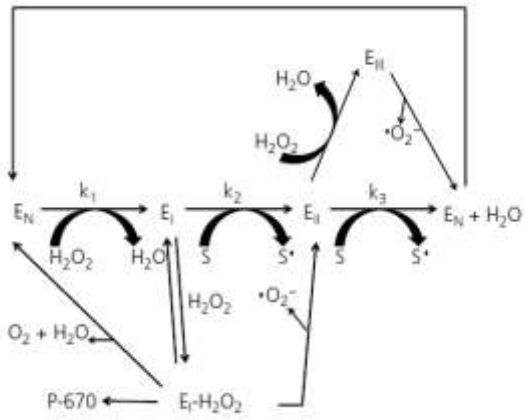

Figure 2.3. Mechanism of enzymatic reaction of SBP (Adopted from Steevensz *et al*. 2014).

Some substrates are not able to form a radical by themselves due to their structure. For such compounds, redox mediators can be used as an electron shuttle (Van der Zee and Cervantes 2009). The mediator is oxidized by the enzyme to a radical, which in turn oxidizes the substrate to a radical. The substrate free radical can then couple to dimers and, possibly, to higher oligomers. Redox mediators can hence be used to expand the range of compounds that can behave as substrates for the enzyme. Some commonly used mediators include veratryl alcohol, violuric acid, 1-hydroxybenzotriazole (HOBT) and triphenylamine (Fabbrini *et al*. 2002). Ali *et al.* (2013) used HOBT as redox mediator for degradation of Crystal Ponceau 6R dye by SBP, which could not be degraded otherwise in the presence of SBP and H_2O_2 alone. Similarly, Alneyadi and Ashraf (2016) used HOBT as a redox mediator for degradation of thiazole pollutants using SBP and CPO. While SBP required HOBT for the enzymatic reaction, CPO did not require the mediator. Instead, a reduction in enzymatic activity was observed with the use of HOBT for CPO degradation

of thiazole because HOBT itself behaves as a substrate for the enzyme, as reported by Mashhadi *et al*. (2019).

2.4.3 SBP inactivation

SBP inactivation can take place reversibly and irreversibly, the latter is generally referred to as suicide pathway. There are three ways in which the enzyme may become deactivated (Feng *et al*. 2013, Steevensz *et al.* 2014, Alneyadi *et al*. 2017):

1. In the presence of excess peroxide, E_{II} can be converted to E_{III}, which is an inactive form of enzyme. E_{III} can be converted back to E_N through the generation of superoxide radical. Hence, this deactivation is reversible, but the conversion back to E_N is too slow (Figure 2.2).

2. P-670 formation (due to opening of heme ring) leads to irreversibly deactivated enzyme (Figure 2.2).

3. The third way of enzyme activation is due to adsorption of the enzyme onto polyphenolic precipitates.

2.4.4 Use of additives to reduce enzyme inactivation

Several methods have been investigated to prevent enzyme inactivation. These include: (1) step addition of H_2O_2; (2) use of additives such as gelatin and polyethylene glycol (PEG); (3) using surfactants such as Triton X-100, sodium lauryl sulphate (SDS) and Span 20. (Al-Ansari *et al*. 2010, Sakurai *et al*. 2003). Sakurai *et al*. (2003) proposed that surfactants such as lauryl trimethyl ammonium bromide (DTAB) are even capable of reactivating the enzyme that has been precipitated by end products of the enzymatic reaction of phenol with *Coprinus cinereus* peroxidase. This was refined by Feng *et al*. (2013) who showed with

SBP that the inactivation is attributed to reversible immobilization of active enzyme onto phenolic precipitates, thereby resulting in a lower specific activity.

Wu *et al*. (1998) carried out a detailed study to discover the reasons for HRP inactivation and utilize PEG to reduce inactivation of the enzyme for removal of phenol from synthetic wastewater. Adsorption of HRP onto polymeric products was observed to be one of the reasons for reduction in enzymatic activity that could be minimized by using PEG. PEG reacts with polymeric products to form a complex instead of the products' reacting with HRP since the polymers have higher affinity for PEG. Enzyme inactivation was still observed but at a relatively slower rate. During the same period, Kinsley and Nicell (1999) found that PEG reduced SBP requirement for removal of phenol from water, thereby increasing the active life of SBP due to interaction between the polymeric products and PEG.

Additives also have an additional benefit of reducing the cost due to reduction in the enzyme usage. Effect of PEG, SDS, Triton X-100 and sodium dodecanoate (SDOD) additives on enzymatic reaction of anilines with SBP were investigated by Mazloum *et al*. (2016). No significant effect was observed by using PEG while SDS not only decreased the enzyme requirement from 0.6 U/mL to 0.3 U/mL for 95% removal of 1 mM aniline but also improved the quality of precipitates and treated water. SDOD and Triton X-100 also reduced enzyme requirement with 1 mM aniline to 0.28 U/mL and 0.4 U/mL, respectively (Mazloum *et al*. 2016). This suggests that PEG effectively works as a non-toxic and cost-effective additive for removal of phenols but not for anilines.

2.5 Azo-dyes

Azo-dyes are xenobiotic and are characterized by the presence of one or more chromophoric groups (-N=N- azo linkage) and usually have sulphonic acid, carboxylic acid or some other electron-withdrawing functional group attached, known as auxochromes. They are highly recalcitrant and have high polarity with log K_{ow} of 3 (Carmen and Daniela 2012). Azo-dyes have a wide variety of applications such as food additives, colourizer in oils, inks, cosmetics, solvents and polishes, for vital staining in microscopy and dyeing cellulose fabrics and leather (Carmen and Daniela 2012, Husain *et al*. 2010).

Auxochromes can alter the physico-chemical properties of a dye by influencing its solubility and making it resistant to degradation by microorganisms (Ali *et al*. 2013). These dyes can be carcinogenic by themselves or can produce carcinogenic products upon azo-cleavage (Chung *et al*. 2016). Release of these dyes in wastewater can lead to eutrophication, reduction in water-gas solubility, interference in photosynthesis and aesthetic issues (Hassaan and El Nemr 2017).

2.6 Compounds studied in this thesis

In this section, toxicity, health concerns and need for treatment for the compounds studied in this thesis are discussed (structures are given in Figure 1.2, above).

2.6.1 Methyl Orange

Methyl Orange (MO) is a mono-azo dye widely used for estimating the alkalinity of water and as an indicator for titrating strong acids and bases. It also has wide usage in the pharmaceutical, printing, food and textile industries (Mittal *et al*. 2007). High usage of this dye results in release of enormous amounts in wastewater streams from industries (Ma *et al*. 2007) The dye is categorized as persistent in the domestic substances list (DSL) of

Canada (Government of Canada 2020). Due to the ionic nature of MO, the dye is non-volatile and less susceptible to aerobic biodegradation in soil and water. Also, it may be adsorbed to sediments and clay and mineral surfaces in water (Evans 1989). Once in the body, MO can undergo reductive azo-bond cleavage through reductive enzymes present in the liver and form toxic aromatic amines that can cause intestinal cancer (Mittal *et al*. 2007).

Various treatment methods have been suggested for removal of the hazardous dye. Adsorption has been widely investigated by researchers (Li *et al*. 2016). Adsorption using chitosan was demonstrated by Saha *et al*. (2010) and the effect of various parameters such as pH, temperature and initial dye concentration were studied. Another study by Habiba *et al*. (2017), used a composite of chitosan/polyvinyl alcohol/zeolite for removal of MO and Congo Red using a flocculation/adsorption technique. Adsorption was dominant at lower MO concentrations while at higher concentrations, flocculation was observed to be the dominant process. Some other adsorption studies used adsorbents such as graphene oxide (Robati *et al*. 2016), mesoporous carbon (Mohammadi *et al*. 2011), lanthanum (III) chloride modified mesoporous carbon (Goscianska *et al*. 2014), iron terephthalate (MOF-235) (Haque *et al*. 2011) and chitosan/magnesium oxide composite (Haldorai and Shim 2014). Composite fiber synthesized from deposition of calcium alginate on multi-walled carbon nano-tubes was used by Li *et al*. (2012). Removal of 65% was observed at pH of 2.0 and the removal decreased with an increase in pH because of competition between $-COO^-$ ions from calcium alginate and MO dye anions that resulted in reduction of the dye uptake. Adsorption however presents a major drawback as the large quantity of sludge generated that necessitates safe disposal (Singh *et al*. 2015).

Some other techniques that have been investigated for removal of MO include photocatalytic degradation using silver, gold and silica nanoparticles coated on silica core-shell (Badr and Mahmoud 2007), reverse osmosis using a spiral-wound polyamide membrane (Al-Bastaki 2004) and zero-valent iron nanoparticles supported on biochar (Han *et al*. 2015). Chiong *et al*. (2016) used SBP for decolourization of 30 mg/L (0.09 mM) MO dye, achieving 81.4% decolourization efficiency at pH 5.0, 2.0 mM H_2O_2 and 0.186 U/mL SBP (guaiacol was used to measure SBP activity). However, no information about reaction products was reported. Dixit and Garg (2018) used *Klebsiella pneumoniae* for degradation of MO using reduced nicotinamide dinucleotide (NADH) as a redox mediator. HPLC analysis of the degradation products showed formation of 4-aminobenzenesulphonic acid (sulfanilic acid (SA)) and N,N-dimethyl-*p*-phenylenediamine (DMPD) after the treatment. Similarly, Parshetti et al. (2009) used *Kocurea rosea* MTCC 1532 for decolourization of MO. GC-MS (gas chromatography-mass spectrometry) revealed formation of SA and DMPD after the treatment. However, the initial dye concentration for complete decolourization was 30 µM which is quite low. Only 40% decolourization was observed for 300 µM MO, even after 120 hours.

2.6.2 Direct Yellow 12

Direct Yellow 12 (DY12) is a bis-azo dye that is extensively used in textile, paper and leather industries, dermatology, cosmetics, food additives, biological staining, ink and paint (Abedi and Nekouei 2011, Ghaedi *et al*. 2012). Since DY12 is ethoxylated, it is highly stable towards acidic and/or alkali solutions (Toor *et al*. 2006). The dye is persistent and has a very strong colour. It has high BOD, does not allow light to pass and has a

considerable effect on aquatic life and photosynthesis of aquatic plants (Abedi and Nekouei 2011).

DY12 does not have phenolic or anilino functional groups normally expected to form free radicals on reacting with SBP. This dye would be appropriate for investigation to see if SBP is capable of cleaving the azo-bond.

Some existing treatment methods for removal of DY12 consist of mostly adsorption techniques: using silver nanoparticles on activated carbon (Ghaedi *et al*. 2012), *Spirulina* algae (Marzbali *et al*. 2017), zero-valent iron nanoparticles (Sohrabi *et al*. 2014) and zinc sulphide and copper nanoparticles on activated carbon (Ghaedi *et al*. 2013). Maddhinni *et al*. (2006) used free and alginate- and acrylamide-immobilized HRP for decolourization of DY12. UV-Visible (UV-VIS) spectrophotometry demonstrated 78% decolourization of 25 mg/L of DY 12 (0.036 mM) using acrylamide-immobilized HRP at pH 4.0 and 2.0 µL/L H_2O_2 as compared to 69% decolourization using free HRP.

2.6.3 *p*-Anisidine

p-Anisidine is an aniline derivative primarily used as an intermediate for manufacture of several azo-dyes and is discharged into the water streams (Lewis 2007). It is also used as a colourant in hair dyes and personal care products and as a reagent in laboratories for evaluating the formation of secondary lipid oxidation products in edible oils (denoted as the anisidine value) (US EPA 2020). Of all the three isomers of anisidine, *p*-anisidine is the most toxic (Chaturvedi and Katoch 2019). It has been reported in Toxics Release Inventory (TRI), 2015 with 1.0 % *de minimis* concentration (US EPA, 2020).

It can cause anoxia by reaction with haemoglobin to form methaemoglobin and has also been reported positive in bacterial mutation assays (IARC 2019, Haworth *et al*. 1983; Thompson *et al*. 1992). Human exposure may occur by inhalation of vapors, ingestion or by skin contact (NIOSH 2020). Although there is no information about the carcinogenicity of *p*-anisidine in humans on short-term exposure, long-term exposure may be carcinogenic. Repeated exposure may even lead to kidney and lung damage, skin allergies, and bronchitis (Pohanish and Sittig 2008). The Henry's constant for *p*-anisidine is $6.60x10^{-8}$ atm m^3/mole (Altschuh J. *et al.* 1999*)* which is quite low. This suggests that it does not have the ability to volatilize from water surface.

Reductive azo-bond cleavage of DY12 results in formation of 4-ethoxyaniline. Due to the easy availability and structural similarity to 4-ethoxyaniline, *p*-anisidine would be a good model compound for study of reactivity with SBP.

To our knowledge, very few studies have been reported for techniques for removal of *p*-anisidine. Adsorption for removal of *o*-, *m*- *and p*-anisidines was utilized by Bardakçı *et al*. (2013), using cobalt supported on pumice as an adsorbent. Fenton's reagent was used by Chaturvedi and Katoch (2019) for removal of *p*-anisidine from wastewater. UV-VIS analysis showed removal of 89% at pH 2.5, 0.05 mM Fe^{2+}, 3.5 mM H_2O_2 and 0.5 mM initial substrate concentration. Mazloum (2014) used SBP for removal of *o*-anisidine (1.0 mM) and achieved 95% removal at pH 5.0, 0.012 U/mL SBP and 1.25 mM H_2O_2.

2.6.4 Azobenzene

Azobenzene is an intermediate in the formation of benzidine and its salts, dyes, insecticides, rubber accelerators and personal care products (US EPA). It is commonly used as a fumigant in greenhouse gases and as a precursor for manufacture of polymers (O'Neil

2006). It is a probable human carcinogen (US EPA 2006). Azobenzene would be an unambiguous model compound for peroxidase-catalyzed azo cleavage. Previous studies for removal of azobenzene include use of kaolinite clay as an adsorbent (Zhang *et al*. 2009) and Fenton's reagent (Fe^{2+}/H_2O_2) by Guivarch *et al*. (2003).

2.7 Azo-bond cleavage

Toxicity of the dye is attributed not to the dye itself but to its degradation products (Bafana *et al*. 2011). As investigated by Seshadri *et al.* (1994), the first step in the degradation of an azo-dye is cleavage of azo-bond since azo-bond is the most labile component of azo-compounds. It can occur through enzyme-mediated reactions (EC 2012). Figure 2.4 shows reductive cleavage of an arylazo-bond leading to the formation of two arylamines with various substituents (Equation 4).

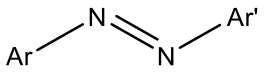

$$\longrightarrow \quad ArNH_2 \quad + \quad Ar'NH_2 \qquad (4)$$

Ar and Ar′ denote aryl groups

Azo-bond cleavage is a degradation pathway for azo-dye degradation by peroxidases. Degradation of azo-dyes by peroxidases generates free radicals that are viable to be attacked by H_2O_2 and oxidize the intermediates to stable intermediates (Bilal *et al*. 2018).

2.8 Azo-bond cleavage studies with dyes

Very few studies to date have focused on azo-bond cleavage in dyes (Ali *et al*. 2013). Nouren *et al*. (2017) conducted a study on azo-bond cleavage in Direct Yellow 4, a bis-azo dye, using citrus lemon peroxidase. The degradation achieved was around 89%, as analyzed using ultra-performance liquid chromatography (UPLC) and the metabolites formed after the cleavage were found to be less toxic than the original dye. Zhang *et al*.

(2012) used CPO for degradation of two azo-dyes, Sunset Yellow and Orange G. Degradation of 98.7% of 0.3 mM Orange G was observed at pH 2.75, 1.0 mM H_2O_2 and 0.05 µM CPO while 77.3% degradation of 0.1 mM Sunset Yellow was observed at pH 2.75, 0.5 mM H_2O_2 and 0.4 µM CPO using UV-VIS. LC/MS (liquid chromatography/mass spectrometry) analysis of reaction products of Orange G showed evidence of symmetrical as well as asymmetrical azo-bond cleavage resulting in formation of eight products. Formation of aniline was proposed but could not be detected in MS.

Another bis-azo dye, Trypan Blue was decolourized by Kalsoom *et al*. (2013) using SBP that reported formation of several intermediates through symmetrical and asymmetrical azo-bond cleavage using HPLC-DAD (Diode Array Detector) and LC-MS/MS analysis with no detail on toxicity of the metabolites. Cordova Villegas *et al.* (2017) studied azo-bond cleavage in Crocein Orange G using HPLC and ESI-MS (electrospray ionization-mass spectrometry). The analysis revealed formation of aniline and coupling products of aniline dimer and trimer after reaction with SBP/H_2O_2.

2.9 Mass spectrometry analysis

Mass spectrometry (MS) is an analytical technique used to identify and quantify molecules on the basis of mass to charge ratio (m/z) of their ions (Sparkman 2000). Several ways of ionization and detection of molecules have been developed for this technique such as ESI, atmospheric solid analysis probe (ASAP), MS/MS (MS^2) analysis and MS/MS/MS (MS^3) analysis.

MS^2 analysis, also known as tandem mass spectrometry consists of two stages. In the first stage, mass selection of a precursor ion (parent ion) takes place and these ions are subsequently fragmented through reaction and mass-analyzed (Niessen 2017). The most

commonly used reaction is through collision with a neutral gas (for example, nitrogen, helium or argon). In the second stage, m/z analysis of the fragmented ions (daughter ions) occurs. The basic principle is the difference in m/z values of parent (m_p^+) and daughter (m_d^+) ion, before and after the ionization reaction (Reaction 5).

$$m_p^+ \longrightarrow m_d^+ + n \text{ (neutral species)} \qquad (5)$$

Ionization can take place through high-energy or low-energy collision (depending upon the type of application) of parent ion with a neutral gas. MS^3 technique involves an additional step of isolation and ion fragmentation, thereby giving additional information about the parent molecule (Ulintz *et al*. 2008).

The ASAP technique uses an ESI or atmospheric pressure chemical ionization (APCI) source for ionization of volatile, semi-volatile or solid samples at atmospheric pressure using a solid probe. Ionization takes place by direct introduction of sample into a stream of heated nitrogen gas (McEwen *et al*. 2005). Compounds having concentrations ≥50 ppb can be detected using ASAP. The primary advantages of this method are ease of implementation and detection of volatile compounds.

The ESI-MS technique is based on time of flight analysis (ToF), wherein high voltage (2.5-6.0 kV) is applied to a solution to convert solutes into molecular ions. Based on their m/z values, the ions reach the detector at different times. This information is used by a computer to create a mass spectrum of the ions. ESI and ASAP are considered to be "soft techniques" since much less fragmentation takes place in comparison to conventional MS techniques (Ho *et al*. 2003, Pitt 2009, Carrizo et al. 2016).

CHAPTER 3: MATERIALS AND METHODS

3.1 Materials

3.1.1 Enzymes

Crude dry solid SBP (E.C. 1.11.1.7, Industrial Grade lot #18541NX, RZ = 0.750, activity 5 U/mg) was purchased from Organic Technologies (Coshocton, OH). Catalase from bovine liver (CAS 9001-05-2, lot #SLBB1797V, activity 2000-5000 U/mg protein) was purchased from Sigma Chemical Company Inc. (Oakville, ON). Both SBP and catalase were stored at -15°C while the solutions prepared were stored in refrigerator at 4°C. Liquid ARP (*Arthromyces ramosus* peroxidase) concentrate (SP-502, activity 1200 U/mL) was purchased from Novzymes (Franklinton, NC) and stored in refrigerator at 4°C.

3.1.2 Enzyme substrates

Methyl Orange (MO) (85% pure), azobenzene (98% pure) and N,N-dimethyl-*p*-phenylenediamine (DMPD) (97% pure) were purchased from Sigma-Aldrich Chemical Company. *p*-Anisidine (>98% purity) and Direct Yellow 12 (DY12) were purchased from Tokyo Chemical Industry (TCI America, Woodrush Way, Portland, OR). Sulfanilic acid (SA) (>90% purity) was purchased from BDH Inc. (Toronto, ON).

3.1.3 Reagents

4-Amino-antipyrine (AAP) was purchased from BDH Inc., ammonium acetate (94% purity) HPLC-grade was obtained from Fluka Analytical (Oakville, ON). Their solutions were kept at room temperature. Hydrogen peroxide (30% w/v) was purchased from ACP Chemicals Inc. (Montreal, QC) and stored at 4°C.

3.1.4 Buffers and solvents

Analytical grade monobasic and dibasic sodium phosphates and hydrochloric acid were purchased from ACP Chemicals Inc. Sodium carbonate, sodium bicarbonate and citric acid were purchased from Sigma-Aldrich, and potassium chloride was purchased from Mallinckrodt Chemical Works (Montreal, QC). HPLC grade water was purchased from EMD Millipore Corporation (Billerica, US) and acetonitrile was purchased from ACP Chemicals Inc.

3.1.5 Others

Syringe filters (0.2 µm, non-sterile) were purchased from Sarstedt (Montreal, QC). 10 mL syringes were obtained from Fischer Scientific Company (Ottawa, ON). Pipettes of adjustable volumes of various sizes (200 µL, 1000 µL, 5000 µL) were purchased from Mandel Scientific (Guelph, ON). 1 mL screw-top HPLC vials were purchased from Waters Corporation (Mississauga, ON). Teflon coated magnetic stirrer bars of various sizes were obtained from Fischer Scientific Company. Pipette tips (100 µL-1000 µL) were purchased from VWR International Inc. (Mississauga, ON) and 5000 µL tips were purchased from Sarstedt. Corning 50 mL centrifuge tubes were purchased from Sarstedt, Inc.

3.2 Analytical and laboratory equipment

3.2.1 UV-VIS Spectrophotometry

An Agilent (Misissauga, ON) 8453 UV-Visible spectrophotometer (λ range of 190 -1100 nm and 1 nm resolution) controlled by a Hewlett Packard Vectra ES/12 computer was used to determine the maximum wavelength (λ_{max}) of substrate, to determine the enzyme activity and to determine the residual peroxide after the reaction. A quartz glass spectrophotometer

cuvette (1000 µL) with 10 mm light path type 104-QS was purchased from Hellma Analytics (Concord, ON).

3.2.2 Centrifuge and pH meter

Centrifugation was done using a Corning LSETM Compact Centrifuge (Tewksbury, MA) with a rotor for 6×50 mL and 6×15 mL centrifuge tubes and a maximum speed of 6000 rpm. pH was measured using an Oakton PC 700 benchtop meter (pH range 0 to 14.00, pH resolution 0.01, ± 0.01 pH accuracy), with an Orion pH electrode (9110DJWP, Ag/AgCl double junction, glass body, ceramic junction, precision 0.02) (Vernon Hills, IL). Calibration buffers at pH 4.00, 7.00 and 10.00 were purchased from ACP Chemicals Inc. while calibration buffer at pH 1.68 was purchased from Hanna Instruments (Laval, QC).

3.2.3 High Performance Liquid Chromatography (HPLC)

To analyze the concentration of aromatic compounds and to identify the reaction products, HPLC (Model 2487), from Waters Corporation (Oakville, ON), with a dual-wavelength absorbance detector (model 2489), binary HPLC pump (model 1525) and autosampler (model 717) operated by Breeze 3.3 software was used. A reverse-phase, Symmetry C18 column (5 µm, 4.6 × 150 mm) from Waters was used.

3.2.4 Other equipment

Other equipment used for the study include a vortex mixer Model K-550-G (50/60Hz, 0.5 Amp, 120 volts) purchased from Scientific Industries, Inc (Bohemia, NY), VWR magnetic stirrers VS-C10 (50-60 Hz, 30Watts) purchased from VWR International Inc. (Mississauga, ON) and analytical balance from A&D Company (San Jose, CA) with precision up to 0.1 mg was used.

3.2.5 Electrospray ionization (ESI) and atmospheric solids analysis probe (ASAP) mass spectrometry

After the enzymatic reaction, samples were analyzed using MS. Since there was no precipitate formation with MO and very light precipitates were formed for *p*-anisidine, the reaction mixtures were used for MS, without any centrifugation. For MO, measurements were completed in ESI(-) and ESI(+) sensitivity modes with 300 µL aliquots of the reaction mixtures following addition of 3 drops of acetonitrile. ASAP in positive sensitivity (ASAP(+)) mode was used for *p*-anisidine and the reaction mixture was used as such without the addition of acetonitrile. Appropriate standards in the respective modes were analyzed to determine the sample peak and any background interference. A high-resolution Waters Xevo G2-XS Time-of-Flight (ToF) mass spectrometer instrument (Oakville, ON) was used for the analysis. The instrument was operated by MassLynx 4.1 version software.

3.3 Analytical techniques

3.3.1 SBP activity determination

Enzyme activity was determined based on the 'Trinder type' assay formulated by Wu *et al*. 1998 according to which 1 unit of activity (U) is defined as the number of micromoles of H_2O_2 converted per minute at pH 7.4 at room temperature, in the assay conditions. The reagent consisted of 25 mg of 4-AAP, 5000 µL of 100 mM phenol in 0.5 mM sodium phosphate buffer at pH 7.4 and 100 µL of 100 mM H_2O_2 made up to 47.5 mL in a volumetric flask. The reagent (950 µL) was then vigorously added to a cuvette containing 50 µL of the enzyme at appropriate dilution so as to produce rapid mixing of the reagent and enzyme. For the SBP stock solution below, runs were conducted at 30, 40 and 50-fold dilution. The reaction proceeds as illustrated in Equation 5:

$$\text{4-AAP + Phenol + } H_2O_2 \xrightarrow{\text{SBP}} \text{pink chromophore } (\lambda_{max} = 510 \text{ nm}) \quad (6)$$

The mixture produces a pink chromophore at 510 nm having an extinction coefficient of 6000 $M^{-1}cm^{-1}$ based on peroxide. The rate of change of absorbance was measured by a UV spectrophotometer using the kinetics function in the software over a period of 30 seconds at intervals of 5 seconds. The change of absorbance should generally be between 0.1-0.2 AU. The detection limit for this activity is 0.1 U/mL. For detection of activities below 0.1 U/mL, the reagent should be concentrated 2- or 4-fold in order for samples larger than 50 uL to be monitored in the same final volume by the spectrophotometer. More information for SBP determination is given in Appendix B.

3.3.2 Enzyme stock solutions

The dry solid enzymes were kept closed at room temperature for 15 minutes before weighing. To prepare the solution, 1.4 g of solid SBP was mixed with 100 mL of distilled water in a conical flask and was gently stirred for 24 hours. The solution was then centrifuged for 25 minutes at 4000 rpm and the supernatant was stored at 4°C. Catalase solution was prepared by adding 0.1 g in 20 mL distilled water with gentle stirring for an hour and then stored at 4°C.

3.3.3 Product analysis by HPLC

In order to determine the residual concentration of the substrates after reaction, HPLC was used. The mobile phase consisted of aqueous phase (A) and organic phase (B) and their relative proportions are listed in Table 3.1. For all of these HPLC methods, an injection volume of 10 µL was used and column temperature was maintained at 30°C.

Table 3.1. HPLC protocol for substrates used in this thesis.

Substrate	Total flow (mL/min)	Phase A	Phase B	Ratio of solvent in A and B (%)		Wavelength (λ_{max})
p-Anisidine	1	Ammonium acetate (5mM)	Acetonitrile	70	30	279 nm (Isosbestic point)
DY12						401 nm
MO						465 nm (Isosbestic point)
SA	0.6			85	15	249 nm
DMPD	0.6			85	15	239 nm
Azobenzene	1	Formic acid (0.1%)		70	30	312 nm

3.3.4 Buffer preparation

Buffers were prepared in accordance with Gomori's method (Gomori 1955). pH 2.0-2.6 was prepared using hydrochloric acid-potassium chloride, pH 2.6-5.5 was prepared using citrate-phosphate buffer, pH 6.0-8.0 was prepared using monobasic-dibasic sodium phosphate buffer and higher pH 9.2-10.0 was prepared using sodium carbonate-bicarbonate buffer.

3.3.5 Batch reactor set-up

Batch reactors were set up in order to determine the degradation of the substrate. The components of each batch reactor included buffer, substrate, enzyme, hydrogen peroxide and water to make up the volume to 20 mL. Concentration of buffer was kept constant at 40 mM for all the experiments. Varied concentrations of hydrogen peroxide and enzyme were used to determine the optimum conditions for substrate degradation. The initial concentration of *p*-anisidine in the batch reactors was 1.0 mM. For MO, chrysophenine,

SA and DMPD, the initial concentrations were 0.50 mM while for azobenzene, it was kept low as 0.125 mM due to solubility issues. The components were mixed uniformly for 3 hours by inserting Teflon-coated magnetic stirrer bars in all the batch reactors and then kept on magnetic stirrer plates at room temperature of 22±3°C. At the end of 3 hours, the reaction was stopped by quenching with excess catalase (to 50 U/mL) that decomposes hydrogen peroxide into water and oxygen, which consequently ends the reaction. The product mixture was filtered using a 0.2 micron filter and then analyzed by HPLC. All experiments, unless otherwise stated, were performed in triplicate. Average values of these results have been shown in the graphs with standard deviations denoted by error bars. Control reactions were set up for all reaction conditions with no hydrogen peroxide or no SBP.

3.3.6 Product determination using mass spectrometry

MS was used to identify the products formed after the enzymatic treatment of the substrates. Standards of the samples were prepared in appropriate buffers. Batch reactions were performed following the protocol mentioned in section 3.3.5 at optimized conditions for each of the substrates. However, buffer concentration was kept low at 10 mM (compared to 40 mM) for *p*-anisidine and 5 mM for MO to avoid interference in MS analysis. At the end of three hours, quenched reaction mixtures were taken for analysis. Very light precipitates were observed for *p*-anisidine which could not be separated while no precipitate was observed in the case of MO, SA and DMPD. Therefore, for all the compounds, the solutions/suspensions were directly used for MS. The ASAP technique was used for *p*-anisidine while ESI was used for MO since the latter was not detectable by the ASAP mode.

3.3.7 Sources of error

Since enzyme activity depends on several factors, such as temperature, reagent stability and mixing, it was performed every day for consistent results. Analytical instruments such as pH meter, pipettors and analytical balance, were calibrated and monitored regularly. All tests were performed in triplicate and error in the observations have been denoted as error bars in all the graphs. Room temperature was tracked regularly as 22±3°C. Light-sensitive samples were kept in the dark during preparation and during the reaction to minimize degradation due to light.

CHAPTER 4: RESULTS AND DISCUSSION

4.1 Optimization of pH

Enzymatic activity of SBP is dependent on pH (Kamal and Behere 2002). Alteration in pH may affect the state of ionization of enzyme, substrate, and/or intermediates formed in the reaction or produce changes in the conformational state of the enzyme (Stenesh 1993). An important catalytic residue of enzyme, distal histidine-42, should be in deprotonated form, to act as catalytic base and arginine-38 should be in protonated form, to act as charge stabilizer. The pH at which ionization states of both arginine and histidine are appropriate, strongly influences the optimum pH of the enzyme (Al-Ansari *et al*. 2011).

For example, pH 6.0 has been found to be the optimal pH for maximum activity of SBP within range of 2.2 to 8.0, using guaiacol to measure the activity (Geng *et al*. 2001) while Sessa and Anderson (1981) reported pH 5.5 to be the optimum for guaiacol within range of 4.0-8.0; a decrease of 20% in activity was observed at pH 4.6 and 6.7. Similar results have been reported by Ghaemmaghami *et al*. (2010) in the range of 2.2 to 10.0 using 4-AAP to determine SBP activity.

pH optimization for *p*-anisidine and MO was performed from pH 3.0 to10.0 based on UV-VIS spectrophotometric measurement at the respective maximum wavelengths. For *p*-anisidine, the maximum wavelength was 232 nm in water, but the extinction coefficient was different in different buffers. Hence, an isosbestic point, 279 nm, was used to achieve same extinction coefficient in all the buffers. For MO, the isosbestic point was at 465 nm. Hence, the calibration curve was plotted at this wavelength. Calibration curves using HPLC are shown in Appendix C.

A stringent enzyme concentration was used so that the effect of pH on substrate degradation can be ascertained clearly. SBP activity of 0.00070 U/mL was used for 1 mM *p*-anisidine and 0.0070 U/mL was used for 0.50 mM MO. H_2O_2 was maintained at sufficient concentration of 0.75 mM for both *p*-anisidine and MO. Figures 4.1 and 4.2 show the amount of substrate remaining under these conditions for *p*-anisidine and MO, respectively. Standard deviations of triplicates are plotted as error bars in the graphs, most not seen because the errors are smaller than the symbol. Controls were set up with no SBP and no peroxide so that the entire removal could be attributed to the enzymatic reaction.

pH 5.5 was observed to be the optimum pH for degradation of *p*-anisidine (pK_a 5.36, Lide 2007). Removal at pH 5.0, 5.5 and 6.5 were comparable, with a difference of only 2% among these three pHs. Similar results have been reported for other anilines as well. Mazloum *et al*. (2015) observed 5.0 to be the optimal pH for removal of aniline (pK_a=4.6) and *o*-anisidine (pK_a=4.5). For *p*-cresidine (2-methoxy-5-methylaniline), Mukherjee *et al*. (2018) observed optimum pH of 4.6, quite close to the pK_a of 4.7 for the compound. Phenylenediamines showed maximum conversion in the pH range of 4.5-5.6 (Al Ansari *et al*. 2009). Most anilines have shown pH optima in the acidic region, in contrast to the basic region, possibly due to a decrease in the catalytic efficiency of enzyme and ionization changes of catalytic residues at higher pH values (Al Ansari *et al*. 2009, Zhang 2019). Similarly, for 2,4-dichlorophenol, no conversion could be observed at pH 3.0 and above 8.0. At pH values above 8.0 and below 3.0, SBP is subject to denaturation. However, the denaturation is more rapid in basic solutions than in acidic solutions (Kennedy *et al*. 2002).

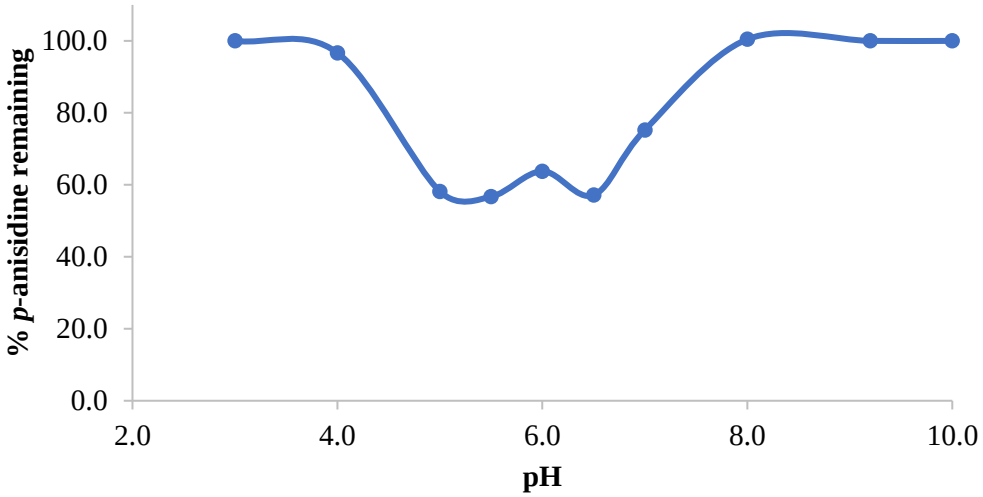

Figure 4.1. Effect of pH on removal of *p*-anisidine. Conditions: 1.0 mM *p*-anisidine; 0.00070 U/mL SBP; 0.75 mM H_2O_2; 40 mM buffer; and 3-h reaction; room temperature, triplicate measurements, standard deviation plotted as error bars.

For MO, pH 4.0 showed maximum removal using 0.0030 U/mL SBP (Figure 4.2). An increase of 18% in conversion was observed at this pH on increasing enzyme concentration to 0.0070 U/mL. The catalytic cycle of SBP is favored at acidic pH since the formation of compound I (Reaction 1) (Section 2.4.2) is dependent on the hydrogen bond between the heme group/H_2O_2 with the catalytic residues: distal histidine-42 (proton acceptor from H_2O_2) and distal arginine-38 (charge stabilizer), while Reactions 2 and 3 are dependent on oxidation state of the substrate (Kalsoom *et al*. 2013, Mukherjee 2019).

Other studies for removal of dyes using SBP have shown similar results. Chiong *et al*. (2016) observed pH 5.0 to show maximum decolourization for 0.015 mM MO. Kalsoom *et al*. (2013) also found maximum decolourization of Trypan Blue at pH 4.0, however, pH 3.0 also showed similar conversion.

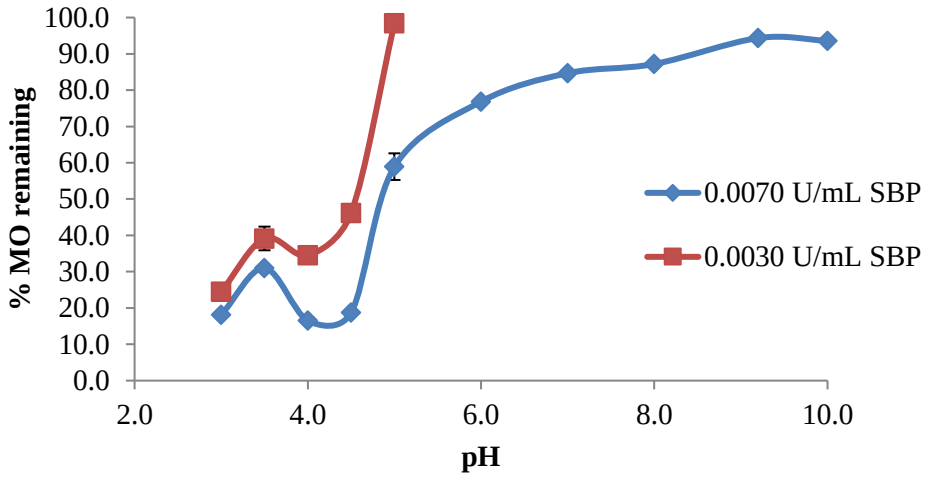

Figure 4.2. Effect of pH on removal of MO. Conditions: 0.50 mM MO; 0.0030 and 0.0070 U/mL SBP; 0.75 mM H_2O_2; 40 mM buffer; and 3-h reaction; room temperature, triplicate measurements, standard deviation plotted as error bars.

Cordova Villegas (2018) decolourized azo dyes, Acid Blue 113 and Direct Black 38 using SBP and observed maximum decolourization at pHs of 4.0 and 3.6, respectively. Miranda-Mandujano *et al.* (2018) observed pH 5.5 to be the optimum for removal of 60 mg/L (0.072 mM) Direct Blue 2, an azo-dye, using SBP. Hence, degradation of azo-dyes using SBP is favored at acidic pH values. The optimum pHs found in this part were used to carry out further optimization experiments.

4.2 Optimization of hydrogen peroxide-to-substrate concentration ratio

Hydrogen peroxide acts a co-substrate to initiate the enzymatic reaction. At low H_2O_2 concentration, the performance of enzyme decreases, while excess H_2O_2 concentrations lead to reaction inhibition. Hence, optimization of H_2O_2 is a crucial factor (Al-Ansari *et al*. 2011, Silva *et al*. 2013, Fernandes *et al*. 2020). Theoretically, one mole of H_2O_2 should oxidize two moles of the substrate and hence the ratio of H_2O_2/substrate should be 0.5.

However, due to formation of dimers and higher oligomers, the ratio approaches 1 or even higher sometimes due to endogenous catalase activity (Ibrahim *et al*. 2001, Mazloum *et al*. 2015, Mukherjee 2019).

More enzyme, 0.0016 U/mL was used than in Figure 4.1 to obtain the results shown in Figure 4.3. The highest conversion of 92% was observed at 1.0 mM H_2O_2 however *p*-anisidine conversion reduced by 18% as H_2O_2 concentration was increased from 1.0 mM to 2.0 mM, shows that H_2O_2 can inhibit the enzymatic activity by causing enzyme inactivation. Thus, the demand of H_2O_2 exceeds the theoretical requirement for higher conversion of *p*-anisidine to the dimer. This is attributed to the formation of soluble higher oligomers during the enzymatic reaction which further act as substrates for SBP and re-enter the enzymatic cycle (Yu *et al*. 1994).

Similar results have been reported for the conversion of anilines and phenols in the past. Caza *et al*. (1994) observed ratios of 1 for removal of *m*-cresol using SBP. Zhang (2019) found a similar trend for removal of Ioxynil wherein conversion efficiency increased as molar ratios of H_2O_2/substrate were increased from 0.5 to 1 and decreased as the ratio reached 3. Hence, 0.1 mM H_2O_2 was the optimum concentration for conversion of 0.1 mM Ioxynil.

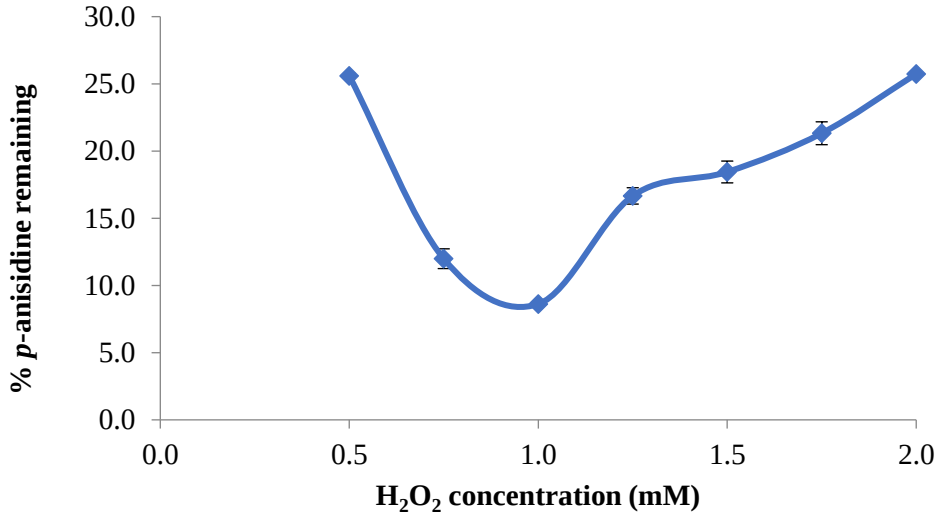

Figure 4.3. Effect of hydrogen peroxide concentration on removal of *p*-anisidine. Conditions: 1.0 mM *p*-anisidine; 0.0016 U/mL SBP; 40 mM pH 5.5 buffer; and 3-h reaction; room temperature, triplicate measurements, standard deviation plotted as error bars.

H_2O_2 optimization for MO is shown in Figure 4.4. Removal of 98% was observed using 1.0 mM H_2O_2 for 0.50 mM substrate. The molar ratio of H_2O_2 to substrate is 2, well above the ratio of 1 for *p*-anisidine. This could be due to the H_2O_2 requirement of the products of azo-bond cleavage of MO. A further increase in H_2O_2 concentration to 2.0 mM reduced the removal to 96%. This is not surprising since H_2O_2 is a co-substrate of the enzyme and hence excess H_2O_2 would not lead to inhibition of enzymatic activity in the presence of limited substrate (Dunford 1999, Kalsoom *et al*. 2013, Silva *et al*. 2013). At 0.50 mM H_2O_2, only 70% removal of MO was observed.

Chiong *et al*. (2016) reported 81% decolourization of (0.09 mM or 30 mg/L) MO at H_2O_2 concentration of 2.0 mM. Cordova Villegas (2017) optimally decolourized 97% of 0.50 mM Direct Black 38 at pH 3.6 using 3 U/mL SBP and 2.5 mM H_2O_2. In the same study, for 1.0 mM Acid Blue 113, 91% and 86% decolourization was achieved at pH 4.0 and 4.6,

respectively, using 2.5 mM H_2O_2. Treatment of 40 mg/L (0.06 mM) Remazol Brilliant Blue R by Silva *et al*. (2013) showed 86% decolourization at pH 7.0 using 200 µM H_2O_2. Stepwise addition of H_2O_2 did not result in any significant improvement in decolourization of the dye in contrast to the findings of Kalsoom *et al*. (2013) wherein degradation of 10 ppm (10 µM) Trypan Blue increased from 60 to 75% on stepwise addition of 64 µM H_2O_2. Thus, for enzymatic conversion of azo dyes H_2O_2/substrate ratios of ≥ 2 seem to be the norm.

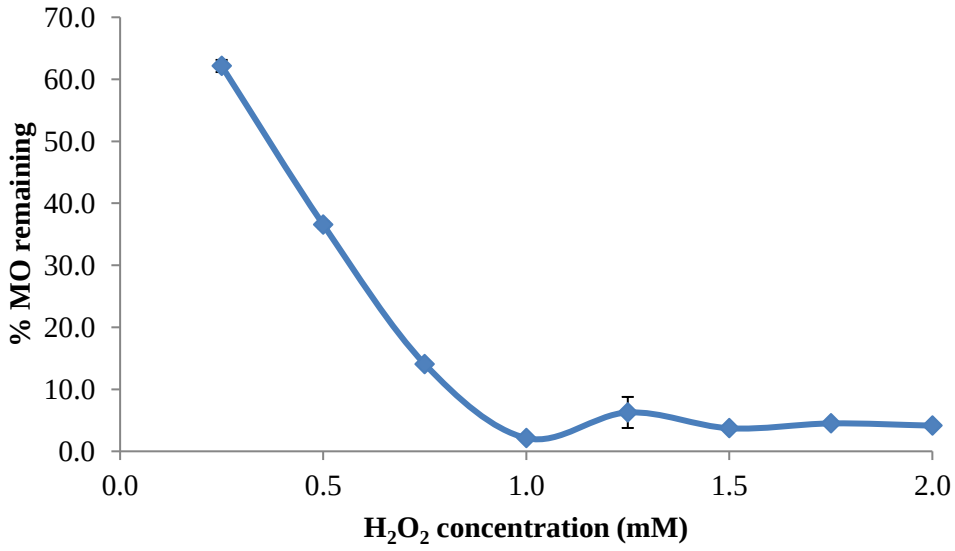

Figure 4.4. Effect of hydrogen peroxide concentration on removal of MO. Conditions: 0.50 mM MO; 0.0070 U/mL SBP; 40 mM pH 4.0 buffer; and 3-h reaction; room temperature, triplicate measurements, standard deviation plotted as error bars.

4.3 Minimum effective SBP

Cost of enzyme is an important parameter that needs consideration for practical applications of enzymatic process in wastewater treatment. Hence, SBP optimization was done to determine the minimum effective concentration of enzyme required for ≥95% removal of *p*-anisidine using optimized pHs and H_2O_2 concentrations.

For *p*-anisidine, Figure 4.5, the minimum effective enzyme for achieving ≥95% removal was observed to be 0.0018 U/mL. *o*-Anisidine (1.0 mM) required 7-fold more SBP for 95% removal at pH 5.0 and 1.5 mM H_2O_2 (Mazloum *et al*. 2015). *p*-Cresidine (1.0 mM), that has a similar structure as *p*-anisidine, required 6-fold more SBP at pH 4.6 and 1.25 mM H_2O_2 (Mukherjee *et al*. 2018).

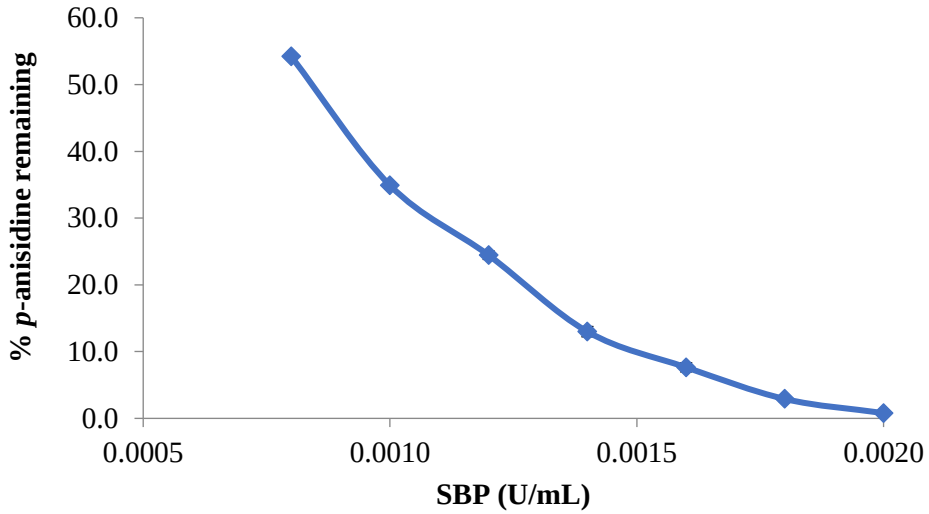

Figure 4.5. SBP optimization for removal of *p*-anisidine. Conditions: 1.0 mM *p*-anisidine; 1.0 mM H_2O_2; 40 mM pH 5.5 buffer; and 3-h reaction; room temperature, triplicate measurements, standard deviation plotted as error bars.

For MO, 0.0070 U/mL was the minimum enzyme required for ≥95% of the dye as demonstrated in Figure 4.6. This enzyme requirement is very low compared to the results achieved by previous researchers for treatment of dyes using SBP. Chiong *et al*. (2016) used 0.186 U/mL (0.5 mL of 0.373 U/mL) SBP (using guaiacol to measure SBP activity) for decolourization of 0.09 mM (30 mg/L) of MO at pH 5.0 and 2 mM H_2O_2 in a one-hour reaction. Cordova Villegas (2017) achieved 98% decolourization of 0.50 mM DB38 using 3.0 U/mL SBP at pH 3.6 and 2.5 mM H_2O_2 while for 1.0 mM AB113, 97% decolourization

was achieved at pH 4.0, 2.5 mM H_2O_2 and 1.5 U/mL SBP during a 3-hour reaction. Higher enzyme requirements for AB113 and DB38 could be attributed to the complex structure of these dyes in contrast to MO (which has no phenolic or primary-amino functional groups) and also to higher substrate concentration in case of AB113. Thus, to our knowledge, MO has the lowest enzyme requirement, relative to its concentration, of those reported.

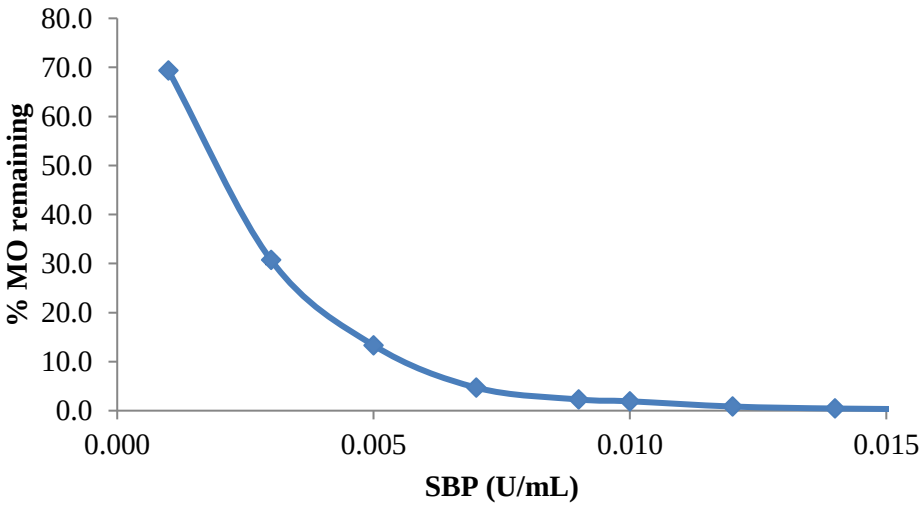

Figure 4.6. SBP optimization for removal of MO. Conditions: 0.50 mM MO; 1.0 mM H_2O_2; 40 mM pH 4.0 buffer; and 3-h reaction; room temperature, triplicate measurements, standard deviation plotted as error bars.

4.4 Summary of optimization experiments

Table 4.1 displays the optimized values for pH, H_2O_2 concentration and SBP activity for achieving ≥95% removal of the substrates.

Table 4.1. Optimized parameters for ≥95% removal of substrates.

Substrate	pH	H_2O_2/substrate (molar ratio)	SBP activity (U/mL)
p-Anisidine (1.0 mM)	5.5	1	0.0018
MO (0.50 mM)	4.0	2	0.0070

4.5 Time course study

Time course study is vital for industrial applications of the treatment process, since it governs the reactor volume which ultimately determines capital and operating costs of the process. Reaction time in the preceding work was chosen as 3 hours, to be consistent with the previous studies done. For the time courses, reactions were done in 125 mL Erlenmeyer flask at the optimum conditions for MO and *p*-anisidine. Aliquots of 6 mL were drawn at intervals and quenched with sufficient catalase to stop the reaction and then analyzed using HPLC.

Rate of enzymatic reaction should be directly dependent on the enzyme concentration. As the reaction proceeds, it decreases, possibly due to inactivation of the enzyme (Section 2.4.3) directly and/or due to the formation of oligomers or reactive radicals. Assuming enzyme to be constant during the initial few minutes of the reaction and the fractional change in [peroxide] to be small, the rate of reaction is dependent only on the substrate concentration. Hence, it is considered to be a pseudo-first-order reaction (Malik Altahir *et al.* 2015). Percent remaining for *p*-anisidine and MO were plotted as a function of time as shown in Figures 4.7 and 4.8, respectively. Rate constants and half-lives were calculated using the integrated first-order rate equation (Equations 6 and 7).

$$C = C_0 e^{-kt} \quad (7)$$

$$t_{1/2} = 0.693/k \quad (8)$$

where k denotes rate constant, $t_{1/2}$ denotes half-life and C_0 and C denote initial and final concentrations, respectively.

For quantitative analysis, the first 3 minutes of the reaction have been fitted to the first-order model. Rate constants and half-lives for *p*-anisidine and MO are given in Table 4.2.

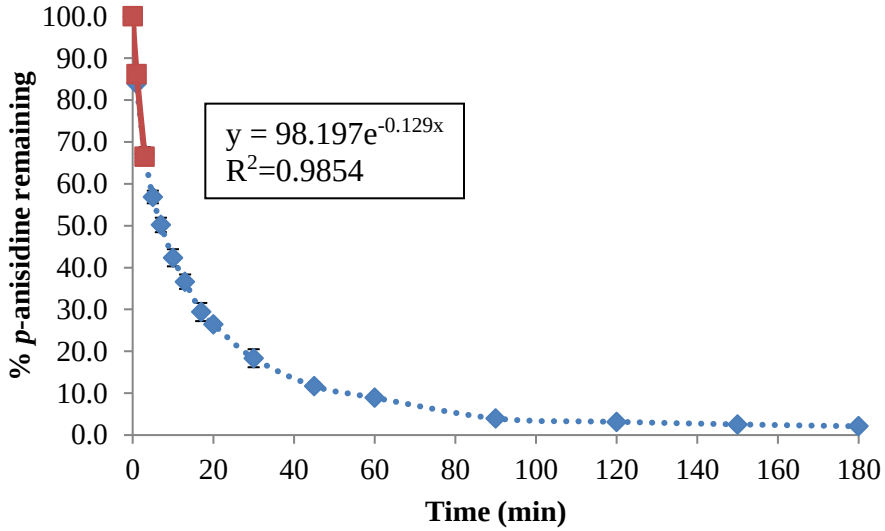

Figure 4.7. Removal of *p*-anisidine with respect to time. Conditions: 1.0 mM *p*-anisidine; 1.0 mM H_2O_2; 40 mM pH 5.5 buffer; and 0.0018 U/mL SBP; room temperature, triplicate measurements, standard deviation plotted as error bars. Blue dashed line represents experimental data and red line represents curve obtained by non-linear regression fitting of first-order reaction equation.

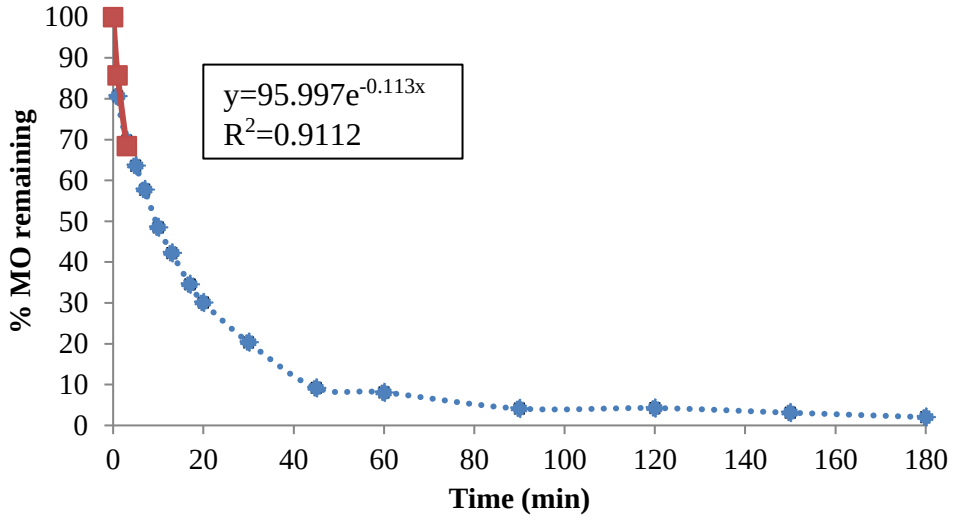

Figure 4.8. Removal of MO with respect to time. Conditions: 0.50 mM MO; 1.0 mM H_2O_2; 40 mM pH 4.0 buffer; and 0.0070 U/mL SBP; room temperature, triplicate measurements, standard deviation plotted as error bars. Blue dashed line represents experimental data and red line represents curve obtained by non-linear regression fitting of first-order reaction equation.

For *p*-anisidine, 70% degradation was achieved in first 17 minutes while 95% degradation was achieved in 90 minutes. For MO, 70% degradation occurred in first 20 minutes of the reaction and 95% removal was observed in 120 minutes. It has been observed in previous studies also that the initial rate of reaction is rapid and it slows as the reaction proceeds. Zhang (2019) observed 74.2% conversion of Bromoxynil in the first 15 minutes of reaction using SBP while for Ioxynil, 74.7% conversion was achieved in 1 minute. Rate constants and half-lives were normalized on the basis of enzymatic activity. These are summarized in Table 4.2.

Table 4.2. Rate constants and half-lives of substrates determined from time-course experiments.

Substrate	Rate constant (min^{-1})	Half-life (min)	Normalized rate constant (min^{-1})	Normalized half-life (min)
p-Anisidine (1.0 mM)	0.13±0.02	5.46±0.84	72±8	0.0097±0.0011
MO (0.50 mM)	0.113±0.035	6.783±2.101	16.1±5.0	0.0476±0.0148

4.6 Mass spectrometry results

Enzymatic reaction of anilines results in the formation of dimers and higher oligomers that precipitate out of the reaction and can eventually be separated by sedimentation/filtration. When SBP reacts with anilines, it results in the formation of free radicals which couple non-enzymatically with C-C, N-N or N-C and *ortho*- and *para*-orientations (Mukherjee 2019). It should be noted here that MS can only suggest probable isomers generated during the enzymatic treatment and cannot be used to determine exact structure of the isomers. For further information about type of coupling, Fourier-transform infrared spectroscopy (FTIR) and nuclear magnetic resonance (NMR) techniques can provide further insight. Structures of probable isomers formed can be interpreted from the molecular formula generated by MassLynx software from high-resolution m/z values within a range of ±5 ppm and ±3 mDa.

ASAP in positive-ion mode (ASAP(+)) was used for product identification of the *p*-anisidine reaction. ESI in both positive-ion (ESI(+)) and negative-ion (ESI(-)) modes was used for MO. ESI(+) was used for DMPD and ESI(-) was used for SA. Appropriate standards were prepared for each of the compounds and analyzed in their respective modes. Reaction solutions/suspensions for both *p*-anisidine and MO, were used as such, without

centrifugation since very light indistinguishable precipitates were observed with *p*-anisidine, while no precipitates were observed in the MO reaction mixture.

Peaks observed in positive-ion mode MS usually have m/z values as the protonated compounds however, in some standards and reaction mixtures, peaks corresponding to both cation radical (simple loss of an electron) and protonated compound have been detected. Symbolism used in MS results presented in this thesis are described here: M is used to denote the standard compound. MH denotes the protonated standard. MHNa denotes protonated standard with a sodium ion (for sulfonate salts). M_2H-2 denotes protonated oxidative dimer and M_2H-4 represents an azo-dimer referred to as the protonated oxidized oxidative dimer. M_3H-4 denotes protonated oxidative trimer. Symbols such as M_3H-4-OCH_2 denote an oxidative trimer that has endured loss of -OCH_2 group. Possible structures corresponding to each of the m/z values (drawn as the parent compounds, not their protonated forms) are shown along with their respective mass spectra. As mentioned earlier, these structures do not denote the exact structures of the compounds and, hence, are just one of the probable isomers.

Carbon and sulphur with isotopes ^{13}C and ^{34}S having relative abundance of 1.07% and 4.25%, respectively, have been correspondingly found in each of the mass spectra (unless noted, the relative intensities of these isotopes compared to the main peak were consistent with expectation). The value at top-right corner of the spectra show the intensity of the signal at which the scan was captured. Values typically between e^4 and e^5 are considered to be of good intensity.

4.6.1 MS for *p*-anisidine standard

For *p*-anisidine (C_7H_9NO), base peak for protonated standard MH with m/z value, 124.0775 is shown in Figure 4.9 with its ^{13}C isotope having m/z value of 125.0789.

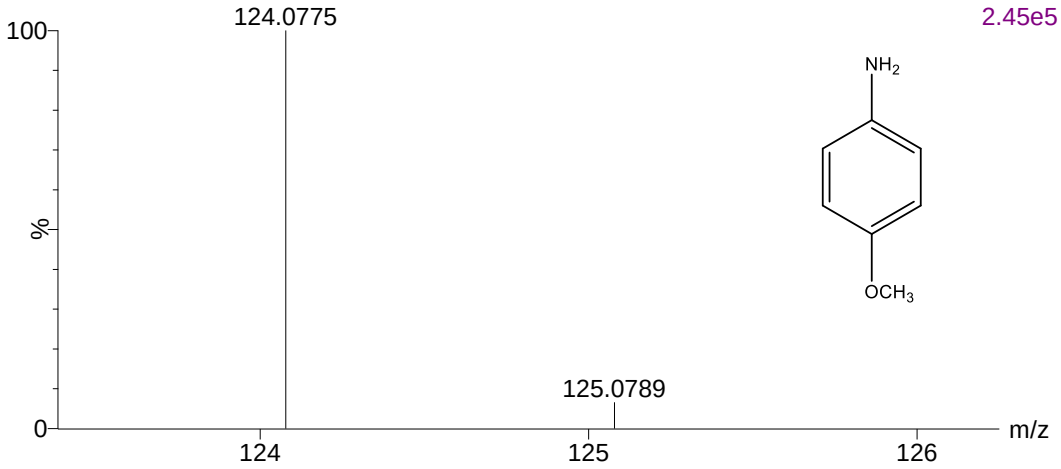

Figure 4.9. ASAP-MS(+) of *p*-anisidine protonated standard with molecular formula, $C_7H_{10}NO$ (MH, m/z=124.0753).

4.6.2 MS for *p*-anisidine reaction mixture

The full-range scan of the enzymatic reaction products of *p*-anisidine is shown in Figure 4.10. This spectrum shows the presence of residual monomer, dimer and other oligomers in the reaction mixture, as illustrated in expanded m/z-scale scans in Figures 4.11 to 4.14. A peak at m/z value of 124.0801 and a ^{13}C peak at 125.0825 in Figure 4.10 show the presence of residual *p*-anisidine monomer after the reaction, since the reaction was run to ≥95% removal, the monomer peak shows the residual 5% *p*-anisidine after 3-h reaction. Protonated azo-dimer (M_2H-4) having molecular formula $C_{14}H_{15}N_2O_2$, with m/z value of 243.1134 is detected in reaction product as shown in Figure 4.11, arbitrarily drawn with a *trans*-bond, and its ^{13}C peak at m/z value of 244.1166. Similar azo-coupled dimers were reported by Mukherjee *et al.* (2018) for *p*-cresidine. A trimer with formula $C_{21}H_{24}N_3O_3$

consistent with M_3H-4, having m/z value of 366.1795 is also detected as shown in Figure 4.12 (arbitrarily drawn with C,N-coupling). Existence of this trimer means that there must have been some non-N,N-coupled dimer as a precursor.

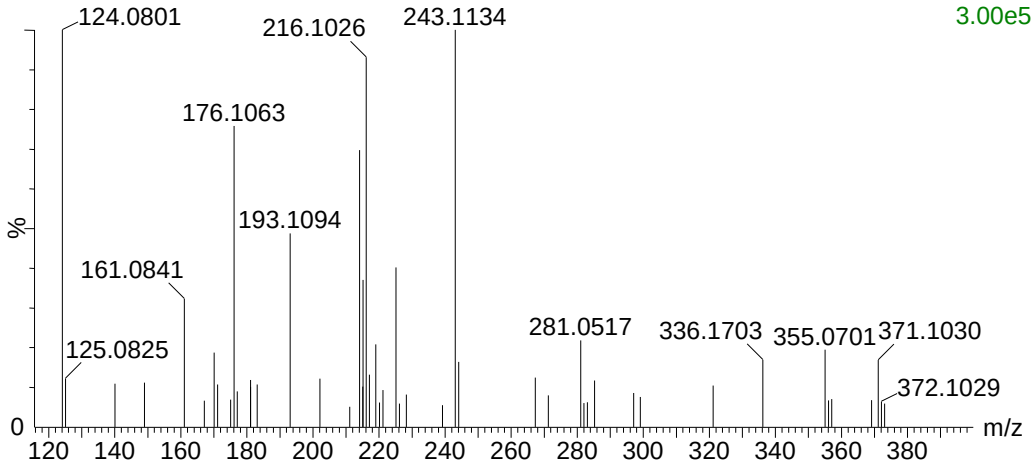

Figure 4.10. ASAP-MS(+) of full-range scan of *p*-anisidine reaction mixture. Conditions: 1.0 mM *p*-anisidine; 1 mM H_2O_2; 40 mM pH 5.5 buffer; 0.0018 U/mL SBP and 3-h reaction.

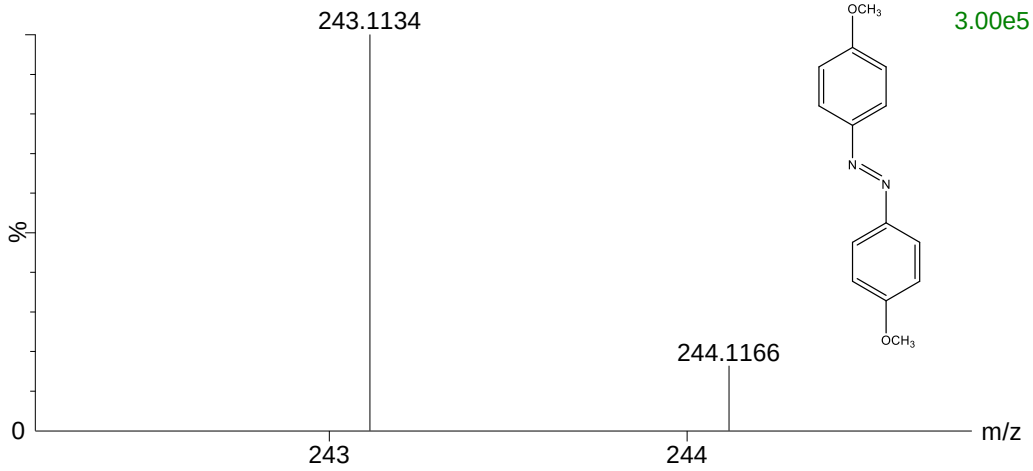

Figure 4.11. ASAP-MS(+) of protonated azo-dimer of *p*-anisidine in reaction mixture supernatant with molecular formula, $C_{14}H_{15}N_2O_2$ (M_2H-4, m/z=243.1132). Conditions: as for Figure 4.10.

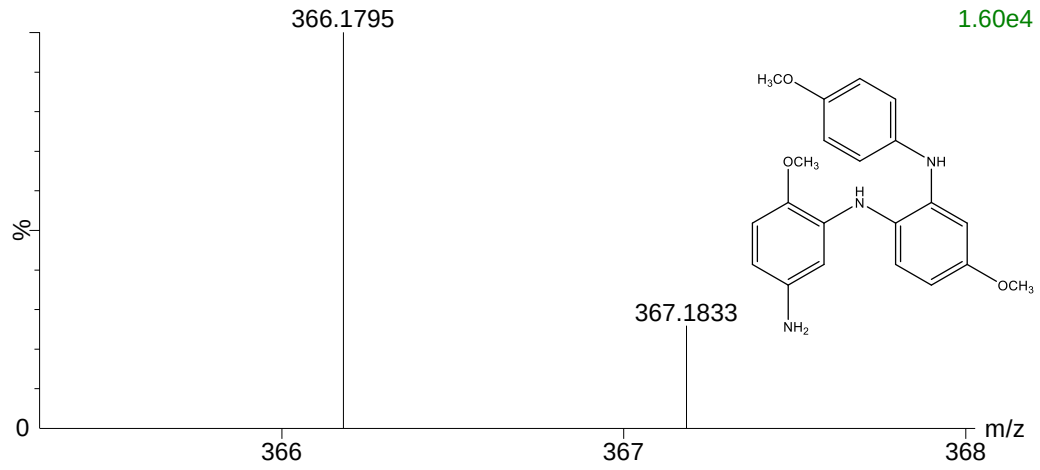

Figure 4.12. ASAP-MS(+) of protonated oxidative trimer of *p*-anisidine in reaction mixture supernatant with molecular formula, $C_{21}H_{24}N_3O_3$ (M_3H-4, m/z=366.1795). Conditions: as for Figure 4.10.

A peak with m/z value of 336.1703 is detected with molecular formula as $C_{20}H_{22}N_3O_2$, as shown in Figure 4.13 along with the peak of its ^{13}C-isomer. This peak corresponds to M_3H-4-OCH_2. Another peak with m/z value of 371.1030 and its ^{13}C-isomer at m/z, 372.1029 correspond to a $C_{22}H_{18}N_3O_3$ protonated oligomer, represented as M_3H-10+C, with a hypothetical molecular structure shown in Figure 4.14.

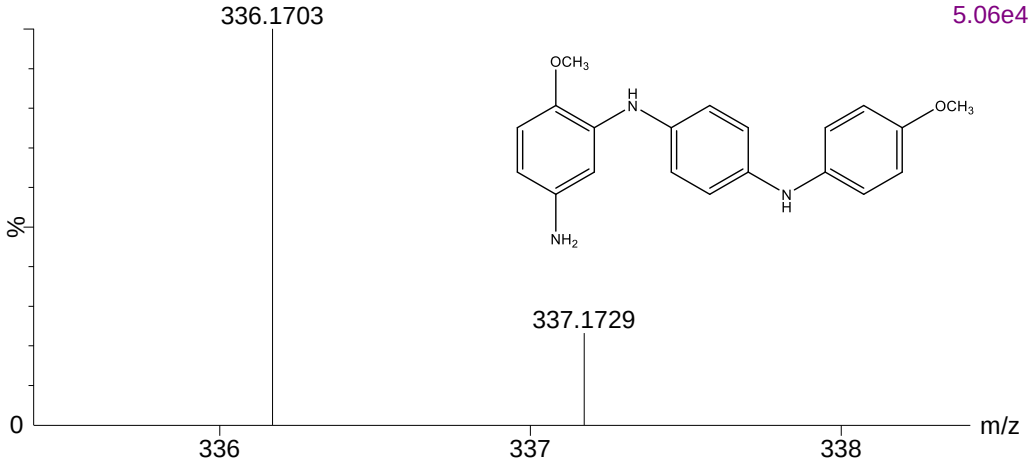

Figure 4.13. ASAP-MS(+) of oligomer of *p*-anisidine in reaction mixture supernatant with molecular formula, $C_{20}H_{22}N_3O_2$ (M_3H-4-OCH_2, m/z=336.1703). Conditions: as for Figure 4.10.

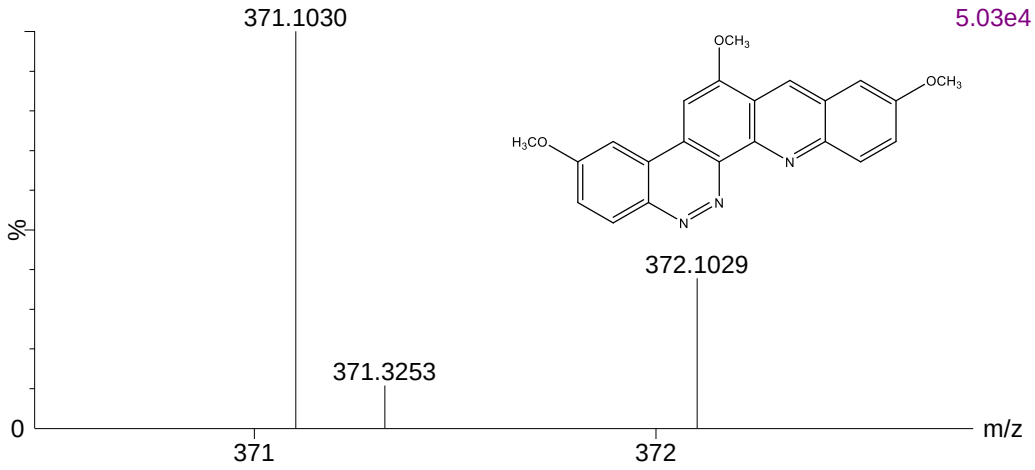

Figure 4.14. ASAP-MS(+) of oligomer of *p*-anisidine in reaction mixture supernatant with molecular formula, $C_{22}H_{18}N_3O_3$ (M_3H-10+C, m/z=371.1030). Conditions: as for Figure 4.10.

4.6.3 MS for MO, SA and DMPD standards

MS for MO standard was done in both ESI(+) and ESI(-) modes. Figure 4.15 shows the mass spectrum in positive-ion mode for protonated standard of MO (M_aHNa; the sub-script a used here is used to distinguish this parent-ion from those SA and DMPD, below), with m/z value of 328.0728. This m/z value corresponds to molecular formula of $C_{14}H_{15}N_3SO_3Na$. Peaks for ^{13}C and ^{34}S isotopes with m/z values of 329.0754 and 330.0722, respectively can be clearly seen in the spectrum. A fragmentation product of MO with m/z value of 306.0913, corresponding to molecular formula of $C_{14}H_{16}N_3O_3S$ is detected (Figure 4.16). This corresponds to M_aH_2. This suggests that Na can be lost and the acid detected by MS. Peaks for ^{13}C and ^{34}S isotopes with exact masses of 307.0946 and 308.0908, respectively are also seen.

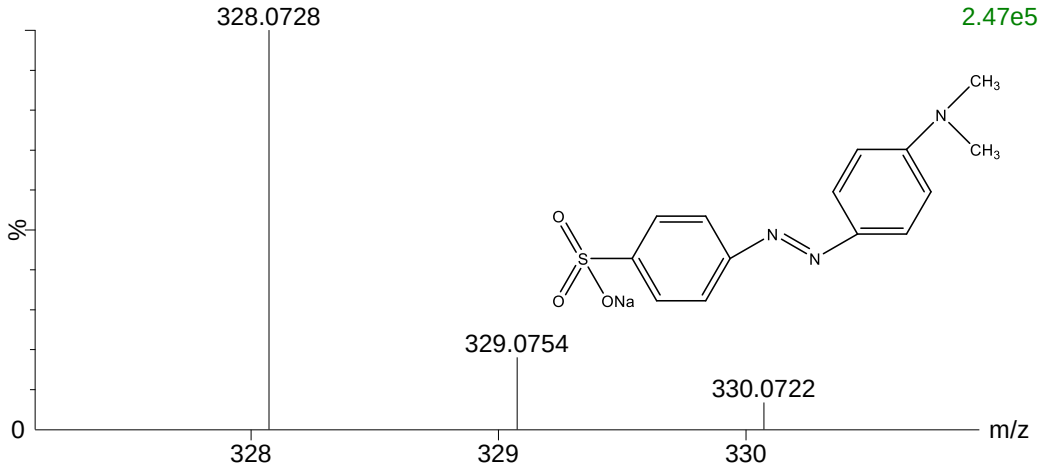

Figure 4.15. ESI-MS(+) of MO protonated standard with molecular formula, $C_{14}H_{15}N_3SO_3Na$ (M_aHNa, m/z=328.0728).

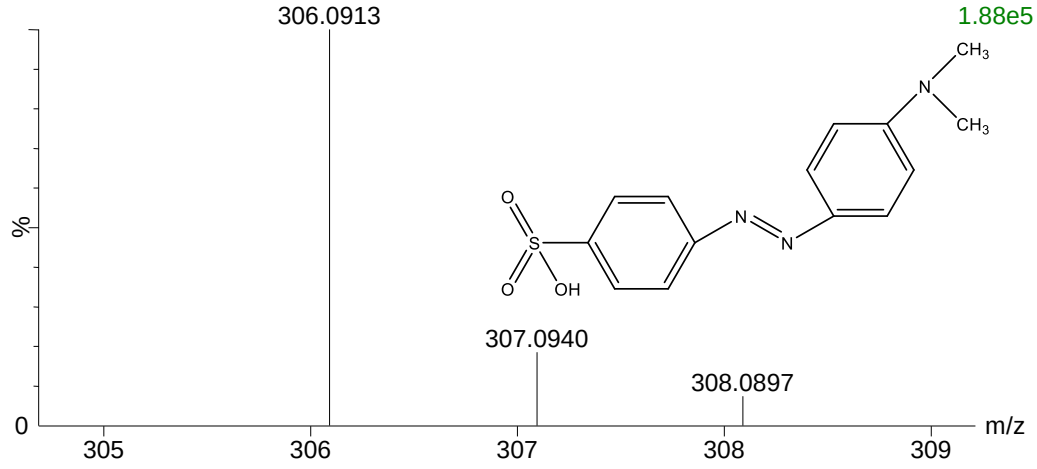

Figure 4.16. ESI-MS(+) of MO protonated standard with molecular formula, $C_{14}H_{16}N_3SO_3$ (MaH_2, m/z=306.0913).

MO in ESI(-) corresponds to m/z value of 304.0753, with ^{13}C and ^{34}S isotopes at m/z values of 305.0781 and 306.0730, respectively, with molecular formula as $C_{14}H_{14}N_3SO_3$ (M_a) (Figure 4.17). This represents MO sulfonate without Na since the analysis is done in negative mode. Fragmentation products for MO standard are also observed. Figure 4.18 shows m/z value of 289.0509, corresponding to molecular formula, $C_{13}H_{11}N_3SO_3$ (M_a-CH_3 or M_aH- CH_2). The ^{13}C peak in this mass spectrum is higher than expected, which could be

because of overlapping of peaks. Another peak is detected at m/z, 240.1137, corresponding to $C_{14}H_{14}N_3O$ (M_a-SO_2 or M_a-SO_3+O) (Figure 4.19). The structure pertaining to this molecular is also shown. The compound is clearly oxygenated but since the position of oxygen cannot be ascertained clearly, it is shown in a generic way in the structure. Previous studies conducted by Mashaddi *et al*. (2019) for MS analysis of indole and HOBT have also reported addition of oxygen in the MS environment. Similar peaks were detected for MO standard and its fragmentation products by Baiochhi *et al*. (2002) at m/z values of 304, 289.2, 240.3 and 156.2 using MS/MS and MS/MS/MS analyses in ESI(-). Chen *et al*. (2008) used MS/MS analysis for MO standard and also observed peaks at m/z ratios of 304.2 289.0, 240.2 and 156.1, suggesting that MO can easily lose a methyl group and -SO_2 group because of its tendency to exist as odd-electron species instead of neutral molecules. The peak at m/z value of 156 could not be detected in this work, probably because in ESI-MS, the compound is subjected to less fragmentation as compared to other techniques (Section 2.9).

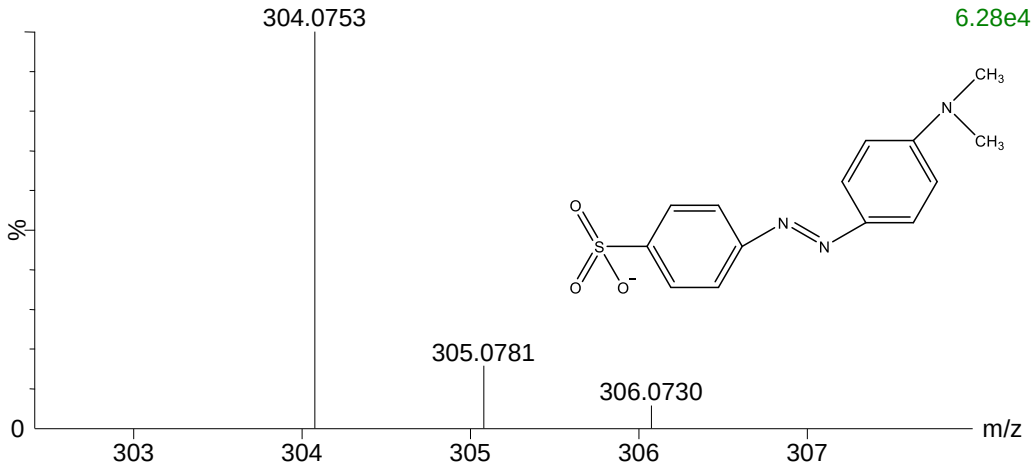

Figure 4.17. ESI-MS(-) of MO standard with molecular formula, $C_{14}H_{14}N_3SO_3$ (M_a, m/z=304.0753).

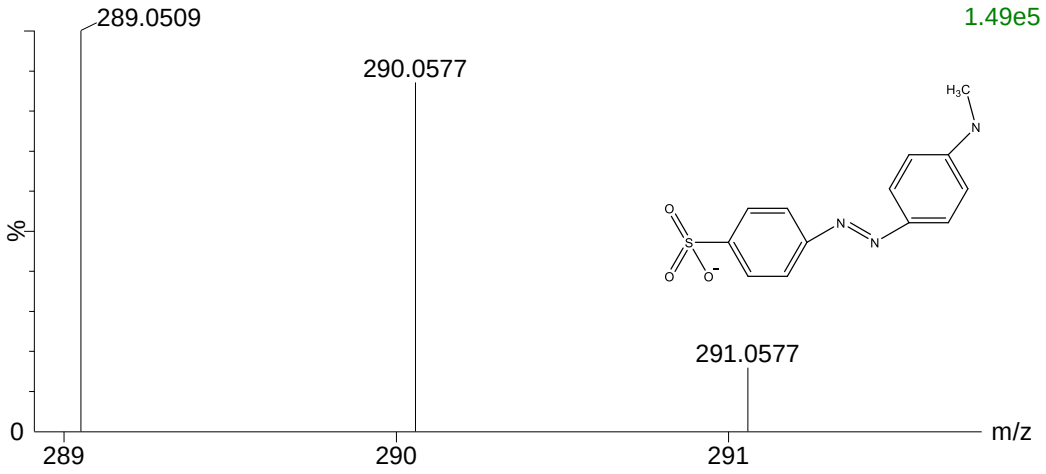

Figure 4.18. ESI-MS(-) of MO fragmentation product of standard with molecular formula, $C_{13}H_{11}N_3SO_3$ (M_a-CH_3, m/z=289.0509).

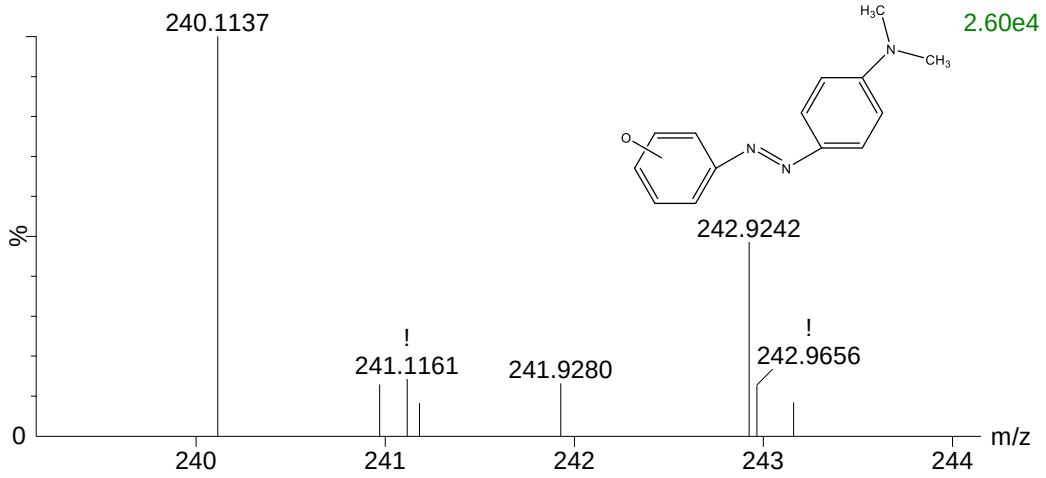

Figure 4.19. ESI-MS(-) of MO fragmentation product of standard with molecular formula, $C_{14}H_{14}N_3O$ (M_a-SO_2, m/z=240.1137).

DMPD protonated standard with m/z value of 137.1066 corresponding to M_bH, with molecular formula $C_8H_{13}N_2$ is detected in ESI(+), as shown in Figure 4.20. Its ^{13}C peak with m/z value of 138.0913 is also observed. A peak for the cation radical was observed for DMPD with exact mass of 136.0997 and its ^{13}C peak at 137.1066. This peak is relatively high with respect to abundance of ^{13}C isotope, possibly due to overlapping of peaks. A

similar peak for cation radical of 4-chloro-*o*-toluidine was reported by Mukherjee (2019) using ESI(+). No peak is detected in negative mode for this compound.

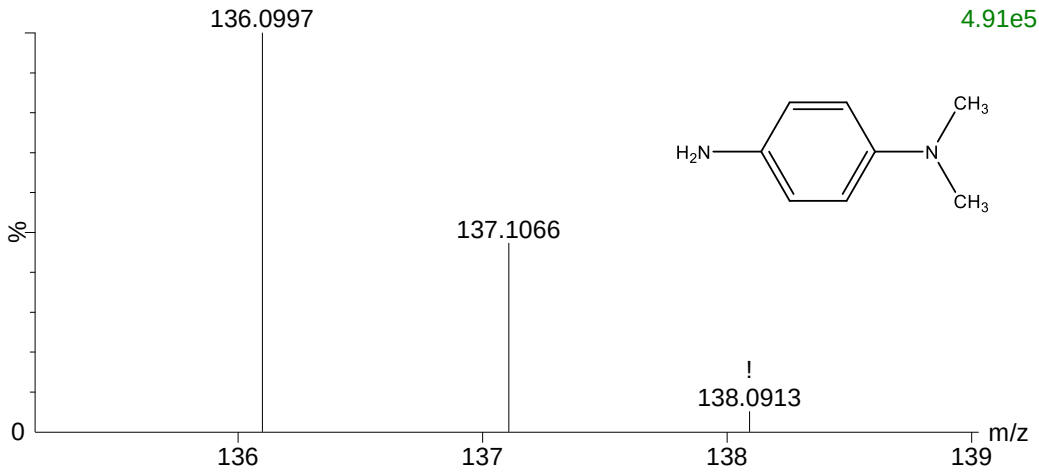

Figure 4.20. ESI-MS(+) of DMPD radical cation standard with molecular formula, $C_8H_{12}N_2$ (M_b, m/z=136.0997), protonated standard with molecular formula, $C_8H_{13}N_2$ (M_bH, m/z=137.1066).

The base peak for SA anion radical standard is detected in ESI(-) with m/z value of 172.0057, corresponding to $C_6H_6NO_3S$, represented as M_c-H (Figure 4.21). ^{13}C and ^{34}S peaks with m/z values of 173.0080 and 174.0077, respectively, are also observed. The intensity of the ^{13}C peak is quite high in comparison to the relative abundance of ^{13}C isotope. This could be due to overlapping of ^{13}C peak with standard molecular ion, M_c. In positive-ion mode, only the peak corresponding to citrate buffer $C_6H_8O_7Na$ with m/z value of 215.0168 is detected. Although buffer concentration was kept as low as 5 mM, SA cannot be detected.

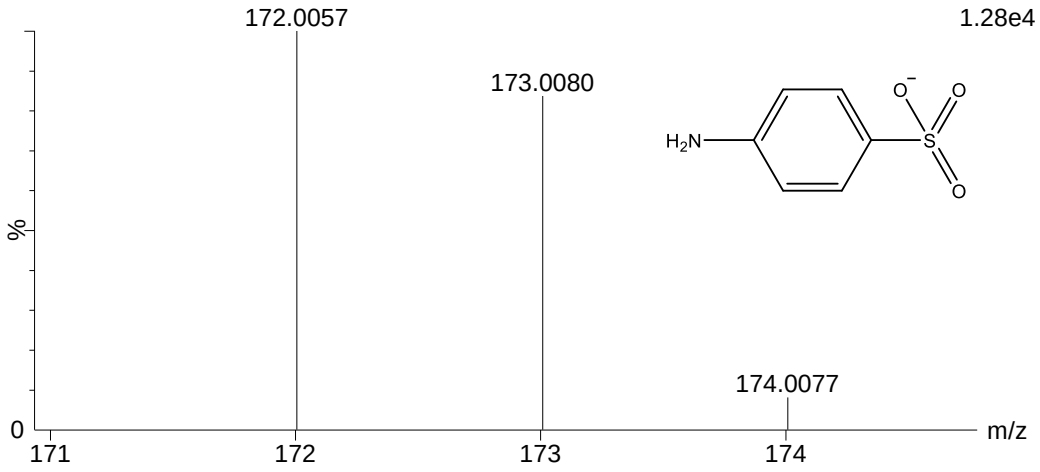

Figure 4.21. ESI-MS(-) of SA radical anion standard with molecular formula, $C_6H_6NO_3S$ (M_c-H, m/z=172.0057).

4.6.4 MS for MO reaction mixture

The mass spectrum for a full-range scan of an MO reaction in ESI(+) is shown in Figure 4.22. The spectrum shows the presence of MO monomer and some of higher oligomers and fragmentation products of the dye formed as a result of azo-bond splitting as follows. Figure 4.23 shows the presence of unreacted MO after the reaction at m/z value of 328.0734 with ^{13}C and ^{34}S peaks at 329.0760 and 330.0711, respectively.

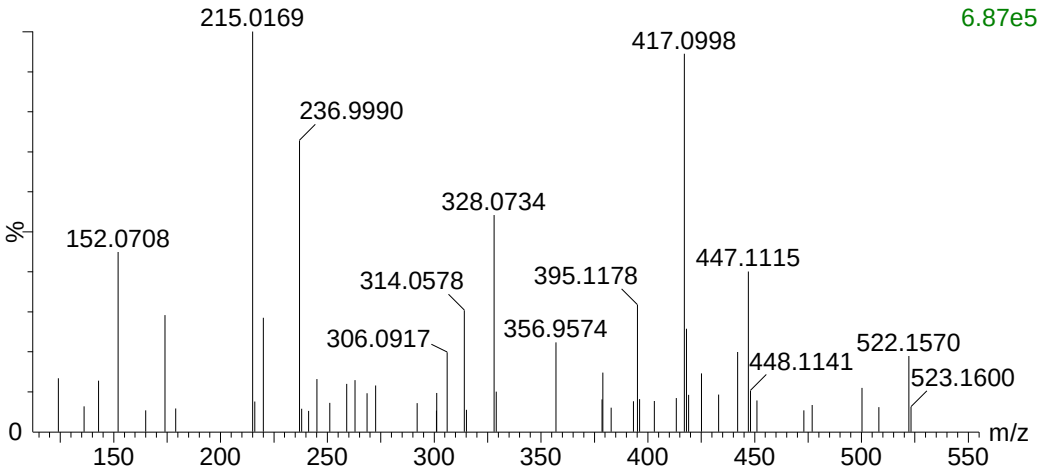

Figure 4.22. ESI-MS (+) of full-range scan of MO reaction mixture. Conditions: 0.50 mM MO; 1 mM H_2O_2; 40 mM pH 4.0 buffer; 0.0070 U/mL SBP and 3-h reaction.

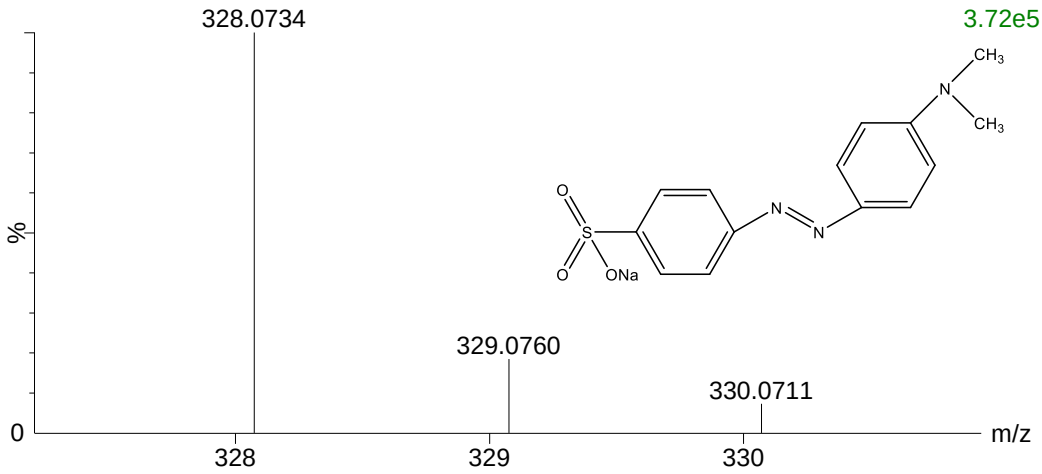

Figure 4.23. ESI-MS(+) of residual MO protonated monomer in MO reaction mixture with molecular formula, $C_{14}H_{15}N_3SO_3Na$ (M_aH, m/z=328.0734). Conditions: as for Figure 4.22.

Similarly, in ESI(-), a peak corresponding to MO monomer is detected, as shown in Figure 4.24, with m/z value of 304.0757 and ^{13}C and ^{34}S peaks at 305.0782, 306.0734, respectively since the reaction proceeded to ≥95% completion. A fragmentation product of MO monomer corresponding to M_a-CH_3 or M_aH-CH_2 at m/z value of 289.0519, similar to the peak detected at m/z value of 289.0509 in the standard (Figure 4.18), is also detected in MO reaction mixture, as illustrated in Figure 4.25. ^{13}C and ^{34}S peaks are detected at m/z values of 290.0583 and 291.0575, respectively.

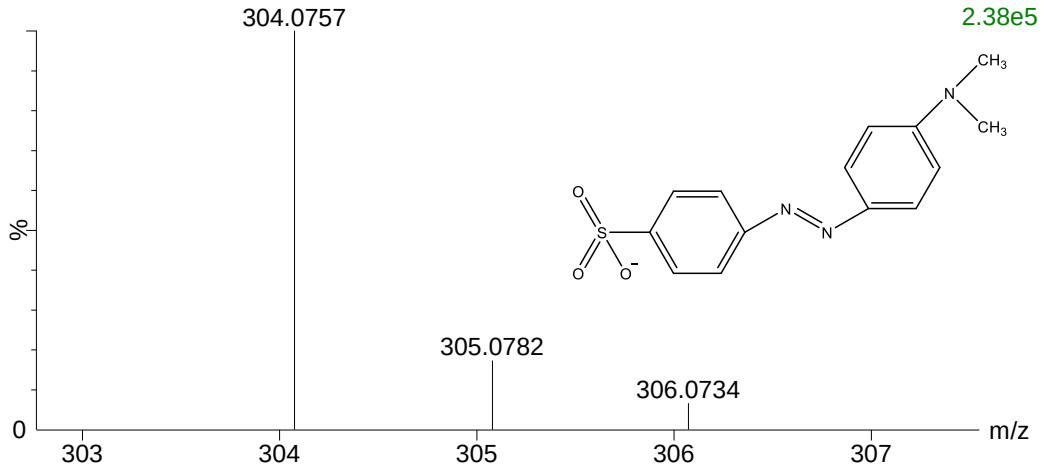

Figure 4.24. ESI-MS(-) of residual MO monomer in MO reaction mixture with molecular formula, $C_{14}H_{14}N_3SO_3$ (M_a-Na, m/z=304.0757). Conditions: as for Figure 4.22.

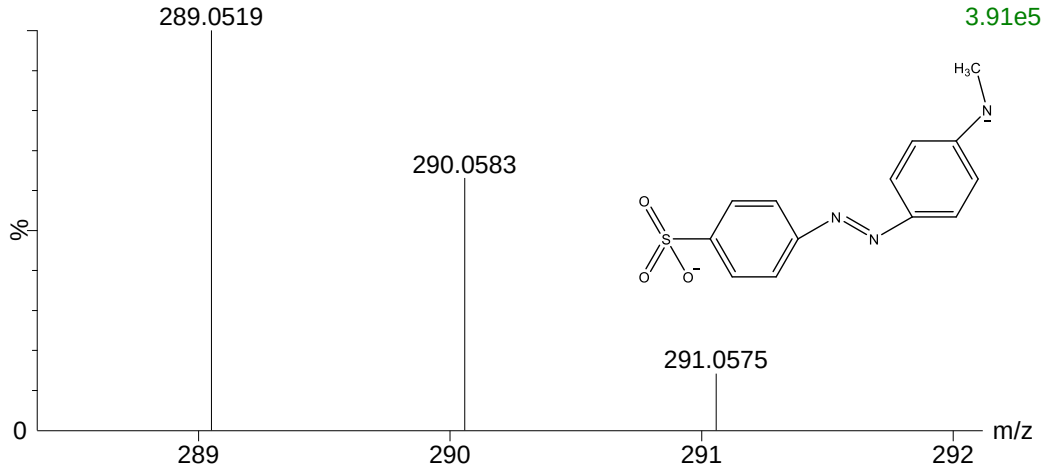

Figure 4.25. ESI-MS(-) of residual fragmentation product of MO monomer in MO reaction mixture with molecular formula, $C_{13}H_{11}N_3SO_3$ (M_a-CH_3, m/z=289.0519). Conditions: as for Figure 4.22.

A peak at m/z value of 136.0760, shown in Figure 4.26 corresponds to radical cation of DMPD, denoted as M_b ($C_8H_{12}N_2$), with a ^{13}C peak at 137.0798. The presence of DMPD in the MO reaction mixture provides the evidence of enzymatic azo-bond cleavage in MO. Some higher oligomers are also detected in the MO reaction solution. A product of regular oxidative hetero-coupling of MO and DMPD with molecular formula of $C_{21}H_{22}N_5SO_3Na$

(M_aM_bH-2-CH_3) and m/z value of 447.1122 is detected, as shown in Figure 4.27. ^{13}C and ^{34}S peaks are detected at m/z 448.1143 and 449.1097, respectively. It should be mentioned here that this peak lies within ±49 ppm of the theoretical range and not within ±5 ppm range that is generally followed for validation of molecular formula. However, the presence of the two isotope peaks (albeit, also not within 5 ppm of their respective theoretical ranges) lends tentative credence to the proposed hetero-dimer structure.

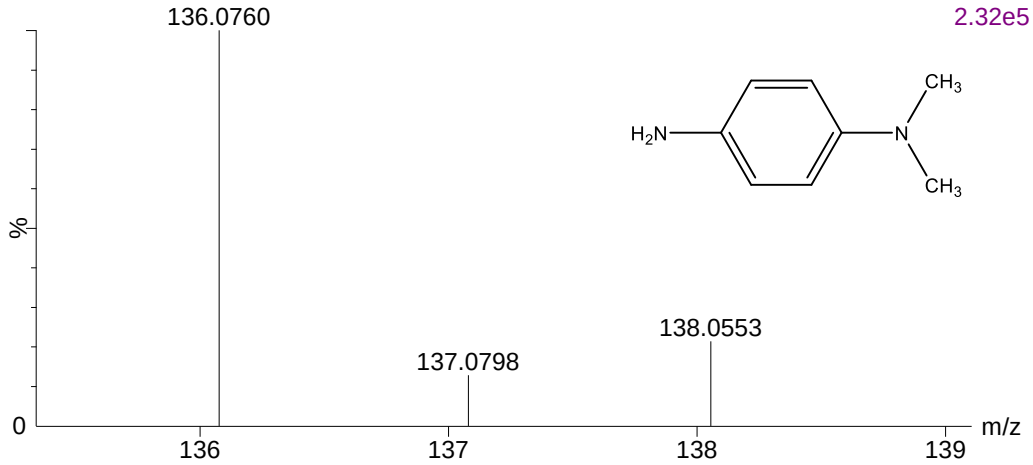

Figure 4.26. ESI-MS(+) of DMPD in MO reaction mixture with molecular formula, $C_8H_{12}N_2$ (M_b, m/z=136.0760). Conditions: as for Figure 4.22.

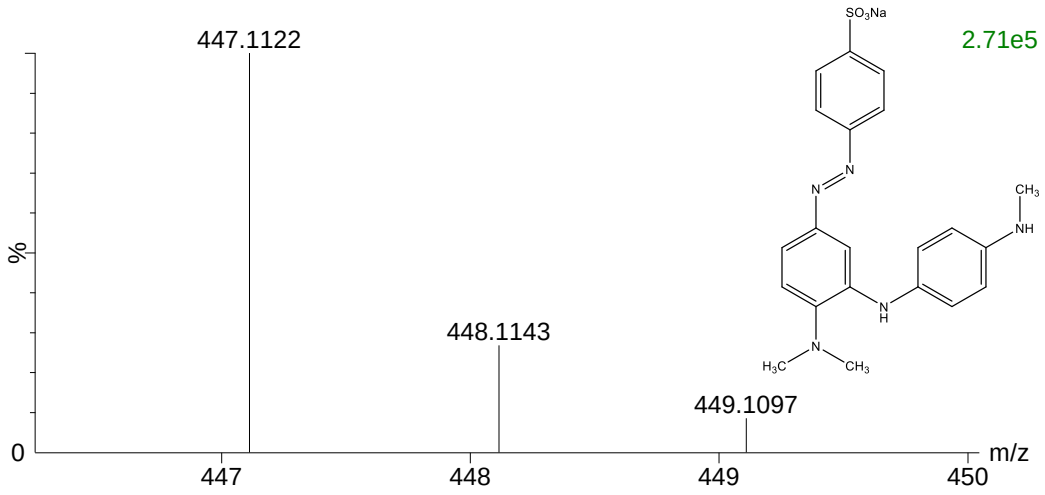

Figure 4.27. ESI-MS(+) of protonated product of oxidative coupling of MO and DMPD in MO reaction mixture with molecular formula, $C_{21}H_{22}N_5SO_3Na$ (M_aM_bH-2-CH_3, m/z=447.1122). Conditions: as for Figure 4.22.

Figure 4.28 shows m/z value of 417.1003, corresponding to molecular formula of $C_{20}H_{18}N_4SO_3Na$ (M_aM_b-2-N-C_2H_6), with ^{13}C and ^{34}S peaks at 418.1032 and 419.1004, respectively. The structure pertaining to this molecular formula is shown in the spectrum (arbitrarily drawn with C-N coupling). This shows coupling of MO and DMPD with loss of nitrogen and two -CH_3 groups. Figures 4.26, 4.27 and 4.28 provide evidence of azo-bond splitting in MO after the enzymatic reaction resulting in formation of DMPD, which further reacted with MO to form hetero-dimers.

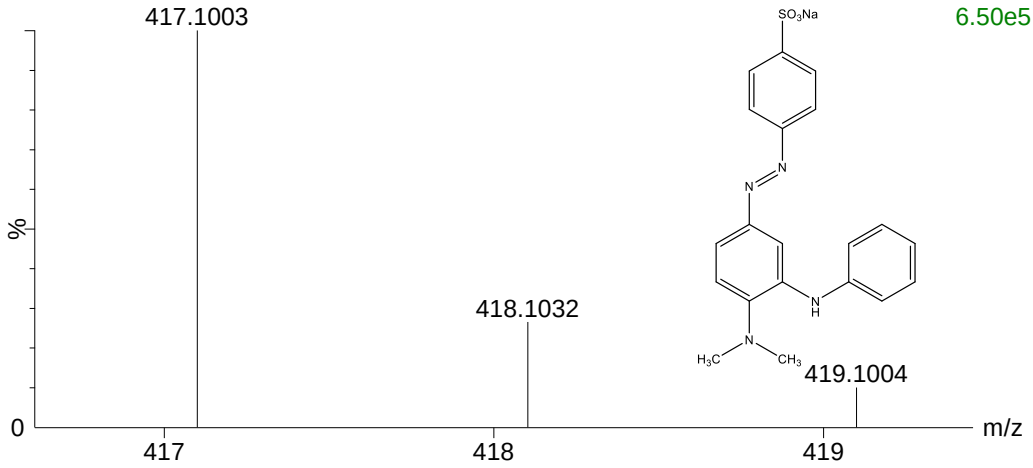

Figure 4.28. ESI-MS(+) of protonated oxidative coupling product of MO and DMPD in MO reaction mixture with molecular formula, $C_{20}H_{18}N_4SO_3Na$ (M_aM_b-2-N-C_2H_6, m/z=417.1003). Conditions: as for Figure 4.22.

The mass spectrum in Figure 4.29 shows m/z value of 522.1570, with ^{13}C and ^{34}S peaks at 523.1601 and 524.1579, respectively, with molecular formula of $C_{27}H_{25}N_5SO_3Na$ ($M_{a2}H$-2-CH_2-N-SO_3Na). This corresponds to protonated oxidative dimer of MO that has endured denitrogenation and loss of -SO_3Na and -CH_3 groups. There is no plausible suggestion for loss of -NCH_3 without the loss of second methyl group, in contrast to MO dimer with m/z value of 508.1417 (discussed in next paragraph) that has lost two methyl groups. Hence, no possible structure is drawn for this structure. Parshetti *et al.* (2010) also observed a fragmentation product of DMPD, with loss of a -CH_3 group at m/z value of 121 after using GC-MS, after decolourization of MO using *Kocuria rosea* MTCC 1532.

Another dimer with m/z value of 508.1417 with molecular formula as $C_{26}H_{23}N_5SO_3Na$ ($M_{a2}H$-2CH_3-N-SO_3Na) is shown in Figure 4.30 (arbitrarily drawn with C-C coupling). ^{13}C and ^{34}S peaks have m/z values of 509.1432 and 510.1409, respectively with loss of one -SO_3Na group, two -CH_3 groups and one nitrogen. Loss of -$N(CH_3)_2$ in this dimer could possibly be attributed to its loss from DMPD. A peak at m/z value of 93, corresponding to

loss of -N(CH_3)$_2$ from DMPD using GC-MS was also reported by Parshetti *et al.* (2010), after decolourization of MO using *Kocuria rosea* MTCC 1532.

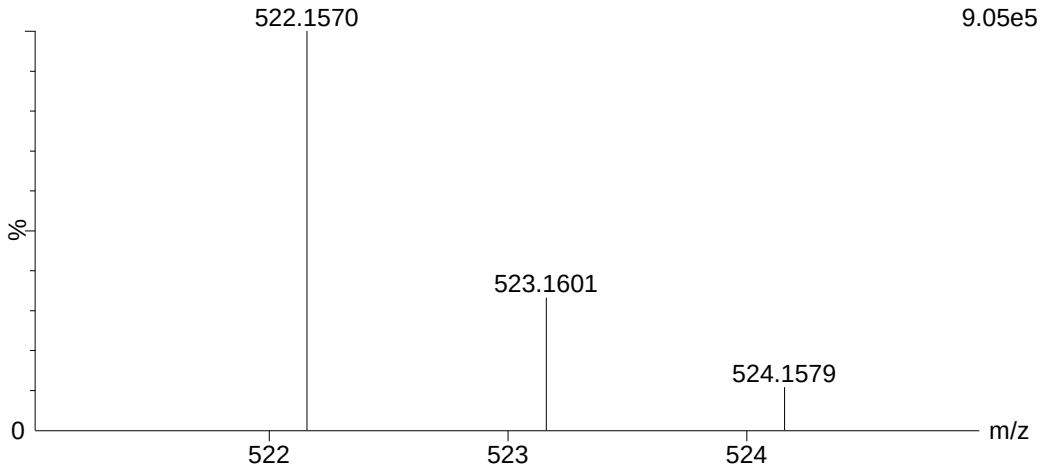

Figure 4.29. ESI-MS(+) of protonated oxidative dimer of MO in MO reaction mixture with molecular formula, $C_{27}H_{25}N_5SO_3Na$ ($M_{a2}H$-2-CH_2-N-SO_3Na, m/z=522.1570). Conditions: as for Figure 4.22.

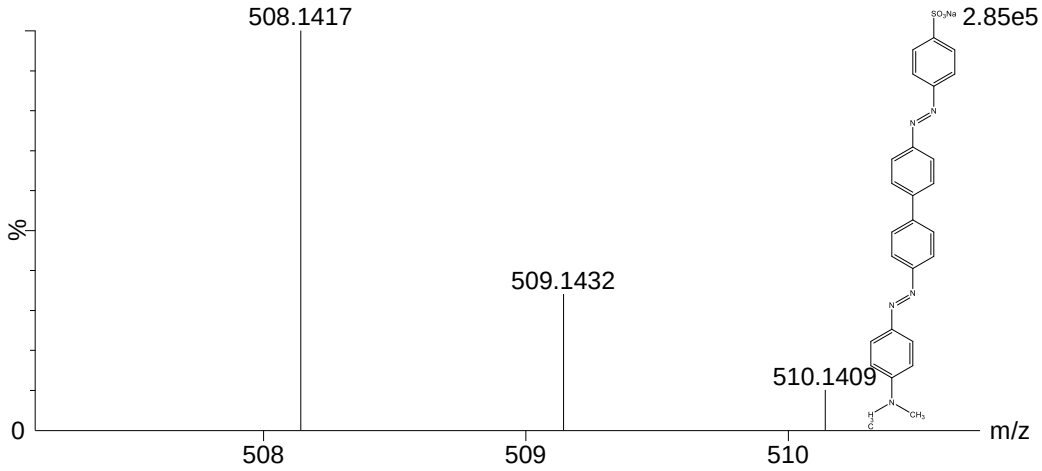

Figure 4.30. ESI-MS(+) of protonated oxidative dimer of MO in MO reaction mixture with molecular formula, $C_{26}H_{23}N_5SO_3Na$ ($M_{a2}H$-2CH_3-N-SO_3Na, m/z=508.1417). Conditions: as for Figure 4.22.

Table 4.3 provides a summary of standards and products of *p*-anisidine and MO with their m/z values and molecular formulae.

Table 4.3. Summary of MS results

m/z value	Compound description	Molecular formula	Symbolic formula
124.0775	*p*-Anisidine protonated standard	$C_7H_{10}NO$	MH
124.0801	*p*-Anisidine protonated residual monomer	$C_7H_{10}NO$	MH
243.1134	*p*-Anisidine protonated azo-dimer in supernatant	$C_{14}H_{15}N_2O_2$	M_2H-4
366.1795	*p*-Anisidine protonated trimer in supernatant	$C_{21}H_{24}N_3O_3$	M_3H-4
336.1703	*p*-Anisidine protonated trimer with loss of -OCH_2 group in supernatant	$C_{20}H_{22}N_3O_2$	M_3H-4-OCH_2
371.1030	*p*-Anisidine protonated oligomer in supernatant	$C_{22}H_{18}N_3O_3$	M_3H-10+C
328.0728	MO protonated standard	$C_{14}H_{15}N_3SO_3Na$	M_aHNa
306.0913	MO protonated standard fragmentation product	$C_{14}H_{16}N_3SO_3$	M_aH_2
304.0753	MO standard	$C_{14}H_{14}N_3SO_3$	M_a
289.0509	MO standard fragmentation product	$C_{13}H_{11}N_3SO_3$	M_a-CH_3
240.1137	MO protonated standard fragmentation product	$C_{14}H_{14}N_3O$	M_a-SO_2
136.0997	DMPD radical cation standard	$C_8H_{12}N_2$	M_b
137.1066	DMPD protonated standard	$C_8H_{13}N_2$	M_bH
172.0057	SA radical anion standard	$C_6H_6NO_3S$	M_c-H
328.0734	MO protonated residual monomer in reaction mixture	$C_{14}H_{15}N_3SO_3Na$	M_aHNa
304.0757	MO monomer in reaction mixture	$C_{14}H_{14}N_3SO_3$	M_a-Na
289.0519	MO residual fragmentation product in reaction mixture	$C_{13}H_{11}N_3SO_3$	M_a-CH_3
136.0760	DMPD radical cation in reaction mixture	$C_8H_{12}N_2$	M_b
137.0798	DMPD protonated standard in reaction mixture	$C_8H_{13}N_2$	M_bH
417.1003	Protonated oxidative product of coupling of MO and DMPD in reaction mixture	$C_{20}H_{18}N_4SO_3Na$	M_aM_b-2-N-C_2H_6

447.1122	Protonated oxidative product of coupling of MO and DMPD in reaction mixture	$C_{21}H_{22}N_5SO_3Na$	M_aM_bH-2-CH_3
522.1570	Protonated oxidative dimer of MO in reaction mixture	$C_{27}H_{25}N_5SO_3Na$	$M_{a2}H$-2-CH_2-N-SO_3Na
508.1417	Protonated oxidative dimer of MO in reaction mixture	$C_{26}H_{23}N_5SO_3Na$	$M_{a2}H$-2CH_3-N-SO_3Na

4.7 Additional evidence for azo-bond cleavage in MO

In addition to MS above, UV-VIS and HPLC techniques provide evidence of azo-bond splitting in MO through enzymatic reaction with SBP. As discussed in Section 4.6.3, detection of DMPD and coupling products of DMPD with MO in the MO reaction mixture using MS confirm azo-bond cleavage in MO. HPLC analysis of the MO reaction mixture and standards of MO, DMPD and SA also support this hypothesis. Figures 4.31, 4.32 and 4.33 show chromatograms of 0.05 mM MO, SA and DMPD standards each. DMPD was observed to undergo peak-splitting under these conditions.

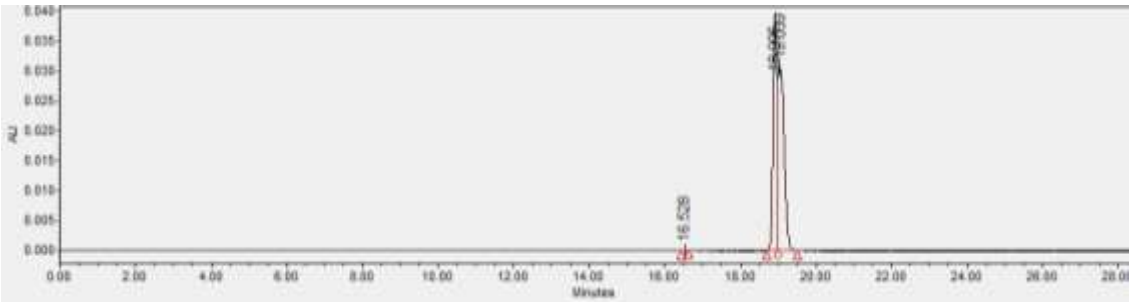

Figure 4.31. HPLC chromatogram of 0.05 mM MO at 465 nm. Mobile phase: 85% ammonium acetate, 15% ACN, total flow rate: 0.6 mL/min.

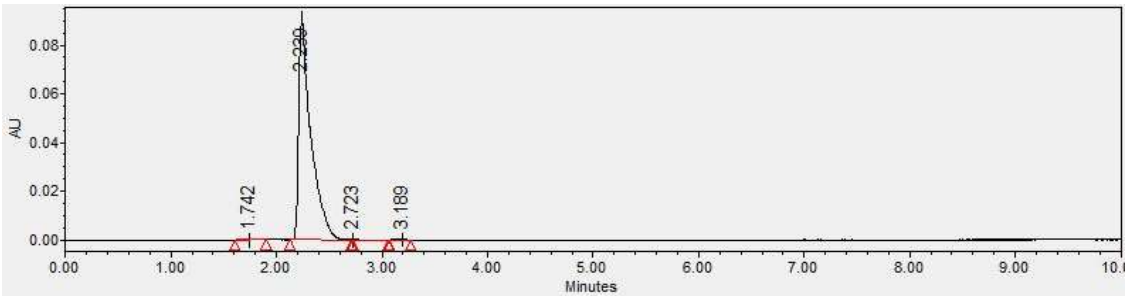

Figure 4.32. HPLC chromatogram of 0.05 mM SA at 249 nm. Mobile phase: 85% ammonium acetate, 15% ACN, total flow rate: 0.6 mL/min.

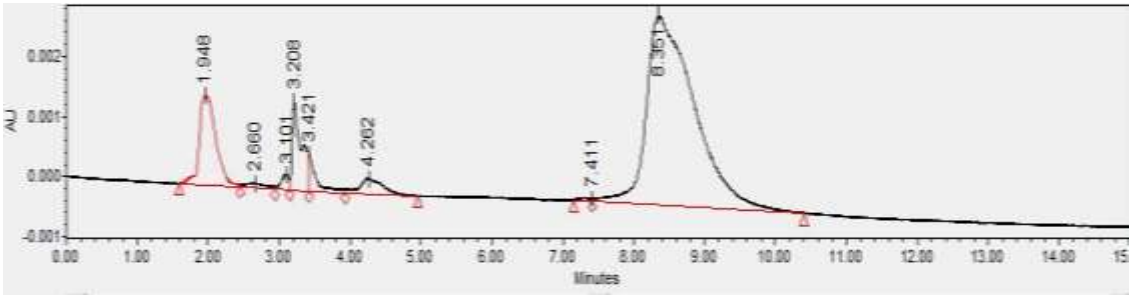

Figure 4.33. HPLC chromatogram of 0.05 mM DMPD standard at 239 nm. Mobile phase: 85% ammonium acetate, 15% ACN, total flow rate: 0.6 mL/min.

Individual batch reactions of 0.50 mM SA and 0.50 mM DMPD were conducted under optimized reaction conditions for MO (Section 4.4) and analyzed using HPLC. Figures 4.34, 4.35 and 4.36 show HPLC chromatograms of MO, SA and DMPD, respectively after 3-hour reaction. Comparing Figures 4.34 and 4.36, peaks observed in the DMPD reaction mixture at retention time of 7.301 and 7.626 min are similar to the peaks found at 7.406 and 7.716 min, respectively in the MO reaction mixture. Similarly, the peak observed at retention time of 2.310 min for SA reaction mixture (Figure 4.35) is analogous to the peak at 2.300 min in MO reaction mixture. HPLC analysis of the SA reaction mixture, no conversion of SA was observed under the optimum conditions for MO. However, no clear HPLC evidence for reaction of DMPD could be found because of splitting of peaks.

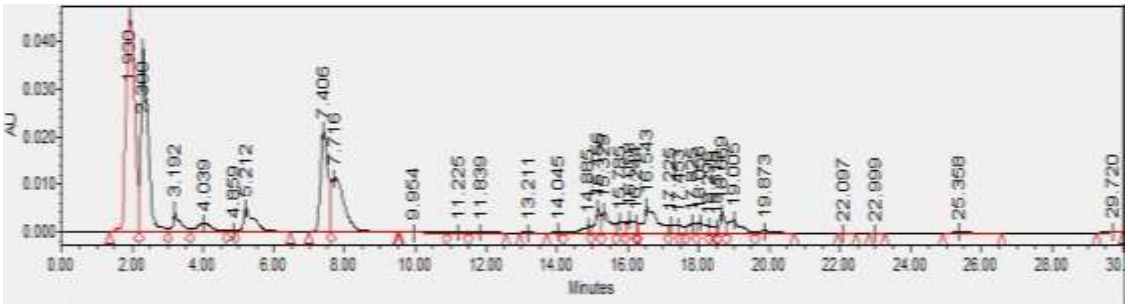

Figure 4.34. HPLC chromatogram of MO reaction mixture at 239 nm. Mobile phase: 85% ammonium acetate, 15% ACN, total flow rate: 0.6 mL/min.

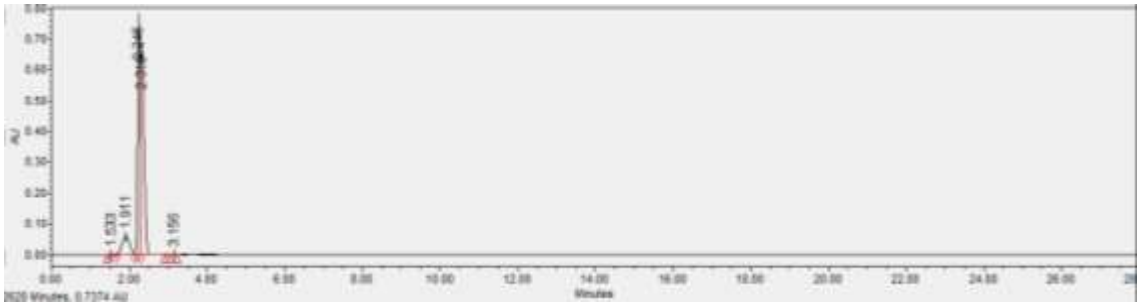

Figure 4.35. HPLC chromatogram of SA reaction mixture at 249 nm. Mobile phase: 85% ammonium acetate, 15% ACN, total flow rate: 0.6 mL/min.

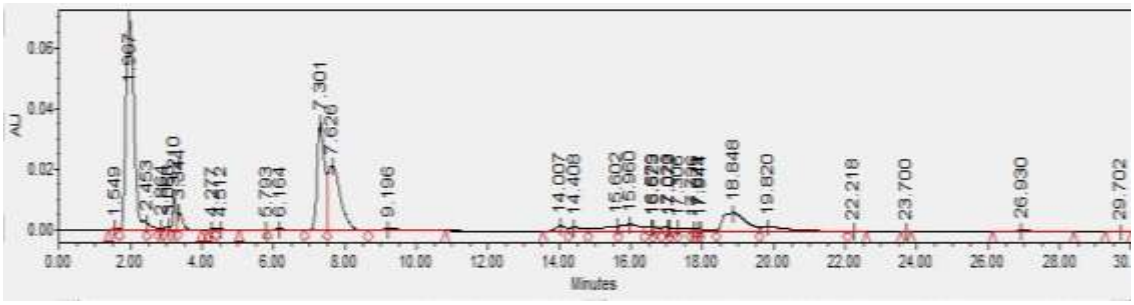

Figure 4.36. HPLC chromatogram of DMPD reaction mixture at 239 nm. Mobile phase: 85% ammonium acetate, 15% ACN, total flow rate: 0.6 mL/min.

UV-VIS spectra of MO, SA and DMPD standards and reaction mixtures are shown in Figure 4.37. MO standard has a strong peak at 465 nm and weak peak at 270 nm. The peak at 465 nm is attributed to conjugated azo-bond structure due to dimethylamino group, while the peak at 270 nm is attributed to $\pi \rightarrow \pi^*$ transition in the aromatic rings (Fan *et al*. 2009).

After the reaction, it was observed that the peaks at 465 nm and 270 nm become weaker, while a new peak at 249 nm was detected. Comparing this peak with SA standard, it could be attributed to SA. Reduction of the peak at 465 nm also suggests azo-bond cleavage (Cai *et al*. 2012, Parshetti *et al*. 2010). No peak was detected at 550 nm, which is a characteristic peak of DMPD. This could possibly be due to further enzymatic reaction of DMPD with SBP. Preliminary reactions conducted on treatment of DMPD using SBP from pH 2.6-10.0 showed maximum removal at pH 6.0.

To our knowledge, this is the first study showing removal of tertiary amines (MO and DMPD) using SBP.

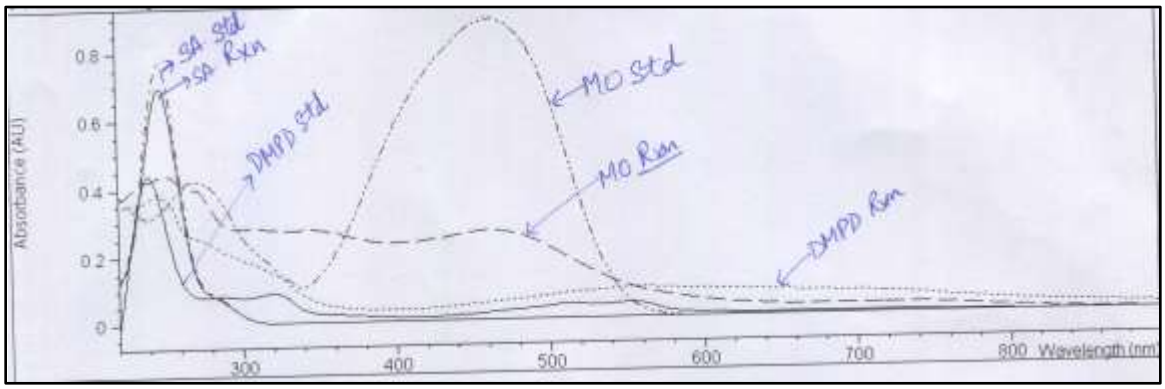

Figure 4.37. UV spectrum of standards and reaction mixtures of MO, SA and DMPD. Conditions: 0.50 mM MO, SA and DMPD, pH 4.0, 1.0 mM H_2O_2, 0.0070 U/mL SBP.

Based on this evidence, it can be stated that SBP results in reductive cleavage of azo bond in MO to form SA and DMPD. These metabolites are known to be non-toxic (Dixit and Garg 2018). Dixit and Garg (2018) also proposed azo-bond splitting of MO into SA and DMPD using HPLC through reaction with *Klebsiella pneumoniae* at pH 7.0. Similarly, Cai *et al*. (2012) and Parshetti *et al*. (2010) also suggested azo-bond cleavage of MO into SA and DMPD using *Shewanella oneidensis* MR-1 and *Kocuria rosea* MTCC 1532, respectively, through GC-MS analysis. However, azo cleavage is not the sole fate of MO

in the enzymatic reaction, as evidenced by the self-coupling products found by MS analysis.

CHAPTER 5: SUMMARY AND CONCLUSIONS

The main focus of this thesis was to investigate the capability of SBP to cleave an azo-bond in model substrate lacking anilino or phenolic functional groups. DY12 was chosen as a realistic model and azobenzene was chosen as the ultimate model for this hypothesis. Azo-splitting was also studied for MO and removal of *p*-anisidine was investigated because it could have been a possible breakdown product of DY12 if azo-bond cleavage occurred. The results are summarized as follows:

1. Experiments conducted for DY12 from pH 1.8-10.0 in the presence of SBP and H_2O_2 exhibited the same removal as in the absence of H_2O_2, suggesting that precipitation of DY12 in the presence of SBP resulted in its removal instead of the enzymatic reaction. Mediator studies conducted using HOBT were also unsuccessful.

2. For azobenzene, 20% removal was observed after the enzymatic reaction and also in the standard (without SBP and H_2O_2) which clearly showed that azobenzene is not a substrate for SBP.

3. Preliminary investigations conducted with *p*-anisidine and MO demonstrated these to be good substrates. Further experiments were conducted to optimize pH, H_2O_2 and minimum enzyme required to achieve ≥95% removal. The pH optima for MO and *p*-anisidine were 4.0 and 5.5, respectively, under stringent conditions of SBP. The H_2O_2 requirements for 0.50 mM MO and 1.0 mM *p*-anisidine were each 1 mM. The minimum effective SBP required for ≥95% removal of the substrates was 0.0018 U/mL for *p*-anisidine and 0.0070 U/mL for MO.

4. Time course studies for MO and *p*-anisidine showed ≥95% removal under optimal conditions within 45 and 90 minutes, respectively. Normalized half-lives for *p*-anisidine and MO with respect to SBP activity were 0.0097 and 0.0476 min^{-1}, respectively.

5. HPLC analysis of standards of SA, DMPD and MO and reaction mixtures of these at optimized conditions for MO, showed formation of DMPD and SA during enzymatic reaction of MO, thus providing evidence of azo cleavage.

6. MS analysis for *p*-anisidine showed formation of dimers, trimers and other coupling products during the enzymatic reaction formed as a result of N-N, N-C or C-C coupling. MS for MO reaction mixture provided evidence of formation of DMPD, coupling products of MO with DMPD and MO dimer, confirming arylazo-bond cleavage in MO and subsequent radical coupling as well as direct self-coupling of MO.

7. The self-coupling of MO and its hetero-coupling with DMPD are the first instances of peroxidase activation of tertiary arylamines to the corresponding radicals.

In conclusion, this study suggests that SBP is capable of cleaving azo-bond. SBP provides a robust, cheap, environmental-friendly and economical alternative for ≥95% removal of MO and *p*-anisidine from wastewater.

CHAPTER 6: FUTURE WORK

The results of this work can be used for removal of MO and *p*-anisidine from wastewater but prior to its implementation to replace the existing treatment methods, some work needs to be done:

1. Toxicity evaluation of polymeric products formed after the enzymatic reaction should be conducted in order to assess environmental impact of soluble reaction products.

2. Matrix effect in real wastewater needs to be studied for practical implication of this method.

3. Cost analysis for this treatment can be conducted to determine economic feasibility of this method.

4. Detailed kinetic studies for enzymatic reaction of *p*-anisidine and MO can be done to calculate K_m (Michaelis constant) and V_{max} (maximum velocity) based on Michaelis-Menten model. This would be useful for treatment process modeling and design.

5. Further insight into the type of coupling and azo-bond cleavage products can be gained through use of FTIR and NMR in combination with MS studies.

Investigation of DY12 as a substrate for SBP can be done using mediators such as violuric acid, veratryl alcohol and HOBT over wide ranges of pH, SBP and H_2O_2. Further investigation of DMPD reactions alone and with MO would be of interest.

BIBLIOGRAPHY

Abedi, S., Nekouei, F. (2011). Removal of direct yellow 12 from water samples by cloud point extraction using Triton X-100 as nonionic surfactant. Journal of Chemistry, 8(4): 1588-1595.

Al-Ansari, M. M., Steevensz, A., Al-Aasm, N., Taylor, K. E., Bewtra, J. K., Biswas, N. (2009). Soybean peroxidase-catalyzed removal of phenylenediamines and benzenediols from water. Enzyme and Microbial Technology, 45(4): 253-260.

Al-Ansari, M. M., Saha, B., Mazloum, S., Taylor, K. E., Bewtra, J. K., Biswas, N. (2011). Soybean peroxidase applications in wastewater treatment. Soybeans: Cultivation, Uses and Nutrition: 189-221. Nova Science Publishers, Inc. Hauppauge, N.Y.

Al-Bastaki, N. (2004). Removal of methyl orange dye and Na_2SO_4 salt from synthetic waste water using reverse osmosis. Chemical Engineering and Processing: Process Intensification, 43(12): 1561-1567.

Aleboyeh, A., Daneshvar, N., Kasiri, M. B. (2008). Optimization of CI Acid Red 14 azo dye removal by electrocoagulation batch process with response surface methodology. Chemical Engineering and Processing: Process Intensification, 47(5): 827-832.

Ali, L., Algaithi, R., Habib, H. M., Souka, U., Rauf, M. A., Ashraf, S. S. (2013). Soybean peroxidase-mediated degradation of an azo dye–a detailed mechanistic study. BMC Biochemistry, 14(1): 35.

Alneyadi, A. H., Ashraf, S. S. (2016). Differential enzymatic degradation of thiazole pollutants by two different peroxidases–A comparative study. Chemical Engineering Journal, 303: 529-538.

Altschuh, J., Brüggemann, R., Santl, H., Eichinger, G., Piringer, O. G. (1999). Henry's Law constants for a diverse set of organic chemicals: Experimental determination and comparison of estimation methods. Chemosphere, 39(11): 1871-1887.

Ba, S., Arsenault, A., Hassani, T., Jones, J. P., Cabana, H. (2013). Laccase immobilization and insolubilization: from fundamentals to applications for the elimination of emerging contaminants in wastewater treatment. Critical Reviews in Biotechnology, 33(4): 404-418.

Badr, Y., Mahmoud, M. A. (2007). Photocatalytic degradation of methyl orange by gold silver nano-core/silica nano-shell. Journal of Physics and Chemistry of Solids, 68(3): 413-419.

Bafana, A., Devi, S. S., Chakrabarti, T. (2011). Azo dyes: past, present and the future. Environmental Reviews, 19(NA): 350-371.

Baiocchi, C., Brussino, M. C., Pramauro, E., Prevot, A. B., Palmisano, L., Marcì, G. (2002). Characterization of methyl orange and its photocatalytic degradation products by HPLC/UV–VIS diode array and atmospheric pressure ionization quadrupole ion trap mass spectrometry. International Journal of Mass Spectrometry, 214(2): 247-256.

Bardakçı, B., Kaya, N., Kalaycı, T. (2013). Anisidine adsorption on Co-supported pumice. Environmental Earth Sciences, 70(2): 849-856.

Beemer, K. W. (2017). Absorption/adsorption properties of peroxidase-catalyzed polyphenolic precipitates using 4-(phenylazo) benzoic acid as a model sorbate. MSc dissertation, University of Windsor, Ontario, Canada.

Bilal, M., Rasheed, T., Iqbal, H. M., Yan, Y. (2018). Peroxidases-assisted removal of environmentally-related hazardous pollutants with reference to the reaction mechanisms of industrial dyes. Science of the Total Environment, 644: 1-13.

Bódalo, A., Gomez, J. L., Gomez, E., Bastida, J., Maximo, M. F. (2006). Comparison of commercial peroxidases for removing phenol from water solutions. Chemosphere, 63(4): 626-632.

Bollag, J. M., Sjoblad, R. D., Liu, S. Y. (1979). Characterization of an enzyme from *Rhizoctonia praticola* which polymerizes phenolic compounds. Canadian Journal of Microbiology, 25(2): 229-233.

Brown, M. A., De Vito, S. C. (1993). Predicting azo dye toxicity. Critical Reviews in Environmental Science and Technology, 23(3): 249-324.

Cai, P. J., Xiao, X., He, Y. R., Li, W. W., Chu, J., Wu, C., Xu, F. (2012). Anaerobic biodecolourization mechanism of methyl orange by *Shewanella oneidensis* MR-1. Applied Microbiology and Biotechnology, 93(4), 1769-1776.

Canadian Textile Industry Association (2013). Weblink: https://www.canadiantextiles.ca/industry. (Accessed: January 2020).

Carmen, Z., Daniela, S. (2012). Textile organic dyes–characteristics, polluting effects and separation/elimination procedures from industrial effluents–a critical overview.

In Organic pollutants ten years after the Stockholm convention-environmental and analytical update (2741): 31. Rijeka, Croatia: IntechOpen, London.

Carrizo, D., Nerín, I., Domeño, C., Alfaro, P., Nerín, C. (2016). Direct screening of tobacco indicators in urine and saliva by Atmospheric Pressure Solid Analysis Probe coupled to quadrupole-time of flight mass spectrometry (ASAP-MS-Q-TOF-). Journal of Pharmaceutical and Biomedical Analysis, 124: 149-156.

Caza, N., Bewtra, J. K., Biswas, N., Taylor, K. E. (1999). Removal of phenolic compounds from synthetic wastewater using soybean peroxidase. Water Research, 33(13): 3012-3018.

Chaturvedi, N. K., Katoch, S. S. (2020). Effect of various parameters during degradation of toxic *p*-anisidine by Fenton's oxidation. Applied Water Science, 10(1): 18.

Chen, L. C. (2000). Effects of factors and interacted factors on the optimal decolourization process of Methyl Orange by ozone. Water Research, 34(3): 974-982.

Chen, T., Zheng, Y., Lin, J. M., Chen, G. (2008). Study on the photocatalytic degradation of methyl orange in water using Ag/ZnO as catalyst by liquid chromatography electrospray ionization ion-trap mass spectrometry. Journal of the American Society for Mass Spectrometry, 19(7), 997-1003.

Chiong, T., Lau, S. Y., Lek, Z. H., Koh, B. Y., Danquah, M. K. (2016). Enzymatic treatment of methyl orange dye in synthetic wastewater by plant-based peroxidase enzymes. Journal of Environmental Chemical Engineering, 4(2): 2500-2509.

Chuah, T. G., Jumasiah, A., Azni, I., Katayon, S., Choong, S. T. (2005). Rice husk as a potentially low-cost biosorbent for heavy metal and dye removal: an overview. Desalination, 175(3): 305-316.

Chung, K. T. (2016). Azo dyes and human health: a review. Journal of Environmental Science and Health, Part C, 34(4): 233-261.

Ćirić-Marjanović, G., Milojević-Rakić, M., Janošević-Ležaić, A., Luginbühl, S., Walde, P. (2017). Enzymatic oligomerization and polymerization of arylamines: state of the art and perspectives. Chemical Papers, 71(2): 199-242.

Cordova Villegas, L.G. (2017). Enzymatic treatment of azo-dyes with soybean peroxidase, PhD dissertation, University of Windsor, Ontario, Canada.

Cordova Villegas, L. G., Mazloum, S., Taylor, K. E., Biswas, N. (2018). Soybean peroxidase-catalyzed treatment of azo dyes with or without Fe° pretreatment. Water Environment Research, 90(8): 675-684.

Dixit, S., Garg, S. (2018). Biodegradation of environmentally hazardous azo dyes and aromatic amines using *Klebsiella pneumoniae*. Journal of Environmental Engineering, 144(6): 04018035.

Dunford, H.B. (1999). Heme Peroxidases. John Wiley and Sons. New York.

El Nemr, A., Hassaan, M. A., Madkour, F. F. (2018). HPLC-MS/MS Mechanistic study of Direct Yellow 12 dye degradation using ultraviolet assisted ozone process. Journal of Water and Environmental Nanotechnology, 3(1): 1-11.

Environment Canada. (2012). The Chemicals Management Plan Substance Groupings Initiative. Aromatic Azo- and Benzidine-Based Substances. Weblink: https://www.ec.gc.ca/ese-ees/9E759C59-55E4-45F6-893A-F819EA9CB053/Azo_Technical%20Background_EN.pdf (Accessed: January 2020).

Evans, L. J. (1989). Chemistry of metal retention by soils. Environmental Science & Technology, 23(9): 1046-1056.

Fabbrini, M., Galli, C., Gentili, P. (2002). Comparing the catalytic efficiency of some mediators of laccase. Journal of Molecular Catalysis B: Enzymatic, 16(5-6): 231-240.

Fan, J., Guo, Y., Wang, J., Fan, M. (2009). Rapid decolourization of azo dye methyl orange in aqueous solution by nanoscale zerovalent iron particles. Journal of Hazardous Materials, 166(2-3): 904-910.

Feng, W., Taylor, K. E., Biswas, N., Bewtra, J. K. (2013). Soybean peroxidase trapped in product precipitate during phenol polymerization retains activity and may be recycled. Journal of Chemical Technology & Biotechnology, 88(8): 1429-1435.

Fernandes, M., Souza, D. H., Henriques, R. O., Alves, M. V., Skoronski, E., Junior, A. F. (2020). Obtaining soybean peroxidase from soybean hulls and its application for detoxification of 2, 4-dichlorophenol contaminated water. Journal of Environmental Chemical Engineering, 8(3): 103786.

Forgiarini, E., de Souza, A. A. U. (2007). Toxicity of textile dyes and their degradation by the enzyme horseradish peroxidase (HRP). Journal of Hazardous Materials, 147(3): 1073-1078.

Freeman H.S., Mock G.N. (2007). Dye application, manufacture of dye intermediates and dyes. In: Kent and Riegel's Handbook of Industrial Chemistry and Biotechnology. 11th ed.; Springer. Boston, MA, 449-590.

Geng, Z., Rao, K. J., Bassi, A. S., Gijzen, M., Krishnamoorthy, N. (2001). Investigation of biocatalytic properties of soybean seed hull peroxidase. Catalysis Today, 64(3-4): 233-238.

Ghaedi, M., Ansari, A., Sahraei, R. (2013). ZnS: Cu nanoparticles loaded on activated carbon as novel adsorbent for kinetic, thermodynamic and isotherm studies of Reactive Orange 12 and Direct yellow 12 adsorption. Spectrochimica Acta Part A: Molecular and Biomolecular Spectroscopy, 114: 687-694.

Ghaedi, M., Sadeghian, B., Pebdani, A. A., Sahraei, R., Daneshfar, A., Duran, C. (2012). Kinetics, thermodynamics and equilibrium evaluation of direct yellow 12 removal by adsorption onto silver nanoparticles loaded activated carbon. Chemical Engineering Journal, 187: 133-141.

Ghaemmaghami, F., Alemzadeh, I., Motamed, S. (2010). Seed coat soybean peroxidase: Extraction and biocatalytic properties determination. Iranian Journal of Chemical Engineering, 7(2): 28-38.

Goscianska, J., Marciniak, M., Pietrzak, R. (2014). Mesoporous carbons modified with lanthanum (III) chloride for methyl orange adsorption. Chemical Engineering Journal, 247: 258-264.

Government of Canada. Detailed categorization results of the Domestic Substances List. Weblink: https://open.canada.ca/data/en/dataset/1d946396-cf9a-4fa1-8942-4541063bfba4 (Accessed: January 2020).

Guivarch, E., Trevin, S., Lahitte, C., Oturan, M. A. (2003). Degradation of azo dyes in water by electro-Fenton process. Environmental Chemistry Letters, 1(1): 38-44.

Habiba, U., Siddique, T. A., Joo, T. C., Salleh, A., Ang, B. C., Afifi, A. M. (2017). Synthesis of chitosan/polyvinyl alcohol/zeolite composite for removal of methyl orange, Congo red and chromium (VI) by flocculation/adsorption. Carbohydrate Polymers, 157: 1568-1576.

Haldorai, Y., Shim, J. J. (2014). An efficient removal of methyl orange dye from aqueous solution by adsorption onto chitosan/MgO composite: A novel reusable adsorbent. Applied Surface Science, 292: 447-453.

Han, L., Xue, S., Zhao, S., Yan, J., Qian, L., Chen, M. (2015). Biochar supported nanoscale iron particles for the efficient removal of methyl orange dye in aqueous solutions. PloS One, 10(7): e0132067.

Haque, E., Jun, J. W., Jhung, S. H. (2011). Adsorptive removal of Methyl Orange and Methylene Blue from aqueous solution with a metal-organic framework material, iron terephthalate (MOF-235). Journal of Hazardous Materials, 185(1): 507-511.

Hassaan, M. A., El Nemr, A. (2017). Health and environmental impacts of dyes: mini review. American Journal of Environmental Science and Engineering, 1(3): 64-67.

Haworth, S., Lawlor, T., Mortelmans, K., Speck, W., Zeiger, E. (1983). Salmonella mutagenicity test results for 250 chemicals. Environmental Mutagenesis, 5(S1): 3-49.

Henriksen, A., Mirza, O., Indiani, C., Teilum, K., Smulevich, G., Welinder, K. G., Gajhede, M. (2001). Structure of soybean seed coat peroxidase: A plant peroxidase with unusual stability and haem-apoprotein interactions. Protein Science, 10(1): 108-115.

Ho, C. S., Lam, C. W. K., Chan, M. H. M., Cheung, R. C. K., Law, L. K., Lit, L. C. W., Ng, K.F., Suen, M.W., Tai, H. L. (2003). Electrospray ionisation mass spectrometry: principles and clinical applications. The Clinical Biochemist Reviews, 24(1): 3.

Holkar, C. R., Jadhav, A. J., Pinjari, D. V., Mahamuni, N. M., Pandit, A. B. (2016). A critical review on textile wastewater treatments: possible approaches. Journal of Environmental Management, 182: 351-366.

Husain, Q. (2010). Peroxidase mediated decolourization and remediation of wastewater containing industrial dyes: a review. Reviews in Environmental Science and Bio/Technology, 9(2): 117-140.

IARC. Monographs on the Evaluation of the Carcinogenic Risk of Chemicals to Humans. Geneva: World Health Organization, International Agency for Research on Cancer, 1972PRESENT. (Multivolume work). Weblink: http://monographs.iarc.fr/ENG/Classification/index.php, p. (8): 76. (Accessed: January 2020)

Ibrahim, M. S., Ali, H. I., Taylor, K. E., Biswas, N., Bewtra, J. K. (2001). Enzyme-catalyzed removal of phenol from refinery wastewater: Feasibility Studies. Water Environment Research, 73(2): 165-172.

International Agency for Research on Cancer. (2019). IARC monographs on the identification of carcinogenic hazards to humans. In List Classif. Agents Classif. by IARC Monogr (Vol. 1).

Kalsoom, U., Ashraf, S. S., Meetani, M. A., Rauf, M. A., Bhatti, H. N. (2013). Mechanistic study of a diazo dye degradation by soybean peroxidase. Chemistry Central Journal, 7(1): 93.

Kamal, J. A., Behere, D. V. (2002). Activity, stability and conformational flexibility of seed coat soybean peroxidase. Journal of Inorganic Biochemistry, 94(3): 236-242.

Kennedy, K., Alemany, K., Warith, M. (2002). Optimisation of soybean peroxidase treatment of 2, 4-dichlorophenol. Water SA, 28(2): 149-158.

Khlifi, R., Belbahri, L., Woodward, S., Ellouz, M., Dhouib, A., Sayadi, S., Mechichi, T. (2010). Decolourization and detoxification of textile industry wastewater by the laccase-mediator system. Journal of Hazardous Materials, 175(1-3): 802–808.

Klibanov, A.M., Alberti, B.N., Morris, E.D., Felshin, L.M. (1980). Enzymatic removal of toxic phenols and anilines from waste waters, Journal of Applied Biochemistry, 2: 414-421.

Knutson, K., Kirzan, S., Ragauskas, A. (2005). Enzymatic biobleaching of two recalcitrant paper dyes with horseradish and soybean peroxidase. Biotechnology Letters, 27(11): 753–758.

Koyuncu, I., Güney, K. (2013). Membrane-based treatment of textile industry wastewaters. Encyclopedia of Membrane Science and Technology. John Wiley & Sons, Inc.1-12. Connecticut.

Krainer, F. W., Glieder, A. (2015). An updated view on horseradish peroxidases: recombinant production and biotechnological applications. Applied Microbiology and Biotechnology, 99(4): 1611-1625.

Lewis, R.J. Sr.; Hawley's Condensed Chemical Dictionary 15th Edition. John Wiley & S ons, Inc. New York, NY 2007: 84.

Li, K., Li, P., Cai, J., Xiao, S., Yang, H., Li, A. (2016). Efficient adsorption of both methyl orange and chromium from their aqueous mixtures using a quaternary ammonium salt modified chitosan magnetic composite adsorbent. Chemosphere, 154: 310-318.

Li, Y., Sui, K., Liu, R., Zhao, X., Zhang, Y., Liang, H., Xia, Y. (2012). Removal of methyl orange from aqueous solution by calcium alginate/multi-walled carbon nanotubes composite fibers. Energy Procedia, 16: 863-868.

Liang, C. Z., Sun, S. P., Li, F. Y., Ong, Y. K., Chung, T. S. (2014). Treatment of highly concentrated wastewater containing multiple synthetic dyes by a combined process of coagulation/flocculation and nanofiltration. Journal of Membrane Science, 469: 306-315.

Lide, D.R. CRC Handbook of Chemistry and Physics. (2007). (88). CRC Press, Taylor & Francis, Boca Raton, FL: 8-47.

Ma, H., Wang, B., Luo, X. (2007). Studies on degradation of methyl orange wastewater by combined electrochemical process. Journal of Hazardous Materials, 149(2): 492-498.

Maddhinni, V. L., Vurimindi, H. B., Yerramilli, A. (2013). Degradation of azo dye with horse radish peroxidase (HRP). Journal of the Indian Institute of Science, 86(5): 507.

Malik Altahir, B., Feng, W., Jasim, H. H., Taylor, K. E., Biswas, N., Bewtra, J. K., Jassim, S. A. (2015). Soybean peroxidase-catalysed removal of benzidines from water. Journal of Environmental Engineering and Science, 10(4): 73-80.

Marzbali, M. H., Mir, A. A., Pazoki, M., Pourjamshidian, R., Tabeshnia, M. (2017). Removal of direct yellow 12 from aqueous solution by adsorption onto spirulina algae as a high-efficiency adsorbent. Journal of Environmental Chemical Engineering, 5(2): 1946-1956.

Mashhadi, N. (2019). Oxidative polymerization of heterocyclic aromatics using soybean peroxidase for treatment of wastewater. PhD dissertation. University of Windsor, Ontario, Canada.

Mazloum, S. (2014). Soybean peroxidase catalysis in removal of anilines and azo- dyes from water. MASc dissertation, University of Windsor, Ontario, Canada.

Mazloum, S., Al-Ansari, M. M., Taylor, K., Bewtra, J. K., Biswas, N. (2016). Additive effect on soybean peroxidase-catalyzed removal of anilines from water. Environmental Engineering Science, 33(2): 133-139.

McEldoon, J. P., Dordick, J. S. (1996). Unusual thermal stability of soybean peroxidase. Biotechnology Progress, 12(4): 555-558.

McEwen, C. N., McKay, R. G., Larsen, B. S. (2005). Analysis of solids, liquids, and biological tissues using solids probe introduction at atmospheric pressure on commercial LC/MS instruments. Analytical Chemistry, 77(23): 7826-7831.

Miranda-Mandujano, E., Moeller-Chávez, G., Villegas-Rosas, O., Buitrón, G., Garzón-Zúñiga, M. A. (2018). Decolourization of Direct Blue 2 by peroxidases obtained from an industrial soybean waste. Water SA, 44(2): 204-210.

Mittal, A., Malviya, A., Kaur, D., Mittal, J., Kurup, L. (2007). Studies on the adsorption kinetics and isotherms for the removal and recovery of Methyl Orange from wastewaters using waste materials. Journal of Hazardous Materials, 148(1-2): 229-240.

Mohammadi, N., Khani, H., Gupta, V. K., Amereh, E., Agarwal, S. (2011). Adsorption process of methyl orange dye onto mesoporous carbon material–kinetic and thermodynamic studies. Journal of Colloid and Interface Science, 362(2): 457-462.

Morsi, R., Bilal, M., Iqbal, H. M., Ashraf, S. S. (2020). Laccases and peroxidases: The smart, greener and futuristic biocatalytic tools to mitigate recalcitrant emerging pollutants. Science of the Total Environment, 136572.

Mousa, M. (2008). Removal of various aromatic compounds from synthetic and refinery wastewater using soybean peroxidase. M.Sc. thesis. University of Windsor, Ontario, Canada.

Mugdha, A., Usha, M. (2012). Enzymatic treatment of wastewater containing dyestuffs using different delivery systems. Scientific Reviews and Chemical Communications, 2(1): 31-40.

Mukherjee, D., Taylor, K. E., Biswas, N. (2018). Soybean peroxidase-induced treatment of dye-derived arylamines in water. Water, Air, & Soil Pollution, 229(8): 283.

Mukherjee, D., Bhattacharya, S., Taylor, K. E., Biswas, N. (2019). Enzymatic treatment for removal of hazardous aqueous arylamines, 4, 4′-methylenedianiline and 4, 4′-thiodianiline. Chemosphere, 235: 365-372.

Mukherjee D. (2019). Treatment of aqueous arylamine contaminants by enzyme-catalyzed oxidative polymerization, PhD dissertation, University of Windsor, Ontario, Canada.

Mukherjee, D., Taylor, K. E., Biswas, N. (2020). Soybean peroxidase-catalyzed oligomerization of arylamines in water: optimization, kinetics, products and cost. Journal of Environmental Chemical Engineering, 103871.

Naghizade Asl, M., Mahmodi, N. M., Teymouri, P., Shahmoradi, B., Rezaee, R., Maleki, A. (2016). Adsorption of organic dyes using copper oxide nanoparticles: isotherm and kinetic studies. Desalination and Water Treatment, 57(52): 25278-25287.

National Institute of Occupational Safety and Health. NIOSH Pocket Guide to Chemical Hazards (full website version). Weblink: https://www.cdc.gov/niosh/npg (Accessed: January, 2020).

Nicell, J. A., Bewtra, J. K., Taylor, K. E., Biswas, N., St. Pierre, C. (1992). Enzyme catalyzed polymerization and precipitation of aromatic compounds from wastewater. Water Science and Technology, 25(3), 157-164.

Niessen, W. M. (2017). MS–MS and MS^n. Encyclopedia of Spectroscopy and Spectrometry (third edition), edited by John C. Lindon, Academic Press, Oxford, 1999, 1675–1681.

Nouren, S., Bhatti, H. N., Iqbal, M., Bibi, I., Kamal, S., Sadaf, S., Sultan M., Kausar A., Safa, Y. (2017). By-product identification and phytotoxicity of biodegraded Direct Yellow 4 dye. Chemosphere, 169: 474-484.

O'Neil, M.J. (ed.). The Merck Index - An Encyclopedia of Chemicals, Drugs, and Biologi cals. Whitehouse Station, NJ: Merck and Co., Inc., 2006. p. 155.

O'Neill C, Hawkes FR, Hawkes DL, Lourenco ND, Pinheiro HM, Delee W (1999) Colour on textile effluents-source, measurement, discharge contents and simulation: a review. Journal of Chemical Technology and Biotechnology, 74:1009–1018.

Parshetti, G. K., Telke, A. A., Kalyani, D. C., Govindwar, S. P. (2010). Decolourization and detoxification of sulfonated azo dye methyl orange by *Kocuria rosea* MTCC 1532. Journal of Hazardous Materials, 176(1-3): 503–509.

Pitt, J. J. (2009). Principles and applications of liquid chromatography-mass spectrometry in clinical biochemistry. The Clinical Biochemist Reviews, 30(1): 19.

Pohanish, R. P., Sittig, M. (2008). Sittig's Handbook of Toxic and Hazardous Chemicals and Carcinogens. William Andrew, Norwich, NY.

Raghu, S., Ahmed Basha, C. (2007). Chemical or electrochemical techniques, followed by ion exchange, for recycle of textile dye wastewater. Journal of Hazardous Materials, 149(2): 324–330.

Rauf, M. A., Ashraf, S. S. (2012). Survey of recent trends in biochemically assisted degradation of dyes. Chemical Engineering Journal, 209: 520-530.

Regelsberger, G., Jakopitsch, C., Engleder, M., Rüker, F., Peschek, G. A., Obinger, C. (1999). Spectral and kinetic studies of the oxidation of monosubstituted phenols and anilines by recombinant *synechocystis* catalase− peroxidase compound I. Biochemistry, 38(32): 10480-10488.

Robati, D., Mirza, B., Rajabi, M., Moradi, O., Tyagi, I., Agarwal, S., Gupta, V. K. (2016). Removal of hazardous dyes-BR 12 and Methyl Orange using graphene oxide as an adsorbent from aqueous phase. Chemical Engineering Journal, 284: 687-697.

Ryan, B. J., Carolan, N., Ó'Fágáin, C. (2006). Horseradish and soybean peroxidases: comparable tools for alternative niches? Trends in Biotechnology, 24(8): 355-363.

Sakurai, A., Masuda, M., Sakakibara, M. (2003). Effect of surfactants on phenol removal by the method of polymerization and precipitation catalysed by *Coprinus cinereus* peroxidase. Journal of Chemical Technology & Biotechnology, 78(9): 952-958.

Seshadri, S., Bishop, P. L., Agha, A. M. (1994). Anaerobic/aerobic treatment of selected azo dyes in wastewater. Waste Management, 14(2): 127-137.

Sessa, D. J., Anderson, R. L. (1981). Soybean peroxidases: purification and some properties. Journal of Agricultural and Food Chemistry, 29(5): 960-965.

Silva, M. C., Torres, J. A., de Sá, L. R. V., Chagas, P. M. B., Ferreira-Leitão, V. S., Corrêa, A. D. (2013). The use of soybean peroxidase in the decolourization of Remazol Brilliant Blue R and toxicological evaluation of its degradation products. Journal of Molecular Catalysis B: Enzymatic, 89: 122-129.

Singh, R. L., Singh, P. K., Singh, R. P. (2015). Enzymatic decolourization and degradation of azo dyes–A review. International Biodeterioration & Biodegradation, 104: 21-31.

Singh, R. S., Singh, T., Pandey, A. (2019). Microbial Enzymes—An Overview. In Advances in Enzyme Technology: 1-40. Elsevier, Netherlands.

Sohrabi, M. R., Amiri, S., Masoumi, H. R. F., Moghri, M. (2014). Optimization of Direct Yellow 12 dye removal by nanoscale zero-valent iron using response surface methodology. Journal of Industrial and Engineering Chemistry, 20(4): 2535-2542.

Spadaro, J. T., Renganathan, V. (1994). Peroxidase-catalyzed oxidation of azo dyes: mechanism of Disperse Yellow 3 degradation. Archives of Biochemistry and Biophysics, 312(1), 301-307.

Sparkman, O. D. (2000). Mass spectrometry desk reference 2. Journal of the American Society for Mass Spectrometry, 12(11): 1144.

Steevensz, A., Cordova Villegas, L. G., Feng, W., Taylor, K. E., Bewtra, J. K., Biswas, N. (2014). Soybean peroxidase for industrial wastewater treatment: a mini review. Journal of Environmental Engineering and Science, 9(3): 181-186.

Stenesh, J. (1993). Core Topics in Biochemistry. Cogno Press. Kalamazoo, Michigan.

Szyguła, A., Guibal, E., Ruiz, M., & Sastre, A. M. (2008). The removal of sulphonated azo-dyes by coagulation with chitosan. Colloids and Surfaces A: Physicochemical and Engineering Aspects, 330(2-3), 219-226.

The National Institute for Occupational Safety and Health (NIOSH). Registry of Toxic Effects of Chemical Substances (RTECS). Weblink: https://www.cdc.gov/niosh-rtecs/BZ532910.html (Accessed: January 2020).

Thompson, D. C., Josephy, P. D., Chu, J. W., Eling, T. E. (1992). Enhanced mutagenicity of anisidine isomers in bacterial strains containing elevated N-acetyltransferase activity. Mutation Research/Genetic Toxicology, 279(2): 83-89.

Toor, A. P., Verma, A., Jotshi, C. K., Bajpai, P. K., Singh, V. (2006). Photocatalytic degradation of Direct Yellow 12 dye using UV/TiO_2 in a shallow pond slurry reactor. Dyes and Pigments, 68(1): 53-60.

Ulintz, P. J., Bodenmiller, B., Andrews, P. C., Aebersold, R., Nesvizhskii, A. I. (2008). Investigating MS^2/MS^3 matching statistics: a model for coupling consecutive stage mass spectrometry data for increased peptide identification confidence. Molecular & Cellular Proteomics, 7(1): 71-87.

U.S. Environmental Protection Agency. Weblink: https://www.epa.gov/sites/production/files/2015-03/documents/list_of_lists.pdf (Accessed: January, 2020).

U.S. Environmental Protection Agency. Chemistry Dashboard. Weblink: https://comptox.epa.gov/dashboard/DTXSID7024532 (Accessed: January, 2020).

United States Department of Agriculture, USDA. (2018). World agricultural supply and demand estimates. Weblink: https://apps.fas.usda.gov/psdonline/app/index.html#/app/topCountriesByCommodity (Accessed: January, 2020).

Van der Zee, F. P., Cervantes, F. J. (2009). Impact and application of electron shuttles on the redox (bio) transformation of contaminants: a review. Biotechnology Advances, 27(3), 256-277.

Van Huystee, R. B., Cairns, W. L. (1982). Progress and prospects in the use of peroxidase to study cell development. Phytochemistry, 21(8): 1843-1847.

Welinder, K. G., Larsen, Y. B. (2004). Covalent structure of soybean seed coat peroxidase. Biochimica et Biophysica Acta (BBA)-Proteins and Proteomics, 1698(1): 121-126.

Wright, H., Nicell, J. A. (1999). Characterization of soybean peroxidase for the treatment of aqueous phenols. Bioresource Technology, 70(1): 69-79.

Won, K., Kim, Y. H., An, E. S., Lee, Y. S., Song, B. K. (2004). Horseradish peroxidase-catalyzed polymerization of cardanol in the presence of redox mediators. Biomacromolecules, 5(1): 1-4.

Wu, Y., Taylor, K. E., Biswas, N., Bewtra, J. K. (1998). A model for the protective effect of additives on the activity of horseradish peroxidase in the removal of phenol. Enzyme and Microbial Technology, 22(5): 315-322.

Xu, F. (1996). Oxidation of phenols, anilines, and benzenethiols by fungal laccases: correlation between activity and redox potentials as well as halide inhibition. Biochemistry, 35(23): 7608-7614.

Xu, P., Singh, A., Kaplan, D. L. (2006). Enzymatic catalysis in the synthesis of polyanilines and derivatives of polyanilines. In Enzyme-Catalyzed Synthesis of Polymers:69-94. Springer, Berlin, Heidelberg.

Yagub, M. T., Sen, T. K., Afroze, S., Ang, H. M. (2014). Dye and its removal from aqueous solution by adsorption: a review. Advances in Colloid and Interface Science, 209: 172-184.

Yu, J., Taylor, K. E., Zou, H., Biswas, N., Bewtra, J. K. (1994). Phenol conversion and dimeric intermediates in horseradish peroxidase-catalyzed phenol removal from water. Environmental Science & Technology, 28(12): 2154-2160.

Zhang, J., Feng, M., Jiang, Y., Hu, M., Li, S., Zhai, Q. (2012). Efficient decolourization/degradation of aqueous azo dyes using buffered H_2O_2 oxidation catalyzed by a dosage below ppm level of chloroperoxidase. Chemical Engineering Journal, 191: 236-242.

Zhang X. (2019). Enzymatic treatment of selected pesticides in aqueous system, MASc dissertation, University of Windsor, Ontario, Canada.

Zhang, X., Hong, H., Li, Z., Guan, J., Schulz, L. (2009). Removal of azobenzene from water by kaolinite. Journal of Hazardous Materials, 170(2-3): 1064-1069.

APPENDICES

Appendix A: UV-VIS spectra of compounds studied

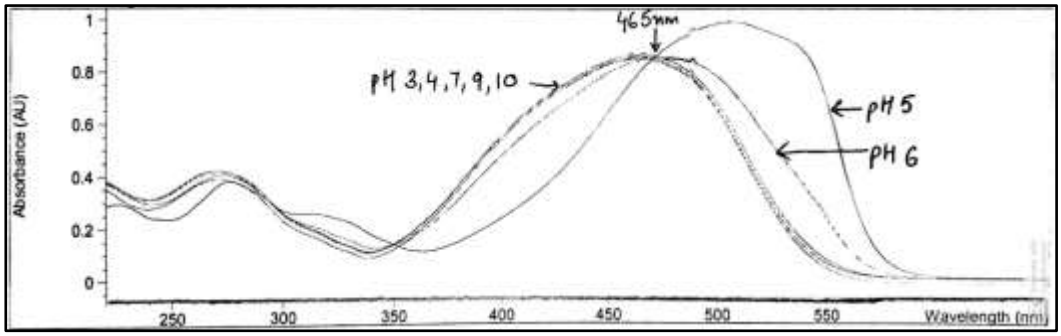

Figure A.1. 0.05 mM MO, approximate extinction coefficient is 17,160 $M^{-1}cm^{-1}$ (at 465 nm)

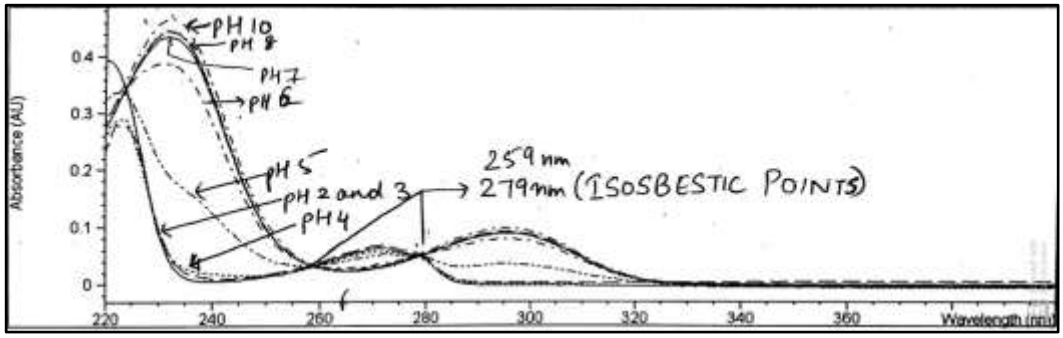

Figure A.2. 0.05 mM *p*-anisidine, approximate extinction coefficient is 990 $M^{-1}cm^{-1}$(at 279 nm)

Appendix B: SBP activity determination

SBP activity was determined using a colorimetric assay by UV-VIS spectrophotometry.

Assay reagent composition:

0.025 g of 4-AAP

100 µL of 100 mM H_2O_2 (prepared by mixing 510 µL of 30% H_2O_2 stock solution in 50 mL distilled water)

5000 µL of 10X concentrate (0.9410 g phenol, 1.3105 g monobasic sodium phosphate and 3.7479 g dibasic sodium phosphate)

42.4 mL distilled water is added to make the total volume of reagent to 47.5 mL.

Enzyme dilution

Enzyme is diluted by a factor of 30, 40 and 50.

Instrument setup

1. Enable kinetics mode in the UV-VIS spectrophotometer

2. Enter the following values:

Wavelength: 510 nm

Cycle time: 30 seconds

Interval time: 5 seconds

Order of reaction: Zero order

Multiplication factor: 200

Procedure for SBP colorimetric assay

1. Blank the instrument with 950 µL of the reagent added to 50 µL distilled water in cuvette

2. Put 50 µL enzyme in the cuvette and place it in the vial holder and lock it

3. Add 950 µL of reagent vigorously to the cuvette and immediately click on start button

4. Monitor the change in absorbance of pink chromophore and note down the rate of reaction

Absorbance change should be within 0.1 to 0.2 AU for 30 seconds.

Multiplication factor of 200 is used in the instrument to achieve initial rate according to the formula mentioned below:

$$SBP\ activity\ \left(\frac{U}{mL}\right) = \frac{initial\ rate\ \left(\frac{AU}{s}\right) * 60\ \left(\frac{sec}{min}\right) * \left(\frac{1000\ \mu L}{50\ \mu L}dilution\right)}{6\ \frac{m}{M\ cm}}$$

$$= 200 * initial\ rate\ \frac{U}{mL}$$

Appendix C: Calibration curves

C.1 HPLC calibration curves

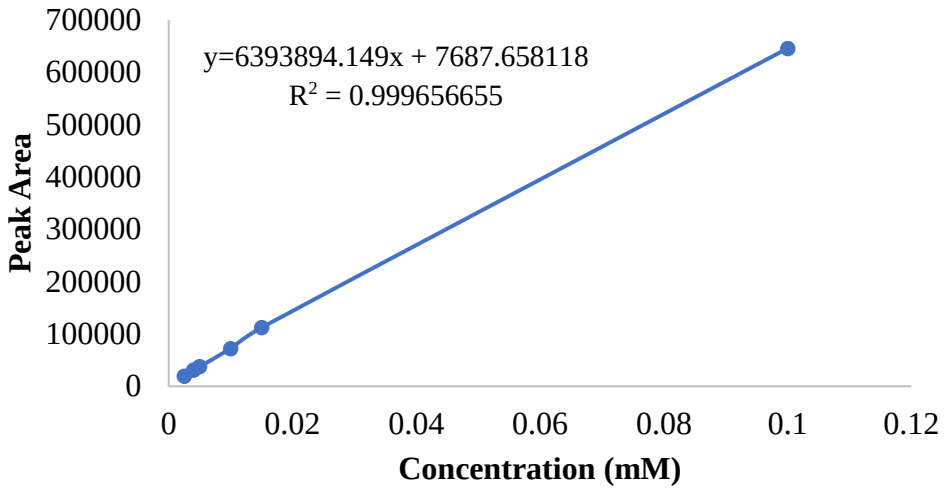

Figure C.1 Standard curve for MO at 465 nm

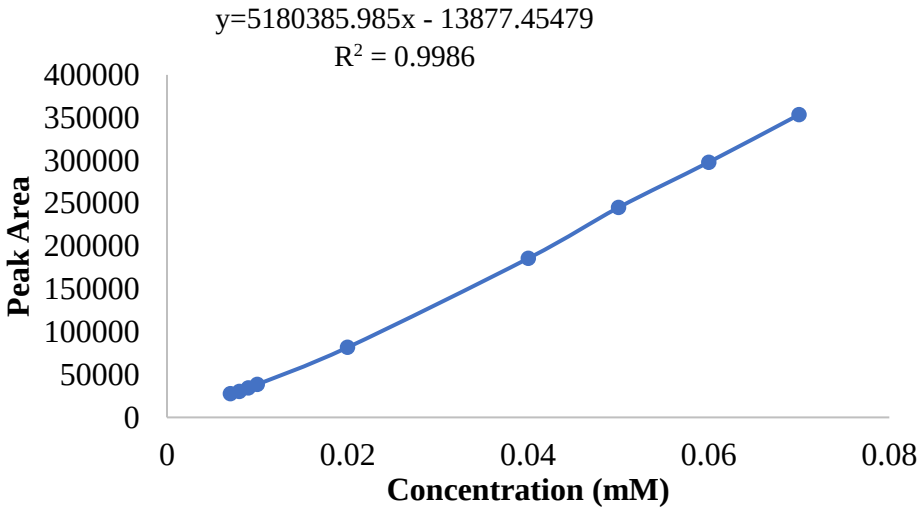

Figure C.2 Standard curve for azobenzene at 312 nm (0.007 mM to 0.07 mM)

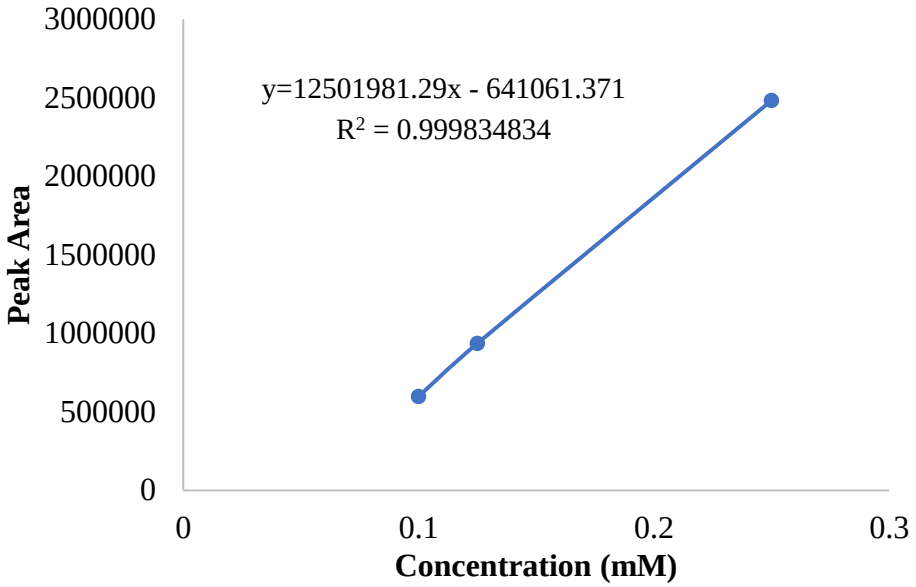

Figure C.3 Standard curve for azobenzene at 312 nm (0.1 mM to 0.25 mM)

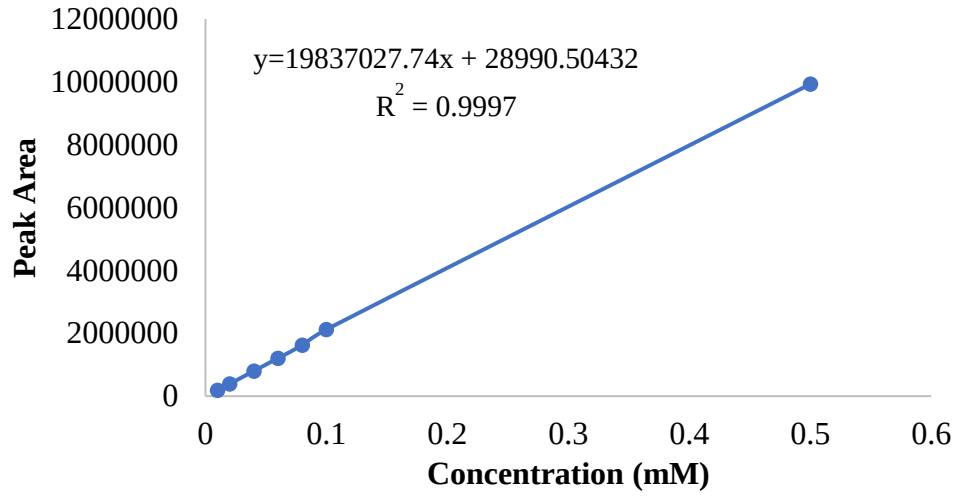

Figure C.4 Standard curve for DY12 at 401 nm

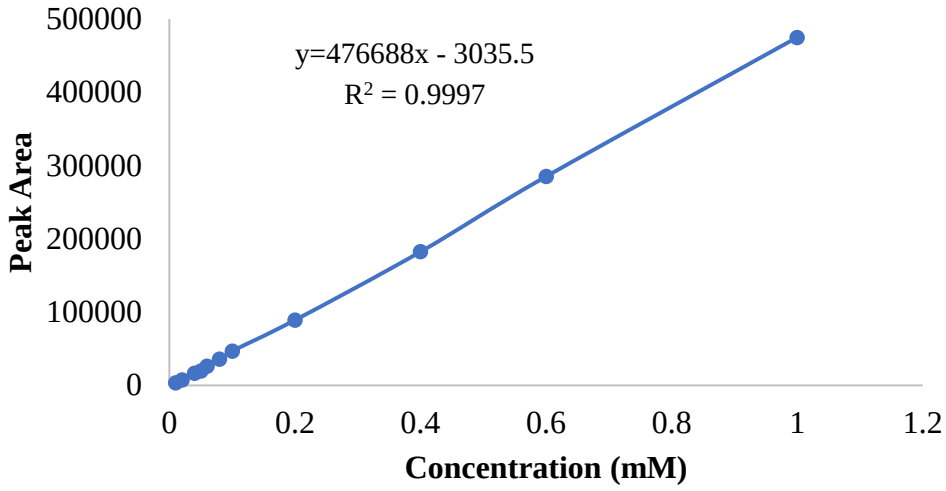

Figure C.5 Standard curve for *p*-anisidine at 279 nm

C.2 UV-VIS calibration curves

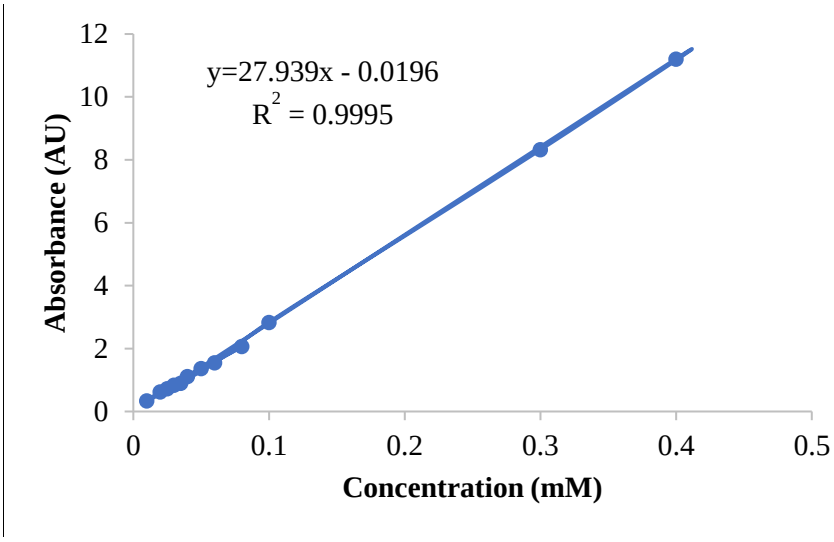

Figure C.6 Standard curve for DY12 at 401 nm

Appendix D: Non-substrates for enzymatic reaction

Direct Yellow 12

Research conducted by Beemer (2017) on removal of 4-(phenylazo)-benzoic acid through adsorption on polyphenolic precipitates formed by SBP, provided evidence of azo-bond cleavage in the absence of anilino or phenolic functional groups. Following this study, DY12 was chosen to be studied in this thesis to investigate the capability of SBP to cleave an azo-bond in the absence of phenolic or anilino functional groups. Preliminary investigation was done using 0.5 mM DY12, 0.75 mM H_2O_2, 40 mM buffer (pH 1.8-10.0) and 1.0 U/mL SBP. A standard was prepared with no SBP and no H_2O_2 at pH 7.0. It was observed that at pH 2.6, 3.0, and 4.0 the orange solution immediately turned to dark brown colour with the formation of mud-like precipitates exhibiting 89% decolourization (maximum) at pH 1.8 by UV-VIS. Above pH 5.0, no significant decolourization was observed with SBP and H_2O_2. Also, no decolourization was observed in the standard. Control experiments were conducted with controls at their respective pHs, with no SBP or no H_2O_2. It was observed that the control with SBP and no H_2O_2 exhibited the same removal of DY12 as with SBP and H_2O_2. Residual H_2O_2 was determined after the 3-h reaction. H_2O_2 remaining in the batch reactor was 88% after the reaction albeit the decolourization of DY12 was 89%. It suggests that only 0.09 mM H_2O_2 was consumed for removal of 0.45 mM DY12, which is not valid since previous studies suggest that the theoretical molar ratio of H_2O_2/substrate should be 0.5 or more (Ćirić-Marjanović *et al*. 2017).

Some more investigation was done using HPLC to validate the results. Removal of 90% was observed at pH 1.8 and 1.0 U/mL SBP without H_2O_2. After 3 hours, the pH of the

batch reactor was raised to 5.0. This resulted in redissolution of the brown precipitates, reverting to an orange solution and decrease in % removal from 90% to 60%. Hence, it was concluded that apparent removal of DY12 could be attributed to precipitation of the dye on SBP and not to the enzymatic reaction.

Mediator studies were conducted by Ali *et al*. (2013) for removal of Crystal Ponceau 6R dye using HOBT with SBP/H_2O_2, Won *et al*. (2004) for removal of cardanol (phenol derivative) with HRP using N-ethyl phenothiazine as mediator, Knutson *et al*. (2005) using 2,2'-azinobis-(3-ethylbenzthiazoline-6-sulfonate), (ABTS) as mediator with laccase for removal of Direct Yellow 11 and Basazol 46L and Khilfi *et al*. (2010) using HOBT as mediator with laccase for treatment of effluents from textile industry. Thus, HOBT was chosen to be studied as a mediator for DY12.

Batch reactions were performed using 0.05 mM DY12, 0.75 mM H_2O_2, 0.75 mM HOBT, 0.1 and 1.0 U/mL SBP and 40 mM pH 3.0 buffer. Decolourization of 44% and 67% was observed with 0.1 and 1.0 U/mL SBP, respectively with the formation of precipitates, both in the presence as well as absence of H_2O_2. This suggested that addition of HOBT as a mediator was unsuccessful in performing enzymatic reaction of DY12 at the above-mentioned conditions.

Azobenzene

Azobenzene was studied as a model compound in this thesis since it is a product of azo-bond cleavage of several dyes and aromatic amines. Due to solubility issues, 0.5 mM stock solution of azobenzene was prepared in 100% ethanol and then diluted to 50%. For batch reactions, 0.125 mM azobenzene in 25% ethanol was used. Preliminary investigation was done from pH 3.0-10.0 with 0.1 U/mL SBP and 0.2 mM H_2O_2 and analyzed using HPLC.

A control was prepared with no SBP and no H_2O_2. Removal of 20% was observed for each of the batch reactors as well as the control. Increments in enzyme concentration from 0.1 to 0.5 U/mL SBP also showed the same results. Hence, it was concluded that azobenzene is not a substrate for SBP.

VITA AUCTORIS

NAME:	Amanpreet Kaur
PLACE OF BIRTH:	Mohali, Punjab, India
YEAR OF BIRTH:	1993
EDUCATION:	Dr. BR Ambedkar National Institute of Technology, Jalandhar, B. Tech, India, 2015
	Dr. BR Ambedkar National Institute of Technology, Jalandhar, M. Tech, India, 2017
	University of Windsor, Department of Civil and Environmental Engineering, MASc., Windsor, ON, 2020